

Rigaku VariMax Dual

Part 2b Analysis Manual with OLEX²

X-ray Laboratory, Nano-Engineering Research Center, Institute of Engineering Innovation, The University of Tokyo

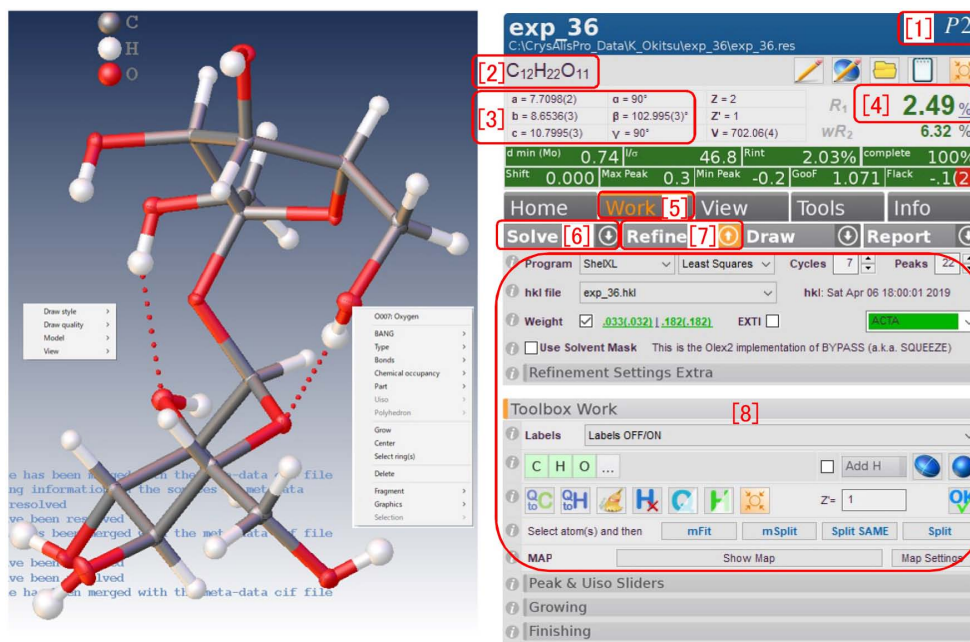


Figure 0: Whole window of OLEX². Molecular structure of sucrose.

The molecular structure of sucrose has been solved with the OLEX² based on 'exp.36.ins' made by the CrysAlis^{Pro}. This was refined by clicking 'Refine [7]' after determination of the initial phases by clicking 'Solve [6]'. '[1] $P2_1$ ' (refer to §B.4.2) [p.41] is the space group, '[2] $C_{12}H_{22}O_{11}$ ' is the molecular formula, '[3] $a, b, c, \alpha, \beta, \gamma$ ' are the lattice constants, and '[4] 2.49' is the R-factor. 'Solve [6]', 'Refine [7]', 'Draw' and 'Report' have been displayed by clicking 'Work [5]'. '↓' on the right of them can be clicked to open their option menus. '↑' on the right of 'Refine [7]' has been clicked to open the option menus shown in the red frame [8].

The molecular model can be 3D-rotated by left click&dragging, be scaled by right click&dragging and be moved parallel by both click&dragging the mouse. Display options can be opened by right-clicking the background. Options of an atom can be opened by right-clicking the atom. Red dashed lines are hydrogen bonds.

Chapter 1 [p.1] describes how to download and install 'OLEX²', 'Shelx' and 'PLATON'. Chapter 2 [p.7] and Chapter 3 [p.20] describes how to solve the molecular structure with the OLEX².

Appendix A [p.30] describes the reasonability of defining the reciprocal lattice. This is strongly recommended to read. The understanding of the reciprocal lattice is necessary for crystallography.

Appendix B [p.34] describes how to determine the space group based on the extinction rule.

Appendix C [p.48] describes the definition of coordinate system and the extinction rule for the trigonal and hexagonal crystal systems.

Contents

1	Download and installation of ‘OLEX²’, ‘SHELX’ and ‘PLATON’	1
1.1	Download and installation of ‘OLEX ² ’	1
1.2	Download and installation of ‘SHELX’	2
1.3	Registration of ‘SHELX’ to ‘OLEX ² ’	4
1.4	Download and installation of ‘PLATON’	4
1.5	Registration of ‘PLATON’ to ‘OLEX ² ’	5
1.6	Registration of the parameter file to the ‘OLEX ² ’	6
2	Example of structure determination with the OLEX² (Sucrose)	7
2.1	Startup of the OLEX ² and opening the project	7
2.2	Determination of the initial phases with the direct method	7
2.3	Concerning the direct method and ‘SHELX’	8
2.4	Refinement of the structure by least-square fitting	9
2.4.1	Refinement with isotropic temperature factors	9
2.4.2	Displaying peaks of electron density that have not been assigned to atoms (Q peaks)	10
2.4.3	Refinement with anisotropic temperature factors	10
2.4.4	Refinement with hydrogens assigned	11
2.4.4.1	Automatical assignment of hydrogens	11
2.4.4.2	Assignment by replacing Q peaks with hydrogens	11
2.4.4.3	Manual assignment of hydrogens	13
2.5	Creation of the report	13
2.5.1	Settings of ‘Collection’	13
2.5.2	Settings of ‘Crystal’	15
2.5.3	Settings of ‘Crystal Image’	15
2.5.4	Settings of ‘Diffraction’	16
2.5.5	Settings of ‘Absorption Correction’	17
2.5.6	Settings of ‘Publication’	17
2.5.7	Settings of ‘Citations’	17
2.5.8	Setting of ‘Reference’	18
2.5.9	Settings of ‘Source Files’	18
2.5.10	Creation of the final report	18
3	Example of structure determination with the OLEX² (α-cyclodextrin)	20
3.1	Opening the project	20
3.2	Determination of the initial phases	20
3.3	The optimization of the molecular structure	22
3.4	Checking the existence of symmetric center	22
3.5	Consideration on the intensities of Q peaks	23
3.6	Separation of disordered atoms	23

3.7	Refinement with isotropic and anisotropic temperature factor	25
3.8	Refinement with hydrogen atoms added	25
	3.8.1 Assignment of methine groups	25
	3.8.2 Assignment of methylene groups	26
	3.8.3 Assignment of hydroxy groups and H ₂ O	27
3.9	Omitting bad reflections	28
3.10	Consideration of extinction effect	28
3.11	Creation of the report	29
A	Reasonability of defining the reciprocal lattice	30
A.1	Bragg's reflection condition	30
A.2	Laue's reflection condition	30
A.3	Ewald's reflection condition (Ewald construction)	31
	A.3.1 Foundation of Ewald construction	31
	A.3.2 Relation between reciprocal lattice vector and Bragg reflection plane	32
A.4	Drawing of Miller and Miller indices	33
B	Determination of space group from extinction rule	34
B.1	Symmetric elements of crystal derived based on the group theory	36
B.2	Symbols of space groups	37
B.3	How to read extinction rules	38
B.4	Examples of extinction rules due to combinations of symmetric elements	39
	B.4.1 Orthorhombic $P2_12_12_1$ (#19)	41
	B.4.2 Monoclinic $P12_11$ [$P2_1$ (#4)]	41
B.5	Mathematical proofs of extinction rules	41
	B.5.1 Extinction rules due to complex lattice	42
	B.5.1.1 Extinction due to base-centered lattice	42
	B.5.1.2 Extinction due to body-centered lattice	42
	B.5.1.3 Extinction due to face-centered lattice	43
	B.5.2 Extinction owing to glide axes	43
	B.5.2.1 Extinction due to axial glide plane	43
	B.5.2.2 Extinction due to double glide plane (e glide plane)	44
	B.5.2.3 Extinction due to diagonal glide plane	44
	B.5.3 Extinction due to screw axes	45
	B.5.3.1 Extinction due to 2_1 screw axis	45
	B.5.3.2 Extinction due to 4_1 screw axis	45
	B.5.3.3 Extinction due to 4_2 screw axis	46
C	Reflection indices and extinction rules in the cases of trigonal and hexagonal crystals	48
C.1	Cases of trigonal system	48
	C.1.1 Diagram shown in <i>International Tables for Crystallography</i> (2006) Vol.A	48
	C.1.2 Real and reciprocal coordinates	49
	C.1.3 Derivation of extinction rule due to 3_1 screw axis	49
	C.1.4 On the absence of extinction due to 2_1 screw axis perpendicular to \mathbf{c}	50
C.2	Case of hexagonal system	51
	C.2.1 Figure shown in <i>International Tables for Crystallography</i> (2006) Vol.A	51
	C.2.2 Coordinates for describing six-fold screw axes	51
	C.2.3 Derivation of extinction rule due to 6_1 screw axis	52

C.2.4	Derivation of the extinction due to 6_2 screw axis	53
C.2.5	Derivation of extinction rule due to 6_3 screw axis	53

List of Figures

0	Whole window of OLEX ² . Molecular structure of sucrose.	i
1.1	Registrtration at the URL of OlexSys	1
1.2	Registration of the user information	1
1.3	Copy of the sign-in URL.	1
1.4	Sign in.	1
1.5	Download of ‘OLEX ² ’.	2
1.6	Installation of ‘OLEX ² ’.	2
1.7	License Agreement.	2
1.8	Settings of ‘Help’ and ‘Auto Update’.	2
1.9	Download of SHELX-2013.	2
1.10	No charge for Academic Use.	2
1.11	Registration of the user information.	3
1.12	Username and password in the e-mail.	3
1.13	Click ‘Downloads’.	3
1.14	Input the user name and password.	3
1.15	Download of the installer.	3
1.16	Execution of the installer.	3
1.17	Choice of files to be installed.	4
1.18	Choice of files to be installed.	4
1.19	Registration of ‘SHELX’ to ‘OLEX ² ’.	4
1.20	How to search ‘PLATON’ homepage.	4
1.21	‘PLATON’ homepage.	4
1.22	Reference and the download sites.	4
1.23	Downloading the PLATON.	5
1.24	Saving ‘platon.zip’.	5
1.25	Expansion of ‘platon.zip’.	5
1.26	Extracted ‘platon.exe’.	5
1.27	Registration of ‘PLATON’ to ‘OLEX ² ’.	6
1.28	The icon of ‘PLATON’ on ‘OLEX ² ’.	6
1.29	The parameter file.	6
1.30	Registration of the parameter file.	6
2.1	Startup of OLEX ² and opening files	7
2.2	Setting of options for Solve	7
2.3	Change of the molecular formula	8
2.4	Molecular structure with the initial phases determined.	8
2.5	Molecular structure with initial phases determined	9
2.6	Result after clicking ‘Refine’ twice	9
2.7	Result after further twice refinement with the weight optimized	9
2.8	Electron density peaks not assigned to any atom (Q peak) and their intensity	9

2.9	Refinement result with an oxygen atom deleted.	10
2.10	Result after further twice refinement with anisotropic temperature factors	10
2.11	Switching the display mode of Q peaks	11
2.12	Setting of the ‘Thermal ellipsoid’ mode.	11
2.13	The molecular structure displayed with the ‘Thermal ellipsoid’ mode.	11
2.14	Molecular model with hydrogens automatically assigned.	11
2.15	Q peaks have been replaced with hydrogens.	12
2.16	The refined structure with hydrogens of hydroxy groups assigned.	12
2.17	The window displayed just after clicking ‘[8] ↓’ in Fig. 2.16 (d).	13
2.18	Setting window of report.	13
2.19	Setting window of ‘Report’	13
2.20	Setting window of ‘Report’	13
2.21	Choice of the first author’s affiliation	14
2.22	Typing the first author’s name and address	14
2.23	The first author’s name	14
2.24	Typing the second author’s name and address	14
2.25	The first and second authors’ name	14
2.26	Addition of the third author’s affiliation	14
2.27	Selection of the affiliation of the third author.	15
2.28	Typing the third author’s name and address.	15
2.29	The third author’s name	15
2.30	Selections of ‘Submitter’ and ‘Operator’.	15
2.31	Selection or typing of crystal information.	15
2.32	Selection or typing of crystal information.	16
2.33	Setting of the parameter file	16
2.34	Information about the absorption correction.	16
2.35	List of the authors and title of the journal	16
2.36	Cover letter to the editor.	16
2.37	Articles that should be cited.	16
2.38	Information concerning the submitted article	16
2.39	Information concerning the the source file	17
2.40	Creation of the report	17
2.41	Conflicting information	17
2.42	Final information concerning the crystal	18
3.1	Loading the file	20
3.2	Molecular structure automatically determined by the AutoChem.	20
3.3	[Ctrl]+[T] can be typed to display these windows.	21
3.4	Settings for determination of the initial phases.	21
3.5	Initial structure obtained by the phase determination	21
3.6	solvent molecule moved by symmetrical operation	21
3.7	Starting the optimization of the molecular structure	22
3.8	Checking the existence of symmetric center	22
3.9	Checking the existence of symmetric center	22
3.10	Anomalous intensity of Maximum Peak	22
3.11	Anomalous intensity of Maximum Peak	23
3.12	Changing the number of displayed Q peaks.	23
3.13	Refined with oxygen replaced from carbon.	24
3.14	The oxygen is dragged to Q peak with [Shift] key pressed.	24
3.15	Starting to separate the disordered oxygens	24
3.16	The disordered oxygen separated to two sites	24

3.17	Refined result with isotropic temperature factors	25
3.18	Refined result with anisotropic temperature factors	25
3.19	Manual addition of hydrogens to carbons	25
3.20	[1]-[7] correspond to Fig. 3.19 [1]-[7].	26
3.21	Methine groups have been assigned.	26
3.22	Refined result after methine groups assigned	26
3.23	Methylene groups have been assigned.	26
3.24	Hydrogens of disordered methylene group have been assigned.	27
3.25	Refined with hydrogens of methine groups added	27
3.26	Refinement with hydrogens of hydroxy groups and H ₂ O added	27
3.27	Refined with hydrogens of hydroxy groups and H ₂ O added	28
3.28	Omitting bad reflections	28
3.29	Result of refinement	28
3.30	Result of refinement with the extinction effect taken into account	28
A.1	Bragg's reflection condition.	30
A.2	Laue's reflection condition.	31
A.3	Ewald sphere	32
A.4	Drawing of Miller and Miller indices	33
B.1	Content of 'process.out' (#1). [Taurine; monoclinic $P2_1/c$ (#14)].	34
B.2	Content of 'process.out' (#2). [Taurine; monoclinic $P2_1/c$ (#14)]	34
B.3	Content of 'process.out' (#3) [Taurine; monoclinic $P2_1/c$ (#14)]. [setting #1] corresponds to '[1] CELL CHOICE 1' in Fig. B.5.	35
B.4	Reflection condition of $P2_1/c$ (#14) described in <i>International Tables for Crystallography</i> (2006) Vol.A. $0k0$ reflections when k is odd and, $h0l$ and $00l$ reflections when l is odd, extinguish.	35
B.5	Drawings for space group $P2_1/c$ (#14) in <i>International Tables for Crystallography</i> (2006) Vol.A. Protein crystals do not belong to this space group absolutely.	37
B.6	Redesignation of space group in CrystalStructure 4.1. (in the case of small molecular-weight crystal).	39
B.7	Drawing for $P\bar{1}$ (#2) in <i>International Tables for Crystallography</i> (2006) Vol.A. Since this space group has symmetric center, protein crystals do not belong to it. The phase problem is simple (0 or π (180°)).	40
B.8	Drawing for $C12/c1[C2/c]$ (#15) in <i>International Tables for Crystallography</i> (2006) Vol.A. Protein crystals do not belong to this space group absolutely since it has glide plane.	40
B.9	<i>International Tables for Crystallography</i> (2006) Vol.A $P2_12_12_1$ (#19).	40
B.10	<i>International Tables for Crystallography</i> (2006) Vol.A $P12_11[P2_1$ (#4)].	40
C.1	<i>International Tables for Crystallography</i> (2006) Vol.A, Symmetric elements. $P3_121$ (#152).	48
C.2	<i>International Tables for Crystallography</i> (2006) Vol.A, Positions of atoms. $P3_121$ (#152).	48
C.3	Real (black) and reciprocal (gray) primitive translation vectors.	49
C.4	<i>International Tables for Crystallography</i> (2006) Vol.A, Symmetric elements. $P6_122$ (#178).	51
C.5	<i>International Tables for Crystallography</i> (2006) Vol.A, Positions of atoms. $P6_122$ (#178).	51

Chapter 1

Download and installation of ‘OLEX²’, ‘SHELX’ and ‘PLATON’

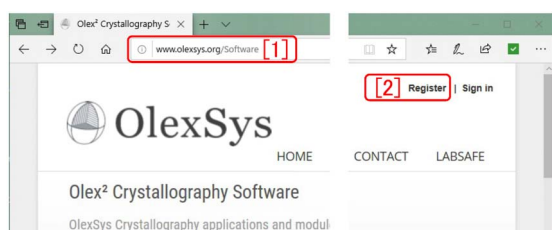


Figure 1.1: Registrtration at the URL of OlexSys

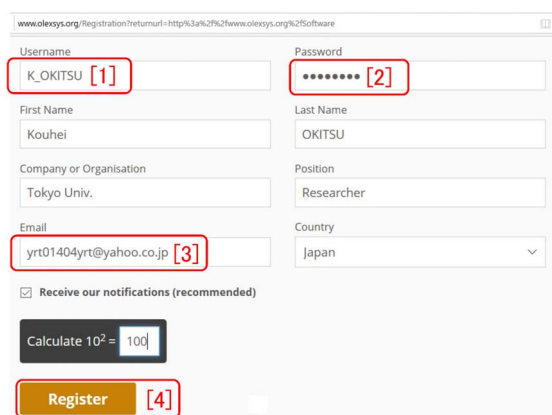
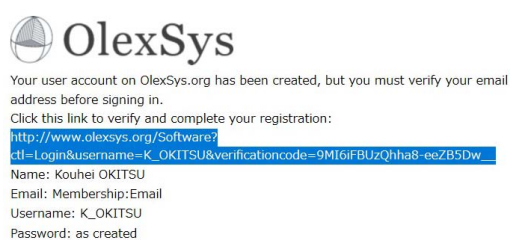


Figure 1.2: Registration of the user information

1.1 Download and installation of ‘OLEX²’

The user information is asked when clicking ‘[2] register’ after entering the URL whose address is shown at ‘[1]’ of Fig. 1.1: <http://www.olexsys.org/software>. By clicking ‘register [4]’ in Fig. 1.2, you can receive an e-mail as shown in Fig. 1.3. You can copy the sign in URL to paste to the browser to login it.

In Fig. 1.4, ‘User name [1]’ and ‘Password



- Login to download our software at www.OlexSys.org/software
- View our documentation at www.olexsys.org/Documentation
- If you subscribed to our mailing list, we will email an occasional newsletter out with important updates and information

Now hurry up and get started with Olex²

Figure 1.3: Copy of the sign-in URL.

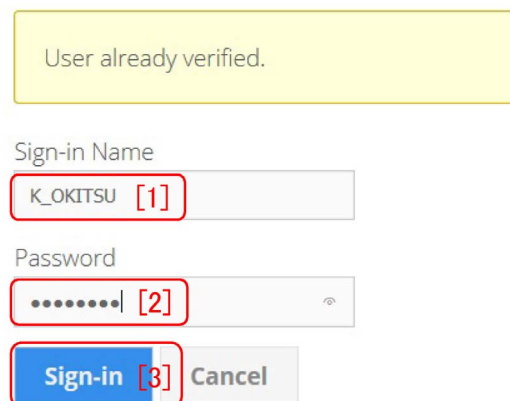


Figure 1.4: Sign in.

‘[2]’ that have been inputted in Fig. 1.2 should be typed to ‘Sign-in [3]’ in Fig. 1.4.

By scrolling down the URL of OlexSys, click ‘[1] Download’ in Fig. 1.5 [p.2], please. ‘[2] Execute’ should be clicked to download and execute ‘[3] olex2-installer.exe’. Then, ‘Install’ in Fig. 1.6 [p.2] should be clicked.

2CHAPTER 1. DOWNLOAD AND INSTALLATION OF ‘OLEX²’, ‘SHELX’ AND ‘PLATON’

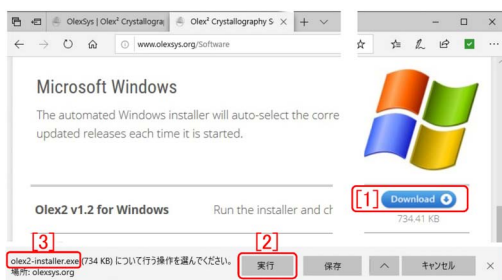


Figure 1.5: Download of ‘OLEX²’.

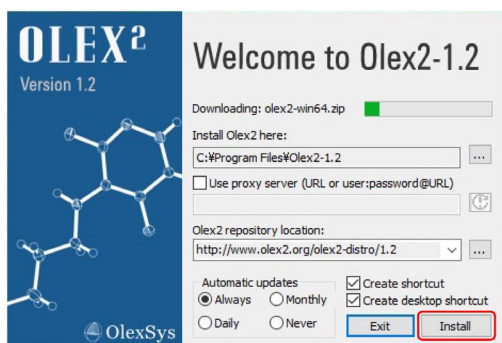


Figure 1.6: Installation of ‘OLEX²’.

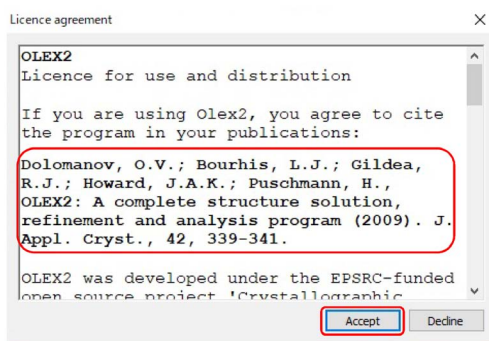


Figure 1.7: License Agreement.

After finishing the installation, ‘License Agreement’ is shown in Fig. 1.7. It should be read to click ‘Accept’. When publishing a paper that reports the results obtained with OLEX², the literature shown in the red frame in Fig. 1.7 should be cited.

For messages about ‘Help’ and automatic update as shown in Fig. 1.8, ‘YES’ is recommended to click.

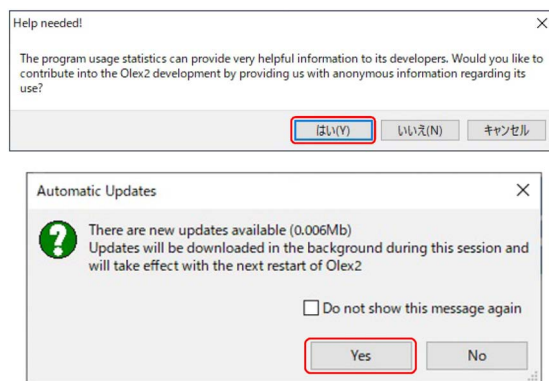


Figure 1.8: Settings of ‘Help’ and ‘Auto Update’.



Figure 1.9: Download of SHELX-2013.

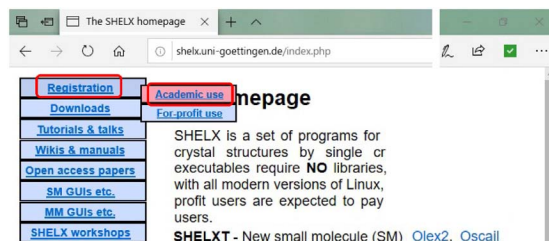


Figure 1.10: No charge for Academic Use.

1.2 Download and installation of ‘SHELX’

In Fig. 1.9, to the URL of SHELX ‘http://shelx.uni-ac.gwdg.de/’ [1] should be accessed to click ‘[2] SHELX-2013’ to display Fig. 1.10. ‘Registration’ and then ‘Academic use’ should be clicked.

In Fig. 1.11, necessary items should be typed to click ‘Submit’. Then, an e-mail in which ‘user name’ and ‘password’ are written as shown in Fig. 1.12, is sent to the e-mail address that has been typed in Fig. 1.11. To the URL as shown in Fig. 1.13, should be accessed again to

SHELX registration for academic use only

"Xtal question" should be the name of space group number 19

First name(s)
 Last name
 Affiliation
 City
 Post/zipcode
 Country
 Email
 Xtal question

Congratulations, your registration was successful.
 The downloading instructions have been emailed to the above address.

Figure 1.11: Registration of the user information.

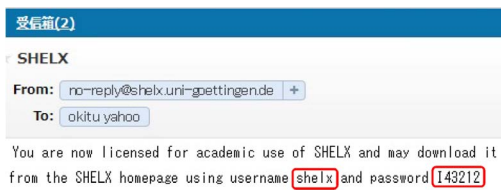


Figure 1.12: Username and password in the e-mail.

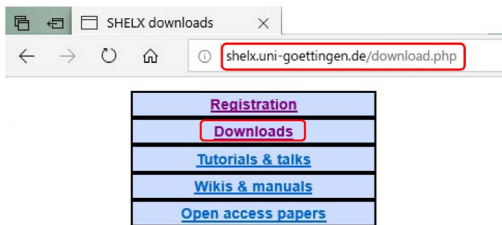


Figure 1.13: Click 'Downloads'.

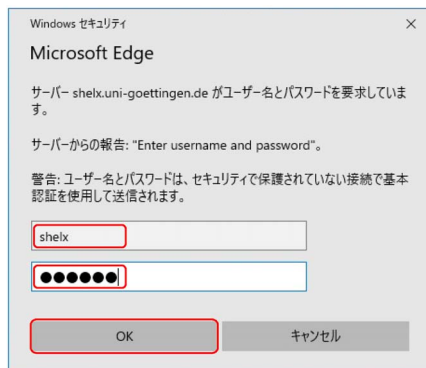


Figure 1.14: Input the user name and password.

click 'Downloads'. In Fig. 1.14, 'User name' and



Figure 1.15: Download of the installer.

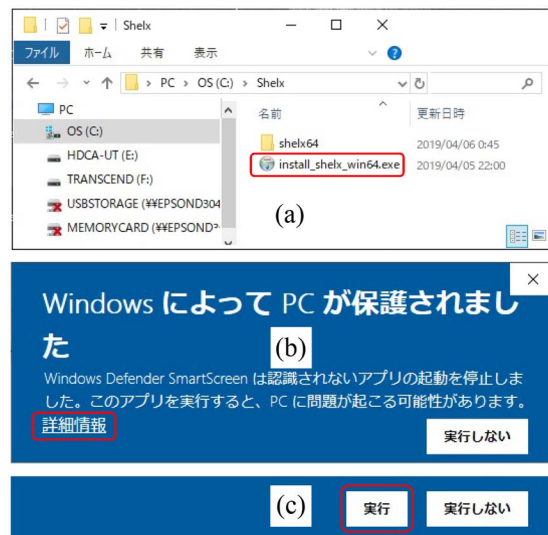


Figure 1.16: Execution of the installer.

'Password' written in Fig. 1.12 should be typed to click 'OK'.

In Fig. 1.15, 'install-shelx-win32.exe' or 'install-shelx-win64.exe' depending on the system of the computer should be right-clicked. It should be saved in a newly made folder 'C:\Shelx' and double-clicked.

In Fig. 1.16 (b), 'Detailed information' should be clicked to open Fig. 1.16 (c). Here, 'Execute' should be clicked to install the SHELX. In Fig. 1.17 [p.4], all programs should be checked to click 'Next'.

In Fig. 1.18 [p.4], installed files are shown.

4 CHAPTER 1. DOWNLOAD AND INSTALLATION OF 'OLEX²', 'SHELX' AND 'PLATON'

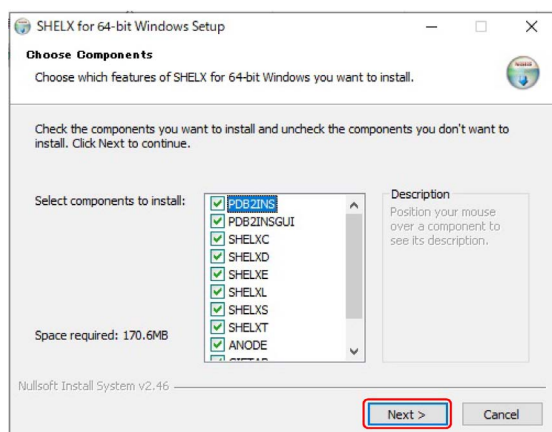


Figure 1.17: Choice of files to be installed.

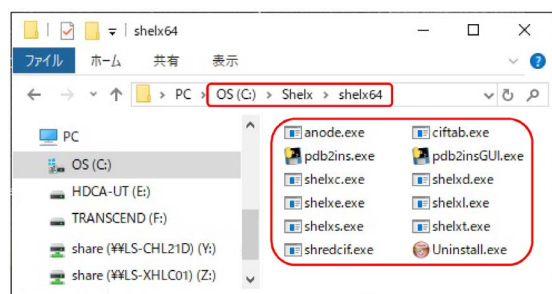


Figure 1.18: Choice of files to be installed.

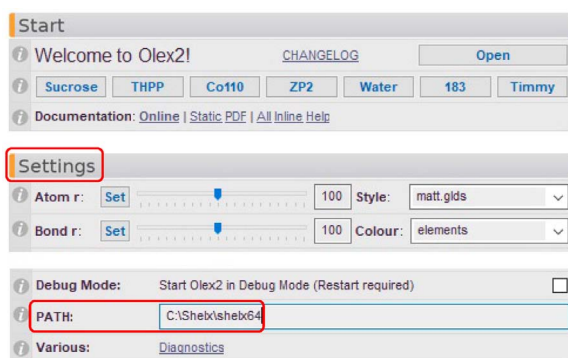


Figure 1.19: Registration of 'SHELX' to 'OLEX²'.

1.3 Registration of 'SHELX' to 'OLEX²'

In Fig. 1.19, a part of menus is shown just after starting the OLEX². 'Settings' bellow 'Start' should be clicked to display many items. In the text box of 'PATH', the folder name 'C:\Shelx\shelx64' should be typed such that



Figure 1.20: How to search 'PLATON' homepage.

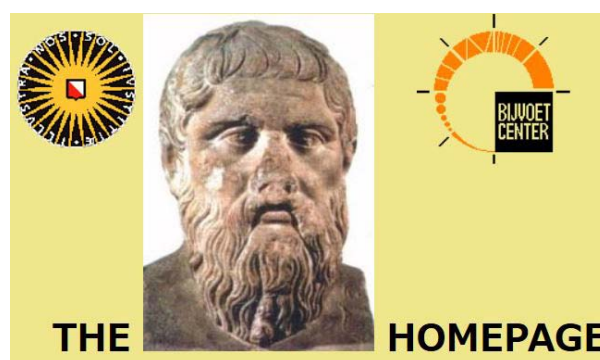


Figure 1.21: 'PLATON' homepage.



Figure 1.22: Reference and the download sites.

the SHELX can be used on the OLEX².

1.4 Download and installation of 'PLATON'

'PLATON' can be downloaded and installed without charge for academic use.

On the Google homepage, 'PLATON homepage' can be typed to find the 'PLATON' home-

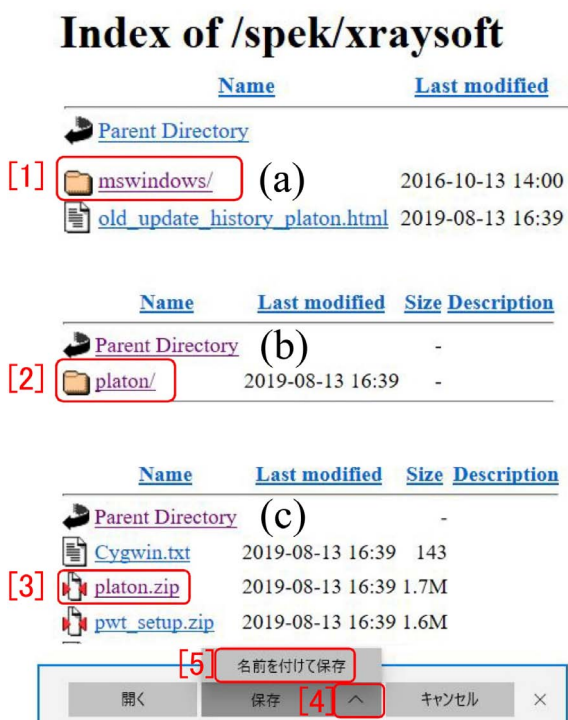


Figure 1.23: Downloading the PLATON.

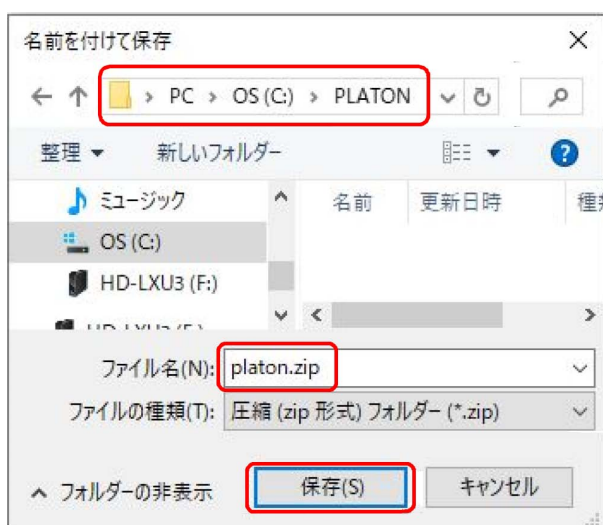


Figure 1.24: Saving 'platon.zip'.

page as shown in Fig. 1.21.

By scrolling down the URL, the reference that should be cited and the sites from which the 'PLATON' can be downloaded, are found.

One of the download sites can be clicked to show Fig. 1.23. '[1] mswindows/' in Fig. 1.23 (a) can be clicked to show Fig. 1.23 (b). '[2] platon/' in it can be clicked to show Fig. 1.23 (c). '[3]

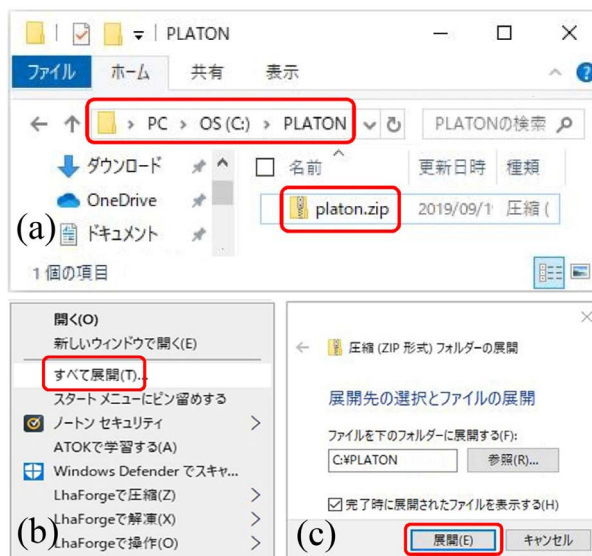


Figure 1.25: Expansion of 'platon.zip'.

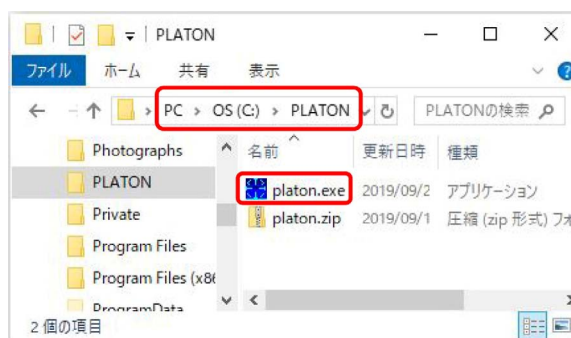


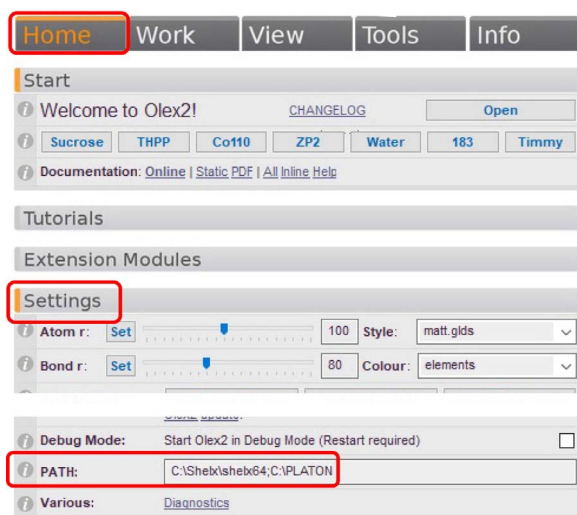
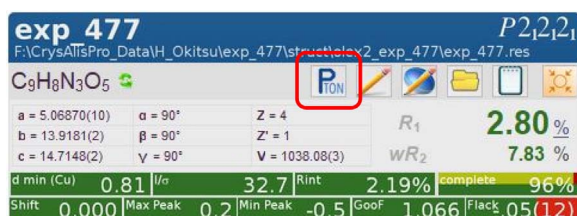
Figure 1.26: Extracted 'platon.exe'.

'platon.zip', '[4] ^' and then '[5] Save as' should be clicked to display Fig. 1.24. 'platon.zip' should be saved in the folder of 'C:\PLATON'.

In Fig. 1.25 (a), 'platon.zip' should be right-clicked to show Fig. 1.25 (b). Here, 'Expand All (T)...' should be clicked to show Fig. 1.25 (c). In Fig. 1.25 (c), 'Expand (E)' should be clicked to expand the file in 'C:\PLATON'. 'platon.exe' can be decompressed as shown in Fig. 1.26.

1.5 Registration of 'PLATON' to 'OLEX²'

'Home' on the upper left of the window of the OLEX² in Fig. 1.27 [p.6] has been clicked to open. Then, 'Settings' can be clicked to let the text box of 'PATH' be shown.

Figure 1.27: Registration of ‘PLATON’ to ‘OLEX²’.Figure 1.28: The icon of ‘PLATON’ on ‘OLEX²’.

Here, ‘C:\PLATON’ should be typed after ‘C:\Shelx\shelx64’ by separating them with a semicolon (;) without space. After closing the OLEX², it can be opened again such that the icon of the PLATON is found as shown in Fig. 1.28 and it can be used.

1.6 Registration of the parameter file to the ‘OLEX²’

‘[2] Rigaku_XtaLAB.P200_007.cif’ in the folder of ‘[1] Program Files\Olex2-



Figure 1.29: The parameter file.

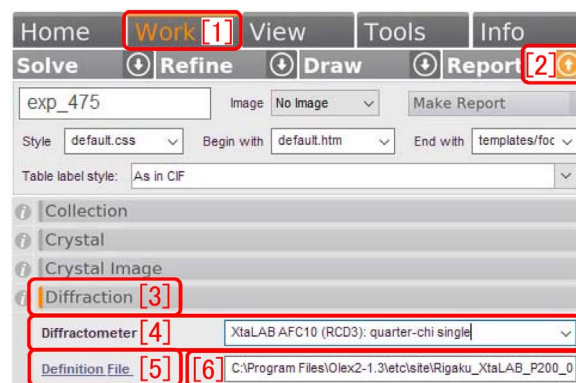


Figure 1.30: Registration of the parameter file.

1.3\etc\site’ in Fig. 1.29 is the parameter file of the apparatus. This file should be placed in the same folder as ‘[1]’. It is available from the same folder in the computer placed near the entrance of the room #333 of the 9th building of the school of engineering.

On the window of the OLEX², ‘Work [1]’ in Fig. 1.30 and then ‘[2] ↓’ on the right of ‘Report’ can be clicked to let the options of ‘Report’ be shown. Here, ‘Diffraction [3]’ and then ‘Definition File [5]’ should be clicked to open the file explorer as shown in Fig. 1.29. In Fig. 1.29, ‘[2] Rigaku_XtaLAB.P200_007.cif’ should be clicked to load it. In Fig. 1.30, ‘XtaLAB AFC10 (RCD): quarter-chi single’ can be selected from the pull-down menu of ‘Diffractometer [4]’.

Chapter 2

Example of structure determination with the OLEX² (Sucrose)

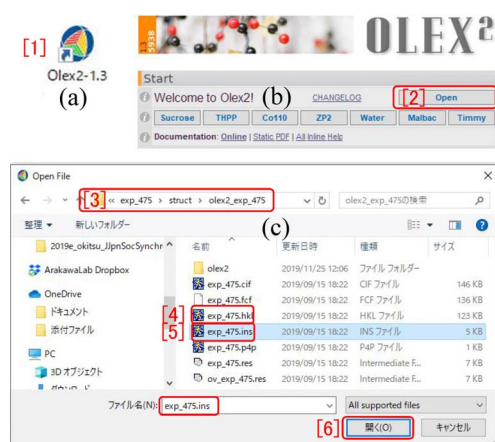


Figure 2.1: Startup of OLEX² and opening files

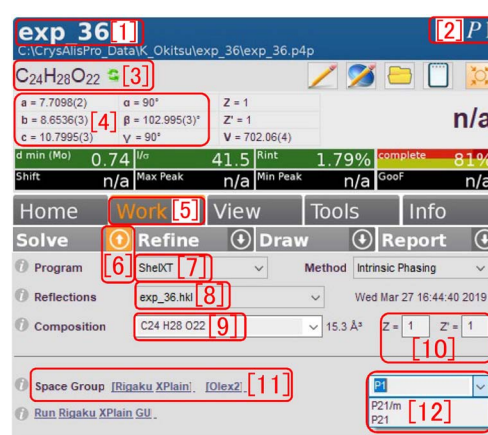


Figure 2.2: Setting of options for Solve

2.1 Startup of the OLEX² and opening the project

By double-clicking ‘[1]’ icon in 2.1 (a), CrysAlis^{Pro} can be started as shown in Fig. 2.1 (b). Fig. 2.1 (c) where the file explorer is displayed, can be opened by clicking ‘[2] Open’ in Fig. 2.1 (b). Here, the folder of ‘[3]’ in which ‘[4] *.hkl’ and ‘[5] *.ins’ exist, should be opened by clicking ‘[6] Open(O)’ with ‘[5] *.ins’ clicked to select it. With this procedure, the files can be loaded.

2.2 Determination of the initial phases with the direct method

In Fig. 2.2, options to determine the initial phases with the direct method have been set.

‘exp_36 [1]’ is the name of the project. ‘[2] P1’ is the default space group that has the lowest symmetry that is the triclinic system without symmetric center. ‘C₂₄H₂₈O₂₂ [3]’ is the formula of molecule in a single unit cell, where the number of hydrogen is wrong. ‘[4]’ are lattice constants that are almost correct.

After clicking ‘Work [5]’, options ‘[7]-[12]’ for ‘Solve’ can be opened by clicking ‘↓ [6]’ on the right of ‘Solve’. The most recommended program ‘ShelXT [7]’ for phase determination has been selected from the pull-down menu. ‘exp_36.hkl [8]’ is the file that has the X-ray diffraction intensities. ‘C₂₄H₂₈O₂₂ [9]’ is the molecular formula that is the same as ‘[3]’. Since there is no symmetric element in the case of ‘[2] P1’, the number of molecule in a symmetric element Z' is the same as the number of molecule in a unit cell Z . By clicking ‘Olex2 [11]’, ‘P21/m’ and ‘P21’ are added as candidates

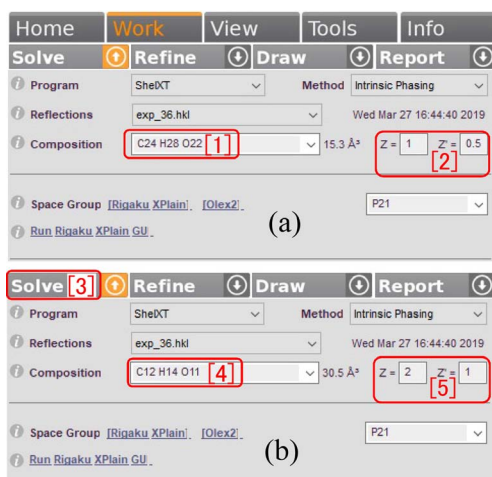


Figure 2.3: Change of the molecular formula

of the space group to the pull-down menu of ‘Space Group [12]’.

With regard to the space groups, refer to Appendix B [p.34], please.

In Fig. 2.3 (a), the molecular formula is ‘C₂₄H₂₈O₂₂ [1]’. In Fig. 2.3 (b), however, the molecular formula and Z' have been changed to be ‘C₁₂H₁₄O₁₁ [4]’ and ‘ $Z' = 1$ ’, respectively, by typing such that ‘ $Z = 2$ ’. Here, in Fig. 2.3 (b), ‘Solve [3]’ can be clicked for obtaining the initial phases to display the molecular model as shown in Fig. 2.4 (b). When a too large molecular model is displayed, click ‘[1]’ on the upper right of Fig. 2.5 (a), please to display the model with a proper size.

The molecular structure in Fig. 2.4 (b) has been obtained by determining the initial phases with ‘[1] ShelXT’ in Fig. 2.4 (a). The number of hydrogen in ‘C₁₂ H₁₄ O₁₁ [2]’ is not correct, yet.

2.3 Concerning the direct method and ‘SHELX’

There is a difficulty in the crystal structure analysis that the phase angles of the crystal structure factor cannot be directly measured while their absolute values can be measured. This difficulty is called the phase problem. The direct method was developed by Hauptman (Herbert Aaron Hauptman; 1917/2/14-2011/10/23) and Karle (Jerome Karle; 1918/6/18-2013/6/6) from 1950’s. The

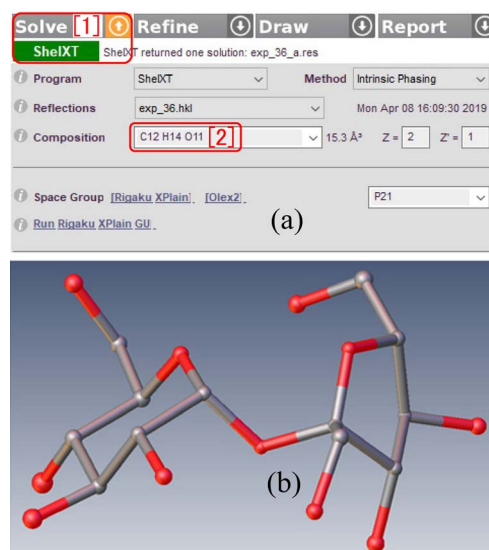


Figure 2.4: Molecular structure with the initial phases determined.

direct method is a purely mathematical method to determine the phases of the crystal structure factors based on the evident fact the electron density in the unit cell is a positive real function. It was rapidly wide-spread after Karle’s wife (Isabella Karle; 1921/12/2-2017/10/3) developed a computer program to solve the phase problem on the computer.

Hauptman and Karle were awarded the Nobel prize for chemistry in 1985 for this work.

SHELX is a series of programs to determine the initial phases with the direct method and refine the molecular structure that has been developed by Sheldrick of the University of Göttingen (George Michael Sheldrick; 1942/11/17-) from 1976. A feature article by Sheldrick titled ‘A short history of SHELX’ was published in *Acta Cryst.* **A64** (2008) 112-122. Due to the large number of citations of this article, IF (Impact Factor) of *Acta Cryst.* **A64** during 2009-2011 reached around 50, which gave a shock to the scientific community. This reveals the excellence of SHELX and also the important role of crystallography in the current chemistry and science.

Sheldrick was awarded the Ewald prize for this work in 2011.

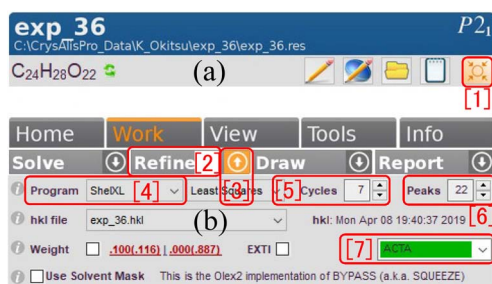


Figure 2.5: Molecular structure with initial phases determined

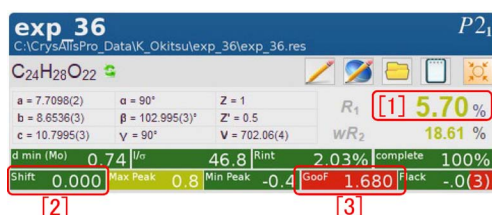


Figure 2.6: Result after clicking 'Refine' twice

2.4 Refinement of the structure by least-square fitting

Fig. 2.5 (b) shows the initial setting of the refinement of structure when starting it. Options '[4]-[7]' when clicking 'Refine [2]' have been opened by clicking '↓ [3]' on the right of 'Refine [2]'. 'ShelXL [4]' has been set (recommended) as the refinement program. Number of fitting done when clicking 'Refine [2]' has been set to be 7 in '[5]'. Number of peaks of electron density that are not assigned to atoms (Q peaks), has been set to be '22 [6]' (number of hydrogen). From the pull-down menu of '[7]', 'ACTA' has been selected (recommended).

The refinement should be done, first with isotropic temperature factors without hydrogens, secondly with anisotropic temperature factors without hydrogens, and finally with anisotropic temperature factors with hydrogens.

2.4.1 Refinement with isotropic temperature factors

Fig. 2.6 shows the result after clicking 'Refine [2]' twice with the settings of Fig. 2.5 (b). The R-factor has been estimated to be '[1] 5.70%'. 'Shift [2]' is 0.000 and green. However, 'Goof [3]

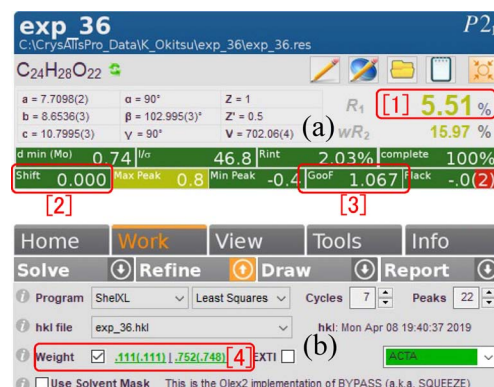


Figure 2.7: Result after further twice refinement with the weight optimized

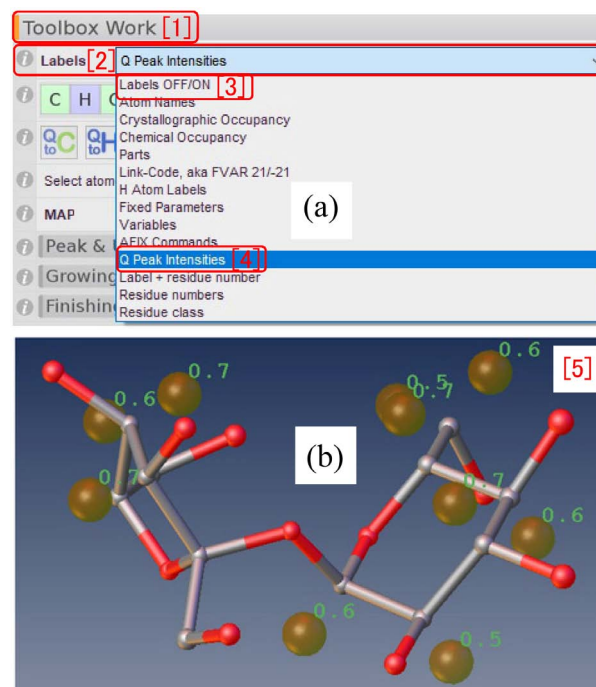


Figure 2.8: Electron density peaks not assigned to any atom (Q peak) and their intensity

[3]' (Goodness of fit) is 1.680 and red. These values estimate the soundness of least-square fitting. The ideal values of 'Shift [2]' and 'Goof [3]' are zero (0) and unity (1), respectively.

Fig. 2.7 (a) shows the result of refinement by typing [Ctrl]+[R] or clicking 'Refine [2]' in Fig. 2.5 (b) with 'Weight [4]' checked in Fig. 2.7 (b). The R-factor has decreased slightly to '[1] 5.51%'. Both 'Shift [2]' and 'Goof [3]' are green which shows that the structure has been refined soundly.

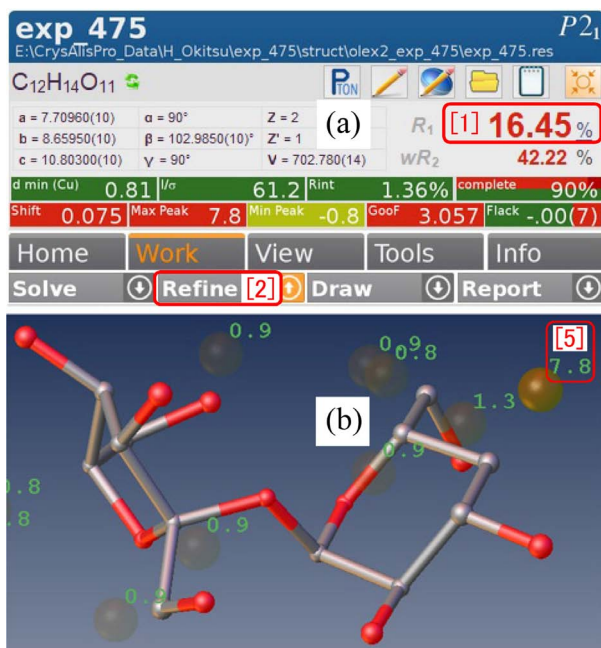


Figure 2.9: Refinement result with an oxygen atom deleted.

2.4.2 Displaying peaks of electron density that have not been assigned to atoms (Q peaks)

In Fig. 2.8 (b) [p.9], peaks of electron density that have not been assigned to any atom (Q peaks) have shown as brown spheres. In Fig. 2.8 (a) [p.9], the pull-down menu of ‘Labels [2]’ bellow ‘Toolbox Work [1]’ has been opened. ‘Q Peak Intensities [4]’ in Fig. 2.8 (a) [p.9] can be clicked to let the Q peak intensities be shown with green characters. The unit is [electrons/Å³]. ‘Q [14]’ in Fig. 2.10 (c) can be clicked to let the Q peaks be displayed, be displayed with bonds or not be displayed (as shown in Fig. 2.11).

After typing [Delete] key to delete the oxygen at ‘[5]’ on the upper right of Fig. 2.8 (b) [p.9], the structure can be reined by clicking ‘Refine [2]’ in Fig. 2.9 (a) or typing [Ctrl]+[R] to display a brown sphere (Q peak) at ‘[5]’ on the upper right of Fig. 2.9 (b). The Q peak intensity ‘7.8’ [electrons/Å³] is also displayed with green characters near here. The peak intensities of the Q peaks in Fig. 2.8 (b) [p.9] are 0.5 ~ 0.7. All of these correspond to hydrogens. After refining the structure with an atom deleted, what it was can be expected from the Q peak intensity.

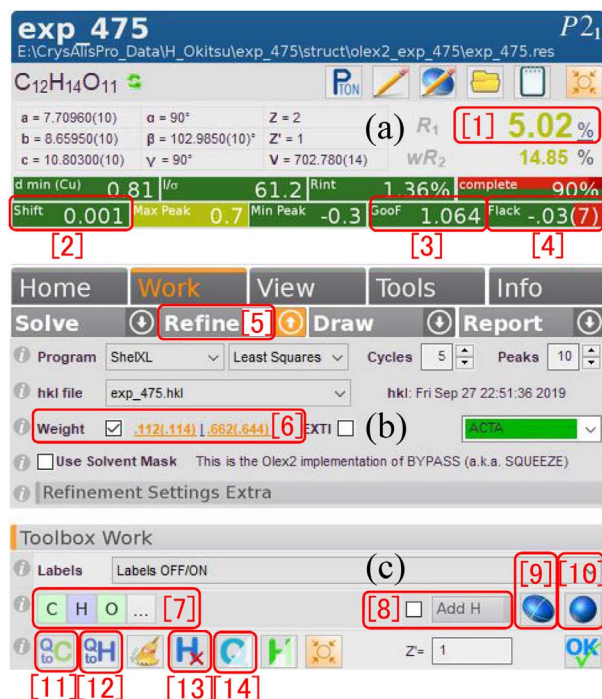


Figure 2.10: Result after further twice refinement with anisotropic temperature factors

The Q peak can be returned to be oxygen by clicking it after clicking ‘O’ of ‘C H O ... [7]’ in Fig. 2.10 (c) or by clicking ‘O’ of ‘C H O ... [7]’ after clicking the Q peak.

2.4.3 Refinement with anisotropic temperature factors

The blue elliptical mark of ‘[9]’ in Fig. 2.10 (c) can be clicked to refine the structure with anisotropic temperature factors. Fig. 2.12 should be displayed by right-clicking the background of the molecular model to click ‘Ellipses & sticks’ in it. By clicking ‘Refine [5]’ in Fig. 2.10 (b) or typing [Ctrl]+[R], the molecular model can be displayed as shown in Fig. 2.13.

In Fig. 2.10 (a), the R-factor has further decreased to ‘[1] 5.02%’ and both ‘Shift [2]’ and ‘Goof [3]’ are green, which means that the structure has soundly been refined. The Flack parameter is approximately 0.0 when the chirality is right but approximately 1.0 when the chirality is wrong. ‘Flack [4] -0.03(7)’ on the right lower of Fig. 2.10 (b) means that it has been estimated to be -0.03 ± 0.07 and then the chirality is right. However, ‘Weight .112(.114) |

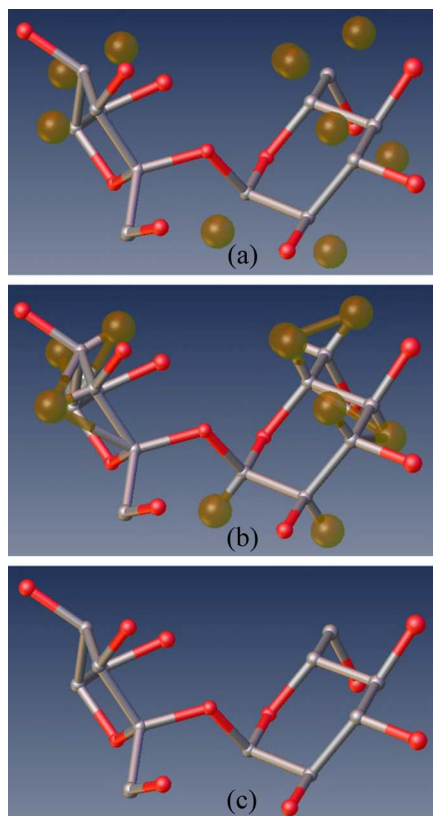


Figure 2.11: Switching the display mode of Q peaks

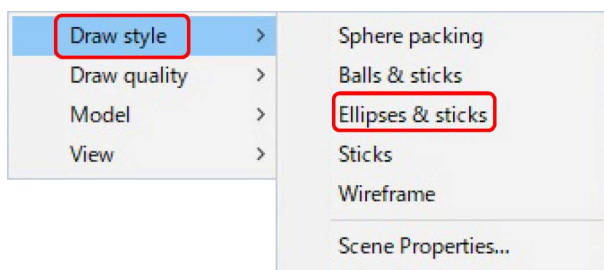


Figure 2.12: Setting of the ‘Thermal ellipsoid’ mode.

.662(.644) [6]’ is displayed with yellow characters. Then, it should be further optimized such that it is displayed with green characters.

2.4.4 Refinement with hydrogens assigned

2.4.4.1 Automatical assignment of hydrogens

Fig. 2.14 shows the molecular model refined with hydrogens automatically assigned by click-

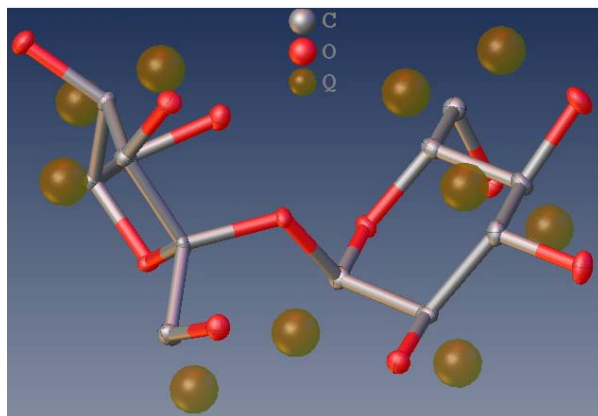


Figure 2.13: The molecular structure displayed with the ‘Thermal ellipsoid’ mode.

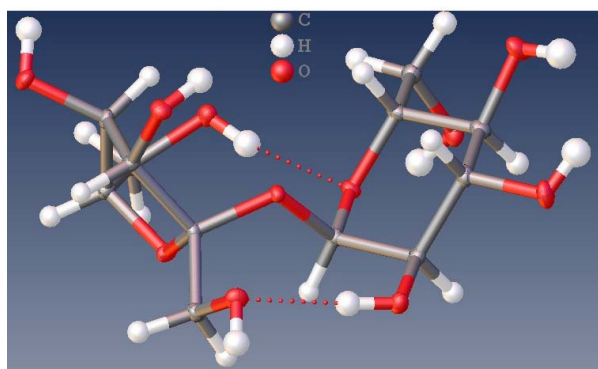


Figure 2.14: Molecular model with hydrogens automatically assigned.

ing ‘[8] Add H’ in Fig. 2.10 (c). When checked between ‘[8]’ and ‘Add H’ in Fig. 2.10 (c), the molecular structure is automatically refined only by clicking ‘[8] Add H’. This is also applied when ‘[9]’ or ‘[10]’ on the right of ‘[8] Add H’ is clicked. ‘H_x [13]’ in Fig. 2.10 (c) can be clicked to cancel the all assignments of hydrogens.

2.4.4.2 Assignment by replacing Q peaks with hydrogens

One molecule of sucrose has 22 hydrogen atoms. By setting ‘[9]’ in Fig. 2.16 (d) [p.12] such that 22 Q peaks are displayed after the refinement, the molecular structure is refined as shown in Fig. 2.15 (a) [p.12]. ‘Q to H [12]’ in Fig. 2.16 (e) [p.12] can be clicked to replace all Q peaks with hydrogens as shown in Fig. 2.15 (b) [p.12].

If ‘Weight ... [10]’ in Fig. 2.16 (d) [p.12] is

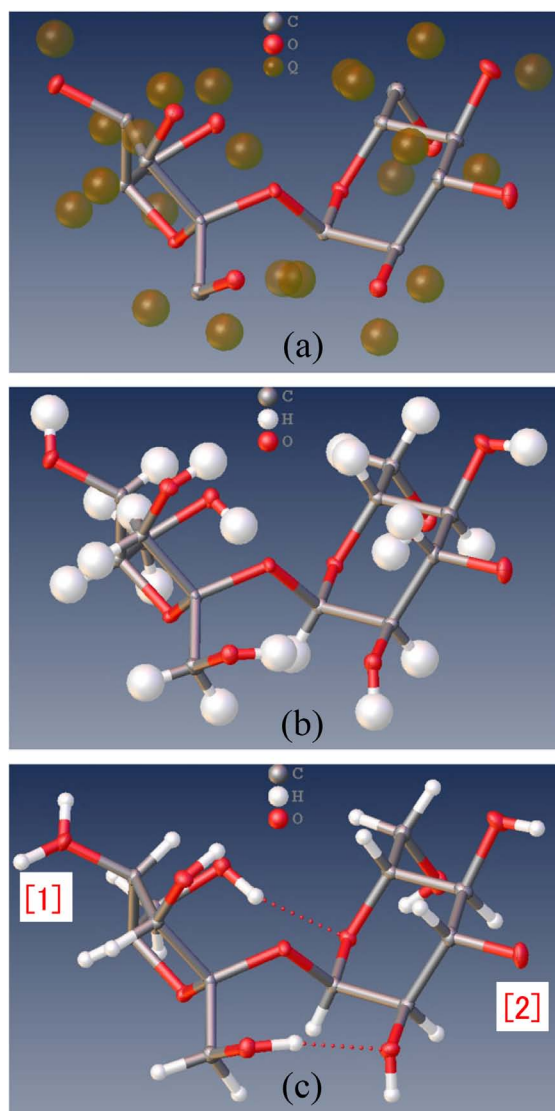


Figure 2.15: Q peaks have been replaced with hydrogens.

displayed with orange or red characters, the structure should be refined with ‘Weight [10]’ checked such that it is displayed with green characters as shown in Fig. 2.6 (d). The refinement can be repeated to show Fig. 2.15 (c). While hydroxy groups are considered to exist at positions of ‘[1]’ and ‘[2]’, there are two and no hydrogens at ‘[1]’ and ‘[2]’. After deleting two hydrogens at ‘[1]’ by typing [Delete] key, the molecular structure can be refined as shown in Fig. 2.16 (a).

After clicking Q peaks of ‘[1]’ and ‘[2]’ to select them, they can be changed to hydrogens by clicking ‘H’ of ‘C H O ... [11]’ in Fig. 2.16 (e). The structure can be refined as shown in Fig.

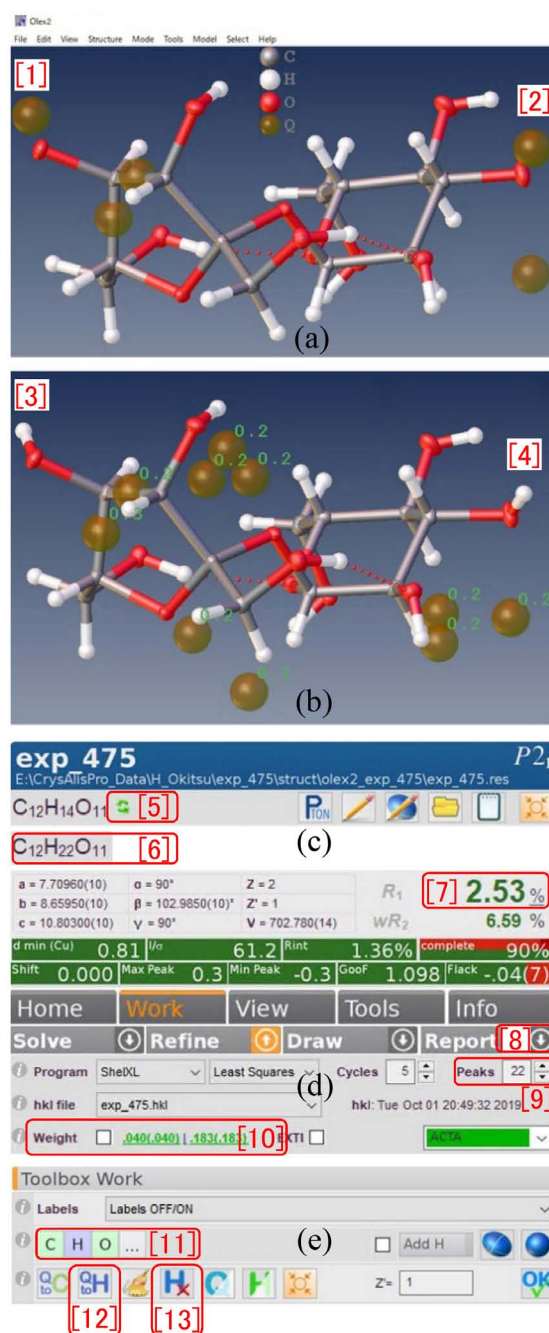


Figure 2.16: The refined structure with hydrogens of hydroxy groups assigned.

2.16 (b). In Fig. 2.16 (c), the R-factor has decreased to ‘[7] 2.53%’. Here, ‘[5]’ can be clicked to such as to display the correct molecular formula as ‘C₁₂H₂₂O₁₁[6]’. Fig. 2.16 (b) shows the final molecular structure of sucrose since all intensities of Q peaks are extremely small values around 0.2 [electrons/Å³].

There is conflicting information!
Some of your files contain conflicting information regarding information that should go into your cif file.
Please select the correct values by clicking on the links below.

	exp_475.cif	exp_475.p4p	exp_475.cif od	User value
diffn_radiation_type Unapplicable (.) Unknown (?)	CuK α	---	Cu K α [1]	? Use
diffn_measured_fraction_theta_max Unapplicable (.) Unknown (?)	0.975	---	0.8636 [2]	? Use
diffn_measured_fraction_theta_full Unapplicable (.) Unknown (?)	0.999	---	1.0000 [3]	? Use

Figure 2.17: The window displayed just after clicking ‘[8] ↓’ in Fig. 2.16 (d).

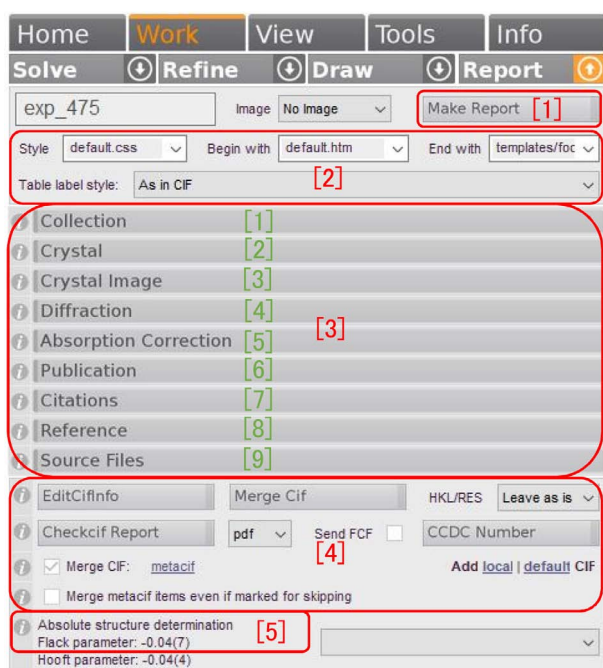


Figure 2.18: Setting window of report.

2.4.4.3 Manual assignment of hydrogens

Hydrogens can also be manually assigned. Refer to the description in §3.8 [p.25], please.

2.5 Creation of the report

‘[8] ↓’ on the right of ‘Report’ in Fig. 2.16 (d) can be clicked to show the window of Fig. 2.17. ‘CuK α [1]’, ‘0.8636 [2]’ and ‘1.0000 [3]’ displayed with green characters, can be clicked to display Fig. 2.18. ‘Make Report [1]’ on the upper right of Fig. 2.18 can be clicked to create the report of html, later. The items in the red frames of ‘[2]’ and ‘[4]’ in Fig. 2.18 should be set as this. In the red frame of ‘Absolute structure determination

Figure 2.19: Setting window of ‘Report’

Figure 2.20: Setting window of ‘Report’

‘[5]’, the Flack parameter has been estimated to be $-0.04(\pm 0.07)$, which means that the chirality of the molecular structure is right.

‘Collection [1]’-‘Source Files [9]’ can be clicked to set parameters of them, which is described in the following subsections.

2.5.1 Settings of ‘Collection’

Fig. 2.20 has been displayed by clicking ‘Collection [1]’ on the upper left of this figure. The text box of ‘Submitter’ in Fig. 2.20 can be clicked to

Sites

The University of Tokyo [School of Business Administration] (a)

The University of Tokyo [School of Business Administration] (b)

Figure 2.21: Choice of the first author’s affiliation

Person details

First Name: Jiro

Middle Name:

Last Name: Todai

Email: jiro-todai@yahoo.co.jp

ORCID Id:

Phone: +81-3-5840-7472

[1]

Update [2] Add as new Delete

[3] OK

Figure 2.24: Typing the second author’s name and address

Person details

First Name: Kouhei

Middle Name:

Last Name: Okitsu

Email: yrt01404yrt@yahoo.co.jp

ORCID Id:

Phone: +81-3-5841-7470

[1]

Update [2] Add as new Delete

[3] OK

Figure 2.22: Typing the first author’s name and address

People

Okitsu, K.
Todai, J.

Figure 2.25: The first and second authors’ name

People

Okitsu, K.

Figure 2.23: The first author’s name

Site details

Institution Name: Nakasu Business University

Name of Department: School of Business

Address: 880-22-5 Nakasu

City: Hakata

Post Code: 810-0880

Country: Japan

[1]

Update [2] Add as new Delete

Figure 2.26: Addition of the third author’s affiliation

display Fig. 2.19 [p.13].

After typing the first author’s affiliation in Fig. 2.19 (b) [p.13], ‘Add as new [1]’ can be clicked to type his (her) name and address in Fig. 2.19 (d) [p.13] as shown in ‘[1]’ of Fig. 2.22. His (her) name as in Fig. 2.23 is displayed in the field of (c) in Fig. 2.19 [p.13]. When the number of the author is one, ‘[2] Add as new’ and then ‘[3] OK’ should be clicked in Fig. 2.22 to finish.

To add the second author whose affiliation is the same as the first author, at first, the affiliation of the first author should be clicked as shown in Fig. 2.21 (b) in the field of (a) in Fig. 2.19 [p.13]. Here, the second author’s name and address should be typed as shown in Fig. 2.24 ‘[1]’. Then, ‘[2] Add as new’ should be clicked such that Fig. 2.25 is displayed in (c) of Fig.

2.19 [p.13]. When the number of author is two, ‘[3] OK’ in Fig. 2.24 should be clicked to finish.

To add the third author whose affiliation is different, at first, his (her) affiliation should be typed in (b) of Fig. 2.19 [p.13] as shown in Fig. 2.26 ‘[1]’. Then, ‘[2] Add as new’ should be clicked such as to display it in (a) of Fig. 2.19 (a) [p.13]. It can be clicked to display Fig. 2.27 (b) such that the third author’s name and address can be typed as shown in Fig. 2.28 ‘[1]’. Here, ‘[2] Add as new’ can be clicked such as to display Fig. 2.29 in (c) of Fig. 2.19 [p.13]. Then, ‘[3] OK’ in Fig. 2.28 can be clicked to finish the

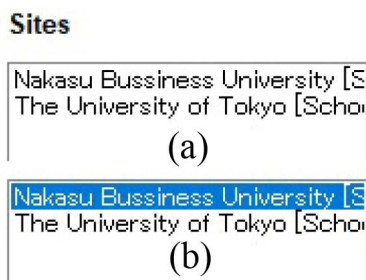


Figure 2.27: Selection of the affiliation of the third author.

Person details

First Name

Middle Name

Last Name [1]

Email

ORCID Id

Phone

Update Delete

Figure 2.28: Typing the third author's name and address.

People

Figure 2.29: The third author's name

creation of the authors list.

'[1] Submitter' in Fig. 2.30 (a) can be clicked to open the authors list as shown in Fig. 2.19 [p.13]. In (a) of Fig. 2.19 [p.13], at first, the affiliation should be clicked as shown in Fig. 2.30 (b). Then, the submitting author can be clicked as shown in Fig. 2.30 (c).

After clicking 'Operator [2]', the operator can also be set with a similar procedure as above.

From the pull-down menus of 'Submitted [3]', 'Collected [4]' and 'Completed [5]' on the bottom of Fig. 2.30 (f), the dates can be selected. Now, all items of 'Collection [1]' on the upper left of Fig. 2.20 [p.13] have been set.

Figure 2.30: Selections of 'Submitter' and 'Operator'.

Figure 2.31: Selection or typing of crystal information.

2.5.2 Settings of 'Crystal'

Fig. 2.31 has been opened by clicking 'Crystal [2]' on the upper left of it. Here information concerning the crystal can be selected or typed. If inputted on the CrysAlis^{Pro}, it has already been set. Even if not, at least, 'Colour [1]' and 'Size & Shape [2]' should be selected or typed.

2.5.3 Settings of 'Crystal Image'

Fig. 2.32 [p.16] has been opened by clicking 'Crystal Image [3]' on the upper left of it. Here, '>' can be clicked to reproduce the optical images of the crystal continuously.



Figure 2.32: Selection or typing of crystal information.

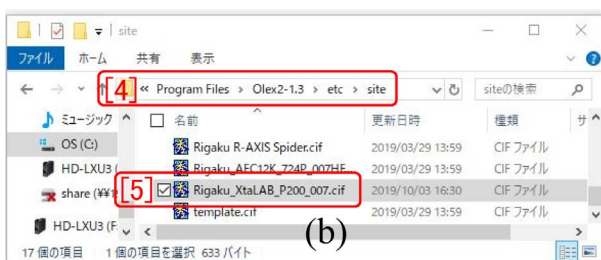
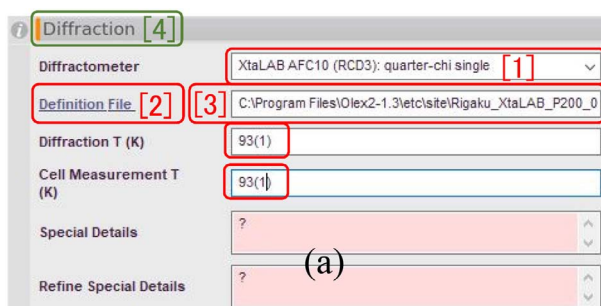


Figure 2.33: Setting of the parameter file

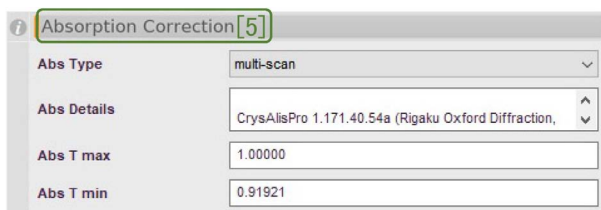


Figure 2.34: Information about the absorption correction.

2.5.4 Settings of ‘Diffraction’

Fig. 2.33 has been displayed by clicking ‘Diffraction [4]’ on the upper left of it. Here, ‘Definition file [2]’ can be clicked to display the file explorer as shown in Fig. 2.33 (b). In Fig. 2.33 (b), ‘[5] Rigaku_XtaLAB_P200_007.cif’ in the folder of ‘[4] Program Files\Olex2-1.3\etc\site’, should be clicked to load it as shown in Fig. 2.33 (a)



Figure 2.35: List of the authors and title of the journal

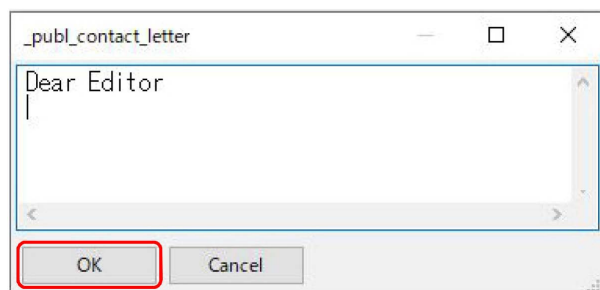


Figure 2.36: Cover letter to the editor.

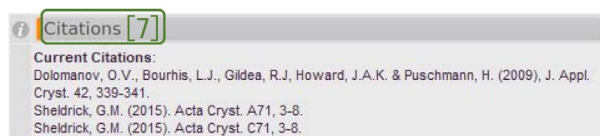


Figure 2.37: Articles that should be cited.

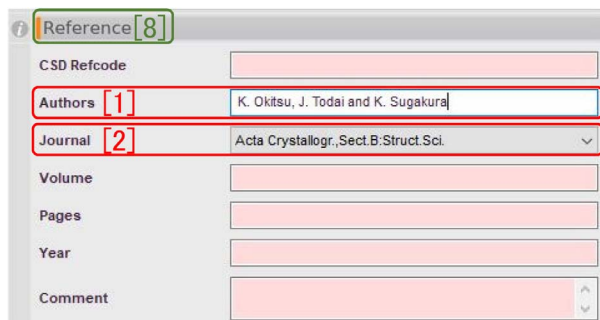


Figure 2.38: Information concerning the submitted article

‘[3]’. Then, the pull-down menu of ‘[1]’ can be found as shown in Fig. 2.33 (a).



Figure 2.39: Information concerning the the source file

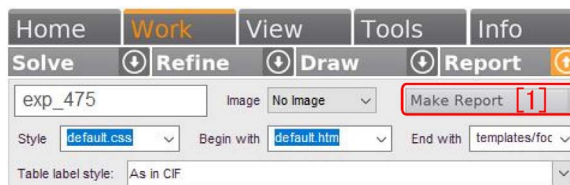


Figure 2.40: Creation of the report

There is conflicting information!
Some of your files contain conflicting information regarding information that should go into your cif file. Please select the correct values by clicking on the links below.

	exp_475.cif	exp_475.p4p	Rigaku_XtaLAB_P200_007.cif	exp_475_acta.cif	exp_475.cif_od	New User Value
computing structure solution	ShelXTL 2018/2 (Sheldrick, 2015)			Sheldrick, 2015		Use
diffn_detector_area_resol_mean	5.8140		5.811		5.8140	Use
diffn_radiation_monochromator	mirror		multi-layer mirror optics		mirror	Use
diffn_detector	CCD plate		FLATUS 200K area detector		CCD plate	Use
diffn_measurement_device_type	XtaLAB AFC10 (BCCD) quarter-circle		Rigaku XtaLAB P200		XtaLAB AFC10 (BCCD) quarter-circle	Use
diffn_source_type	Rigaku (Cu) X-ray DW Source		micromax007		Rigaku (Cu) X-ray DW Source	Use
diffn_source	Rotating-anode X-ray tube (Cu) wavelength		rotating-anode X-ray generator		Rotating-anode X-ray tube (Cu) wavelength	Use
computing publication material	Olex2 1.3 (Dolomanov et al., 2009)			Olex2 1.3 (Dolomanov et al., 2009)		Use
publ_section_references	Dolomanov, O.V., Bourhis, L.J., Gildea, P.J., Howard, J.A.K., Puschmann, H. (2009), J. Appl. Cryst. 42, 339–341; Sheldrick, G.M. (2015), Acta Cryst. A71, 3–8; Sheldrick, G.M. (2015), Acta Cryst. C71, 3–8			Sheldrick, 2015; Sheldrick, G.M. (2015), Acta Cryst. A71, 3–8; Sheldrick, G.M. (2015), Acta Cryst. C71, 3–8; Dolomanov, O.V., Bourhis, L.J., Gildea, P.J., Howard, J.A.K. and Puschmann, H. (2009), J. Appl. Cryst. 42, 339–341		[1] Use
computing molecular graphics	Olex2 1.3 (Dolomanov et al., 2009)			Olex2 1.3 (Dolomanov et al., 2009)		Use
computing structure refinement	ShelXL 2018/3 (Sheldrick, 2015)			Sheldrick, 2015		Use

Figure 2.41: Conflicting information

2.5.5 Settings of ‘Absorption Correction’

Fig. 2.34 has been opened by clicking ‘Absorption Correction [5]’ on the upper left of it. In the CrysAlis^{Pro}, empirical correction is necessarily applied to taking into account the absorption effect based on the expected crystal shape from the comparison of X-ray intensities of equivalent reflections. Information concerning the absorption correction is described in Fig. 2.34. If the absorption correction has been performed based on the measured crystal shape, information concerning this method is also described.

2.5.6 Settings of ‘Publication’

Fig. 2.35 has been displayed by clicking ‘Publication [6]’ on the upper left of it. In ‘[2]’ of Fig. 2.35, three author’s names are listed. They have

been inputted in Figs. 2.19 [p.13]-2.29 [p.15]. The ‘Contact Author [1]’ can be selected from the pull-down menu in Fig. 2.35. The order of the authors can be changed by clicking the arrow of ‘[2]’ in Fig. 2.35. ‘Add Author [3]’ can be clicked to add another author into the list. ‘Requested Journal [4]’ can be selected from the pull-down menu. ‘Journal Style [5]’ can also be selected from the pull-down menu. ‘Contact Letter [6]’ in Fig. 2.35 can be clicked to show Fig. 2.36 in which a contact letter to the editor can be typed. ‘OK’ on the lower left of it can be clicked to finish.

2.5.7 Settings of ‘Citations’

Fig. 2.37 has been opened by clicking ‘Citations [7]’ on the upper left of it. These three articles should necessarily be cited when the OLEX² and the ShelX have been used.

2.5.8 Setting of ‘Reference’

Fig. 2.38 [p.16] has been displayed by clicking ‘Reference [8]’ on the upper left of it. In ‘Authors [1]’, the authors that have been set in Fig. 2.35 [p.16] are listed. ‘Journal [2]’ can be selected from the pull-down menu.

2.5.9 Settings of ‘Source Files’

Fig. 2.39 [p.17] has been opened by clicking ‘Source Files [9]’ on the upper left of it. Here, information concerning the source files is described.

2.5.10 Creation of the final report

‘Make Report [1]’ on the right of Fig. 2.40 [p.17] can be clicked to let Fig. 2.41 [p.17] be displayed. ‘Use’ on the right of Fig. 2.41 [p.17] can be clicked to open the browser on which Fig. 2.42 is opened. In this file, the space group, the lattice parameters, the crystal size and all other information concerning the crystal are described.

exp_475

Table 1 Crystal data and structure refinement for exp_475.

Identification code	exp_475
Empirical formula	C ₁₂ H ₁₄ O ₁₁
Formula weight	334.23
Temperature/K	93(1)
Crystal system	monoclinic
Space group	P2 ₁
a/Å	7.70960(10)
b/Å	8.65950(10)
c/Å	10.80300(10)
α/°	90
β/°	102.9850(10)
γ/°	90
Volume/Å ³	702.780(14)
Z	2
ρ _{calc} /cm ³	1.579
μ/mm ⁻¹	1.261
F(000)	348.0
Crystal size/mm ³	0.24 × 0.22 × 0.2
Radiation	Cu Kα (λ = 1.54184)
2θ range for data collection/°	8.4 to 144.526

Figure 2.42: Final information concerning the crystal

To be continued

Chapter 3

Example of structure determination with the OLEX² (α -cyclodextrin)

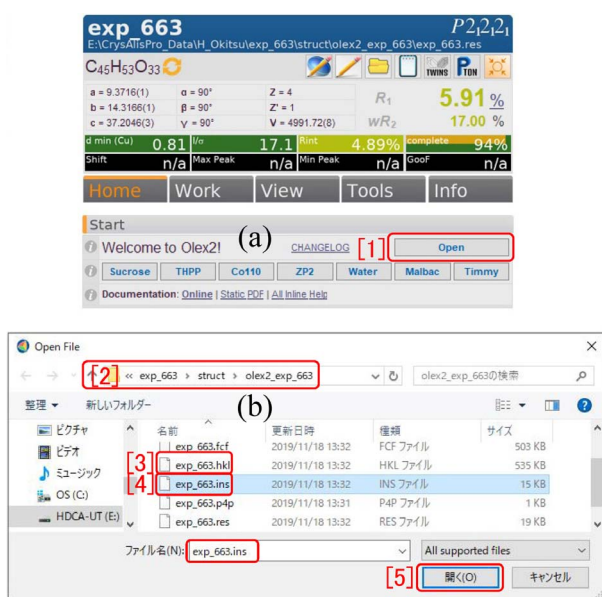


Figure 3.1: Loading the file

3.1 Opening the project

[1] Open' on the lower right of Fig. 3.1 (a) can be clicked to let Fig. 3.1 (b) be shown. In the folder of project '[2] ... exp_663\struct\olex2_exp_663', in Fig. 3.1 (b), '[3] exp_663.hkl' and '[4] exp_663.ins' are found. After selecting '[4] exp_663.ins', '[5] Open(O)' on the lower right should be clicked. Fig. 3.2 shows the molecular structure automatically determined by 'AutoChem' in the OLEX². By typing [Ctrl]+[T], this window can be changed such as to display only the text as shown in Fig. 3.3 (a). By typing [Ctrl]+[T] again, Fig. 3.3 (a) can be changed such as to display only the molecular model as shown in Fig. 3.3 (b). By

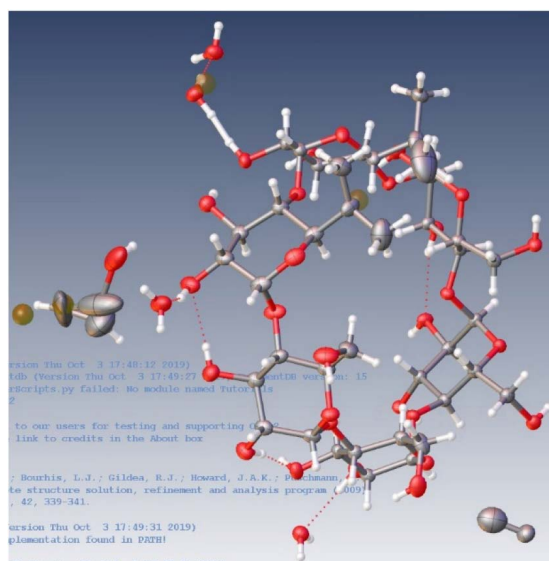


Figure 3.2: Molecular structure automatically determined by the AutoChem.

typing [Ctrl]+[T] once more, both the molecular model and the text can be displayed as shown in Fig. 3.2, which is recommended.

3.2 Determination of the initial phases

In Fig. 3.4 (b), 'Work [1]' and then '↓ [2]' on the right of 'Solve [3]' can be clicked to display 'Solve' options. 'ShelXT [4]' is recommended to select from the pull-down menu since this is recognized to be the most excellent as the phase determination program. 'Solve [3]' can be clicked to start the initial phase determination. It is time consuming due to the large size of the

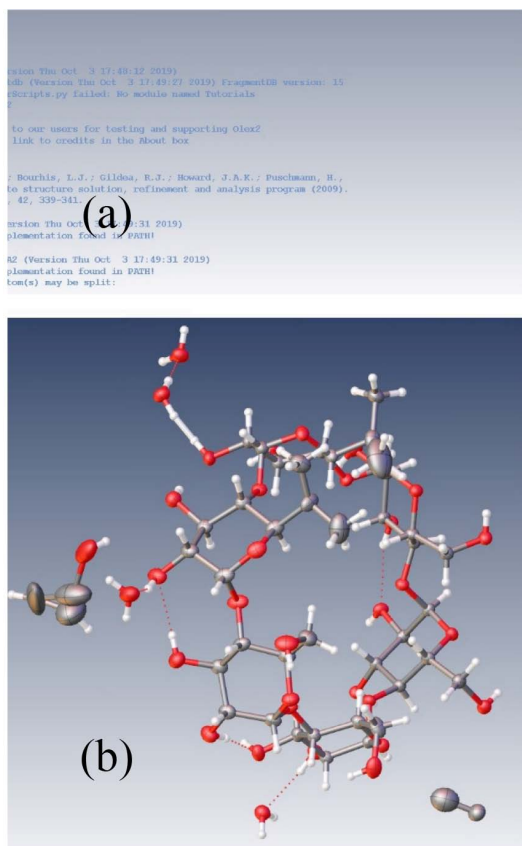


Figure 3.3: [Ctrl]+[T] can be typed to display these windows.

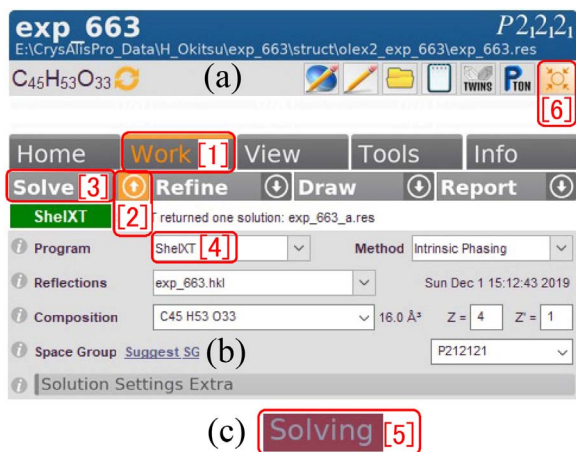


Figure 3.4: Settings for determination of the initial phases.

molecule to determine the initial phases. Then, ‘Solving [5]’ as shown in Fig. 3.4 (c) is displayed for one minute or so on the upper right corner of the molecular model display region.

At first, the initial structure model of the

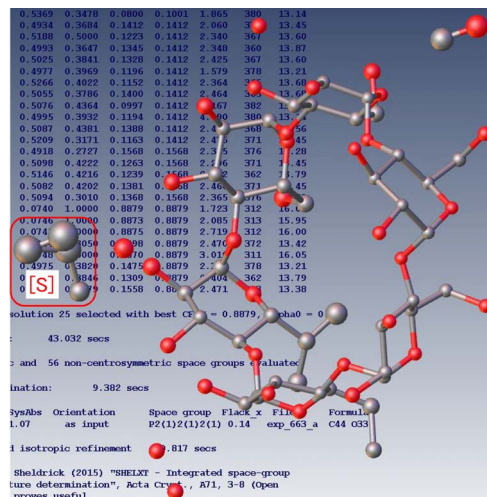


Figure 3.5: Initial structure obtained by the phase determination

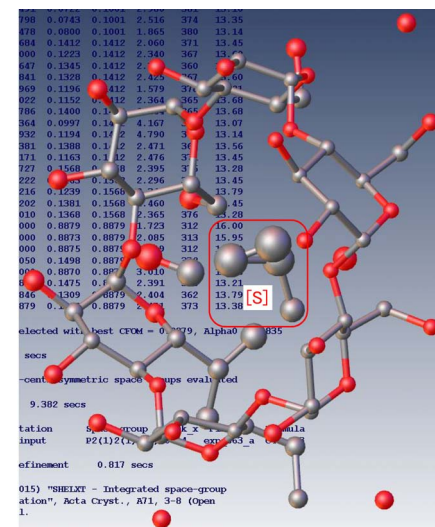


Figure 3.6: solvent molecule moved by symmetrical operation

molecule is displayed as shown in Fig. 3.5. By clicking ‘[6]’ on the right of Fig. 3.4 (a), ‘Solvent molecule [S]’ on the left of Fig. 3.5 can be moved to inside the ring as shown in Fig. 3.6. While only one molecule of the solvent is displayed following the rule that just one symmetric unit is displayed, the solvent molecules exist both inside and outside of the ring.

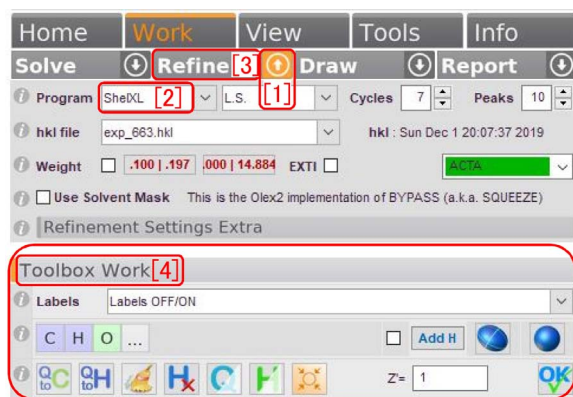


Figure 3.7: Starting the optimization of the molecular structure

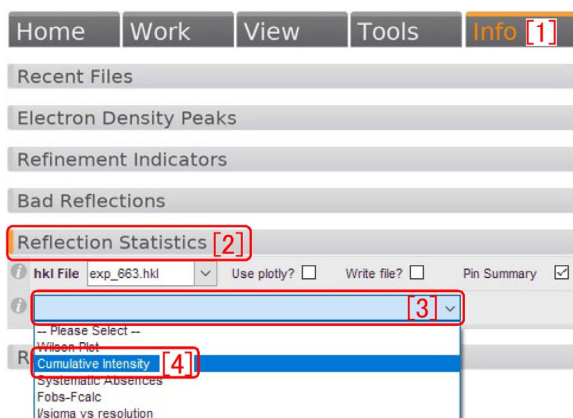


Figure 3.8: Checking the existence of symmetric center

3.3 The optimization of the molecular structure

Fig. 3.7 shows the initial window to start the optimization of the molecular structure.

At first, '↓ [1]' can be clicked to set the options for optimization.

After selecting 'ShelXL [2]' which is recommended, the optimization can be repeated by clicking 'Refine [3]' or typing [Ctrl]+[R]. Here, tools in 'Toolbox Work [4]' can be used.

As described in chapter 2 [p.7], the optimization of the molecular structure should be done in the order of optimization with isotropic temperature factors without hydrogen, that with anisotropic temperature factors without hydrogen and that with anisotropic temperature factors and hydrogen atoms.

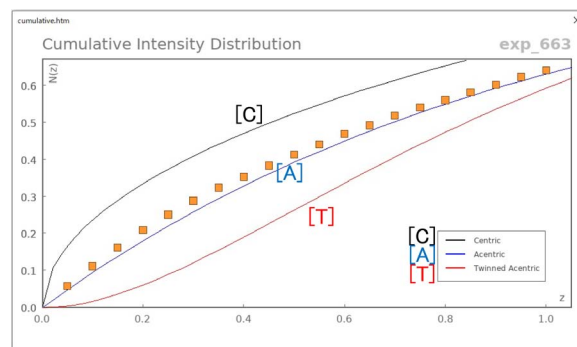


Figure 3.9: Checking the existence of symmetric center



Figure 3.10: Anomalous intensity of Maximum Peak

In the following sections, items that have not been described in chapter 2 are described.

3.4 Checking the existence of symmetric center

After finishing the optimization of the molecular structure, 'Info [1]' on the upper right of Fig. 3.8 should be clicked. After opening 'Reflection Statistics [2]' in Fig. 3.8, 'Cumulative Intensity [4]' should be selected from the pull-down menu of '[3]' to display Fig. 3.9. Here, three curves '[C] Centric', '[A] Acentric' and '[T] Twinned Acentric' correspond to crystals with symmetric center, those without symmetric center and twinned crystals without symmetric center, respectively. It can be found that the crystal whose structure to be solved does not have symmetric center since square marks are plotted in the vicinity of '[A] Acentric'. This is reasonable since the space group $P2_12_12_1$ (orthorhombic #19) displayed on the upper right of Fig. 3.4 (a) [p.21] does not have symmetric center and α -cyclodextrin has a chiral molecular structure.

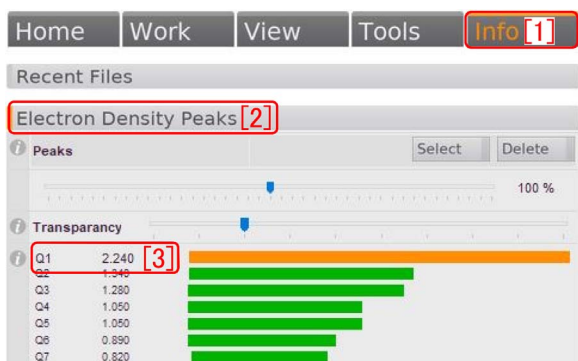


Figure 3.11: Anomalous intensity of Maximum Peak

3.5 Consideration on the intensities of Q peaks

‘MaxPeaks 2.2 [1]’ in Fig. 3.10 is a warning that the maximum intensity of Q peak 2.2 [electrons/Å³] which is a peak of electron density not assigned to any atom, is too large. In Fig. 3.11, ‘Info [1]’ and then ‘Electron Density Peaks [2]’ have been clicked to open. The intensities of Q peaks are displayed on a bar chart. ‘Q1 2.240 [3]’ on the left of the yellow bar is also a warning that the maximum intensity (2.240 [electrons/Å³]) of Q peak is too large.

In Fig. 3.12 showing the molecular model, number of Q peaks displayed can be decreased by scrolling the mouse wheel to the near direction as shown in Figs. 3.12 (a), 3.12 (b) and 3.12 (c). In Fig. 3.12 (c), only one Q peak is found which is nothing but the largest electron density peak as shown in Figs. 3.10 and 3.11.

The molecule of α -cyclodextrin is a molecule of cyclic oligosaccharide that consists of glucoses linked with glycosidic bonds. Therefore, Q peaks labelled with C, C, Q and C in Fig. 3.12 (c) are actually disordered oxygen atoms. When attention is focused on Q and C on the rightmost of Fig. 3.12 (c), oxygen atoms exist at either of these sites with an occupancy ratio of approximately 1 : 1. The situation is similar to the above case also for the first and second leftmost C. In the following section, the procedure to separate these disordered oxygens is described.

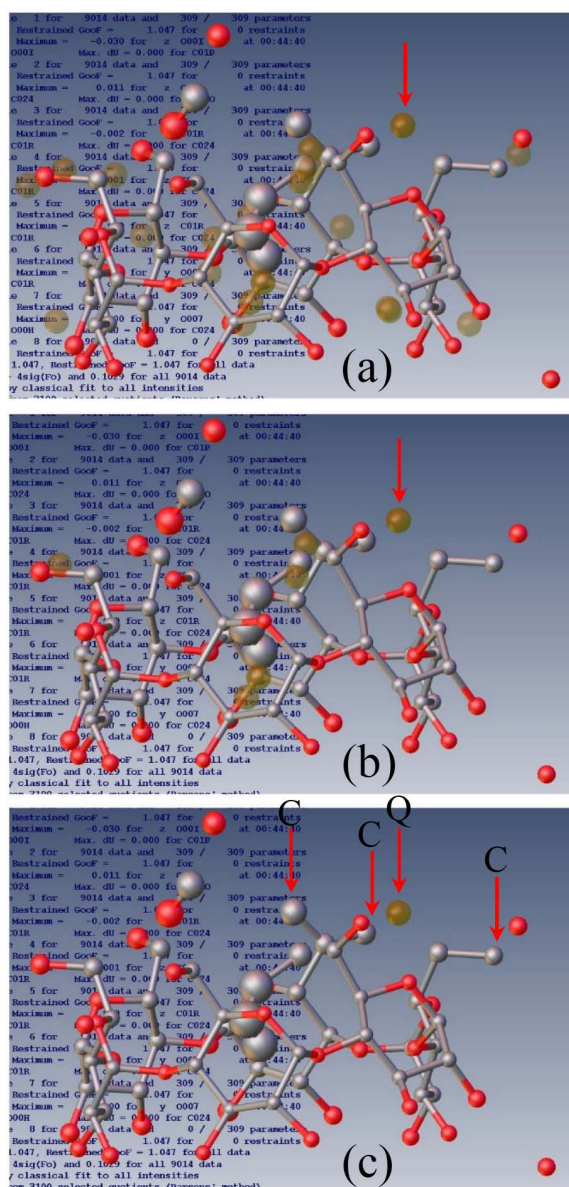


Figure 3.12: Changing the number of displayed Q peaks.

3.6 Separation of disordered atoms

After three carbons indicated with red arrows in Fig. 3.12 (c) are deleted or replaced to oxygens, the molecular structure can be refined by typing [Ctrl]+[R] or clicking ‘Refine [3]’ in Fig. 3.7 as shown in Fig. 3.13 [p.24].

The procedure to separate a pair of Q peak and oxygen on the right of Fig. 3.13 [p.24] into oxygens disordered at two sites, is described referring Figs. 3.14-3.16 [p.24] as follows. At

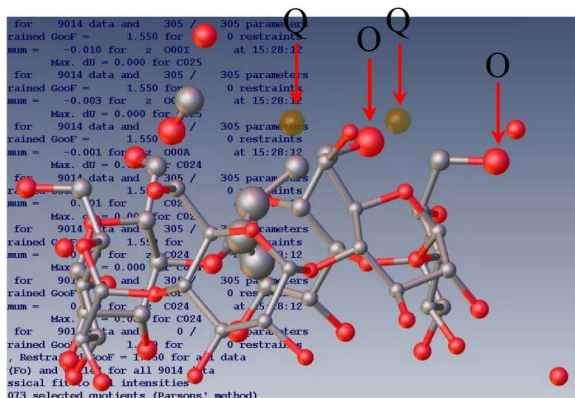


Figure 3.13: Refined with oxygen replaced from carbon.

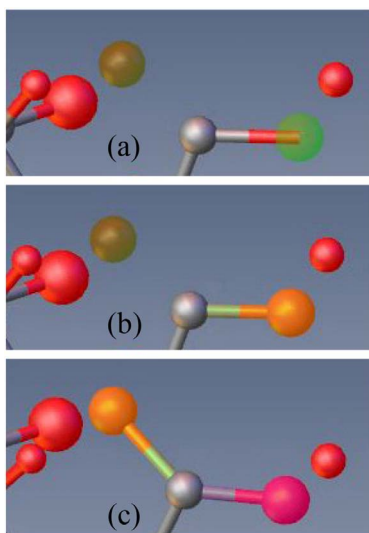


Figure 3.14: The oxygen is dragged to Q peak with [Shift] key pressed.

first, the oxygen atom should be clicked to let it be displayed as a green sphere as shown in Fig. 3.14 (a). Next, in Fig. 3.15, ‘Tools [1]’, ‘Disorder [2]’ and then ‘[3] mSplit’ should be clicked such that an orange band is displayed on the bottom of Fig. 3.15. Further, the orange sphere as shown in Fig. 3.14 (b) should be click&dragged to the position of Q peak with [Shift] key pressed as shown in Fig. 3.14 (c). The positions of the orange sphere and the Q peak should three-dimensionally coincide with each other. The molecular model should be rotated by click&dragging it without [Shift] key pressed such that the positions of the orange sphere and the Q peak can be adjusted also in

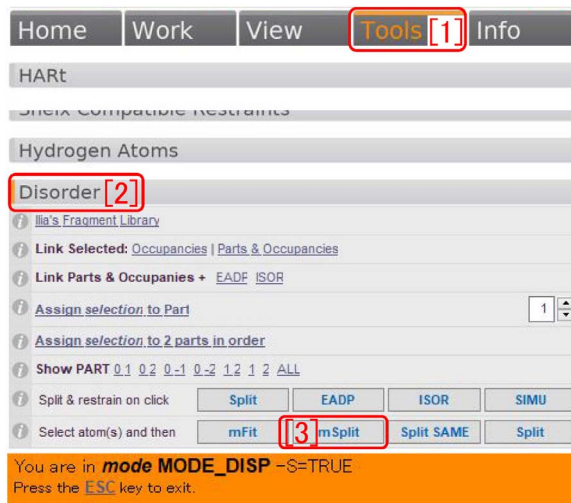


Figure 3.15: Starting to separate the disordered oxygens

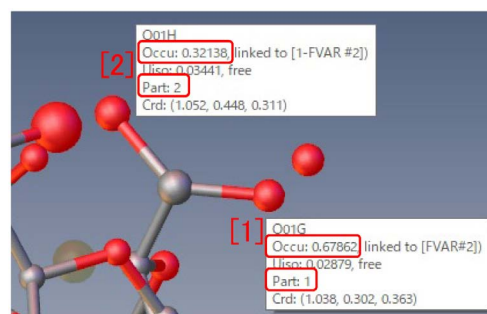


Figure 3.16: The disordered oxygen separated to two sites

the depth direction of Fig. Fig. 3.14 (c). [Esc] key can be clicked to escape from the peak separation mode.

The molecular structure with the disordered oxygen separated can be refined by typing [Ctrl]+[R] or clicking ‘Refine [3]’ in Fig. 3.7 [p.22] as shown in Fig. 3.16. By placing the mouse cursor on the oxygens at ‘[1]’ and ‘[2]’, labels can be displayed for several seconds around there. The labels show the occupancies of oxygen at sites [1] and [2] are 0.67862 and 0.32138, respectively.

The similar procedure can be applied to separating the pair of Q peak and oxygen at upper central part of Fig. 3.13

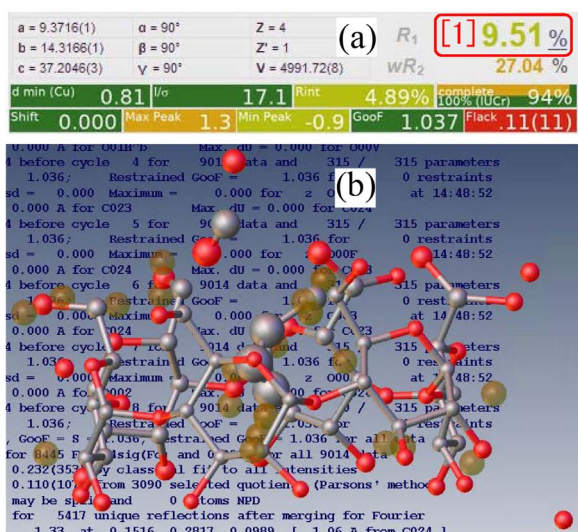


Figure 3.17: Refined result with isotropic temperature factors

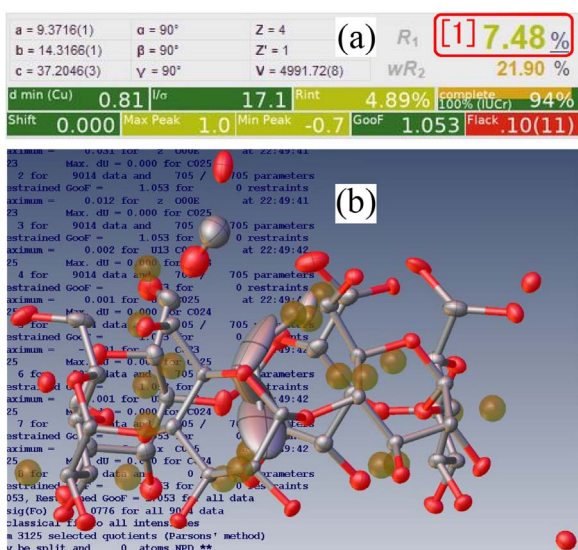


Figure 3.18: Refined result with anisotropic temperature factors

3.7 Refinement with isotropic and anisotropic temperature factor

Similarly to the case of sucrose, after refining the structure under the assumption of isotropic temperature factors such that the R-factor comes to be '[1] 9.51%' as shown in Fig. 3.17, the temperature factor should be changed to anisotropic such that the R-factor comes to be

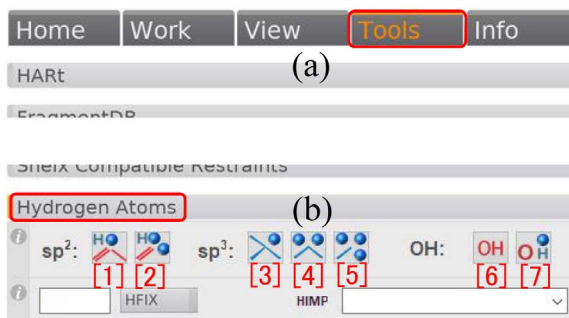


Figure 3.19: Manual addition of hydrogens to carbons

'[1] 7.48%' as shown in Fig. 3.18 (a).

The temperature factor can be changed from isotropic to anisotropic by clicking '[9]' and vice versa by clicking '[10]' on the lower left of Fig. 2.10 (c) [p.10].

3.8 Refinement with hydrogen atoms added

In the case of sucrose, the automatic assignment of hydrogen as in §2.4.4.1 [p.11] and the assignment by changing Q peaks to hydrogens as in §2.4.4.2 [p.11] have been described. However, how to manually assign hydrogen atoms is described in this section.

'Tools' in Fig. 3.19 (a) and then 'Hydrogen Atoms' in Fig. 3.19 (b) can be clicked such as to display icons indicated by [1]-[7] on the bottom. These can be clicked to display the orange bands of '[1] Carbon of benzene ring', '[2] Carbon of ethylene group', '[3] Carbon of methine group', '[4] Carbon of methylene group', '[5] Carbon of methyl group', '[6] Oxygen of hydroxy ion' and '[7] Oxygen of hydroxy group' as shown in Fig. 3.20 [p.26] to assign them. [Esc] key can be clicked to escape from these modes.

In the next subsection, how to assign carbon of methine group, carbon of methylene group and oxygen of hydroxy group, are described.

3.8.1 Assignment of methine groups

Peaks of electron density due to hydrogens of methine groups have relatively large values since the parent atoms are supported by three atomic bonds like a tripod.

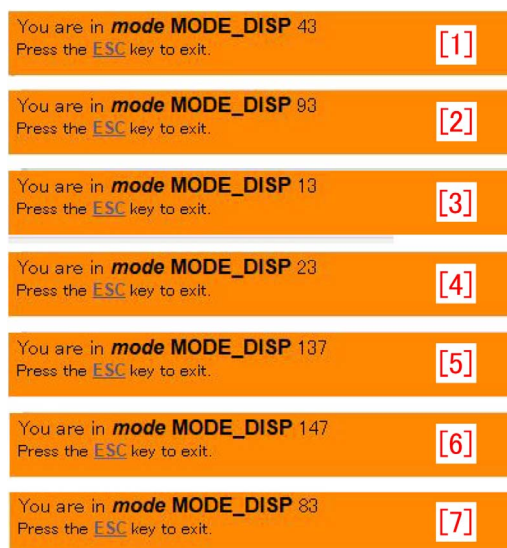


Figure 3.20: [1]-[7] correspond to Fig. 3.19 [1]-[7].

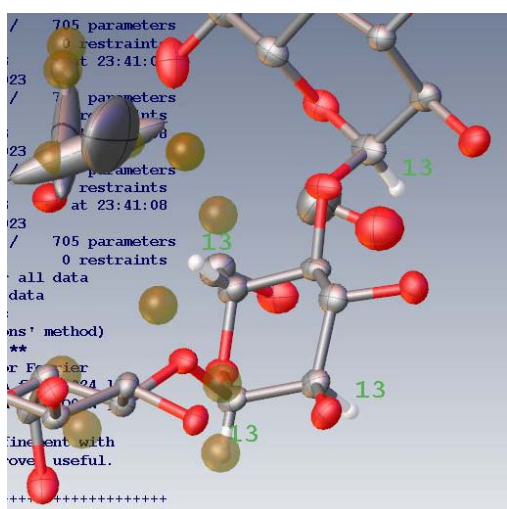


Figure 3.21: Methine groups have been assigned.

‘[3]’ in Fig. 3.19 (b) [p.25] can be clicked to let the orange band of Fig. 3.20 [3] be displayed. Here, carbons of methine groups can be clicked to assign them such that green labels of ‘13’ are displayed as shown in Fig. 3.21.

After clicking carbons of all methine groups to assign them, [Ctrl]+[R] can be typed about ten times to refine the structure to display Fig. 3.22. As shown on the upper right of Fig. 3.22 (a), the R-factor has decreased to 6.54%. On the lower right of Fig. 3.22 (b), Q peaks due to hydrogens of methylene groups are found.

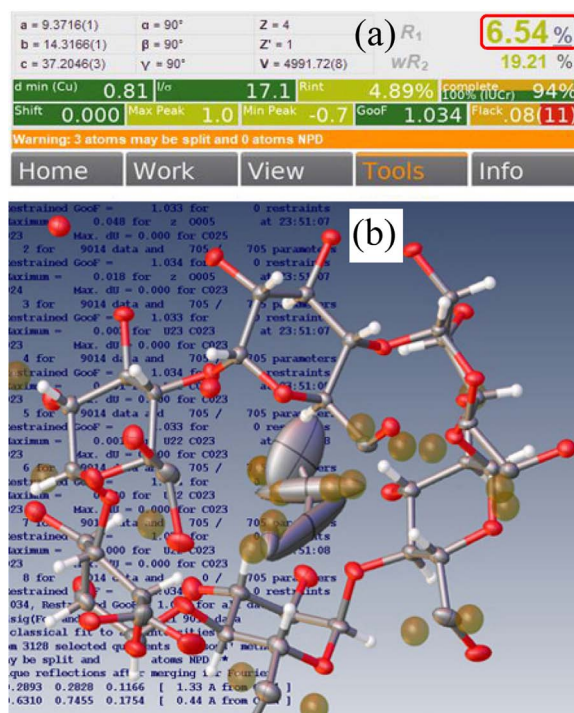


Figure 3.22: Refined result after methine groups assigned

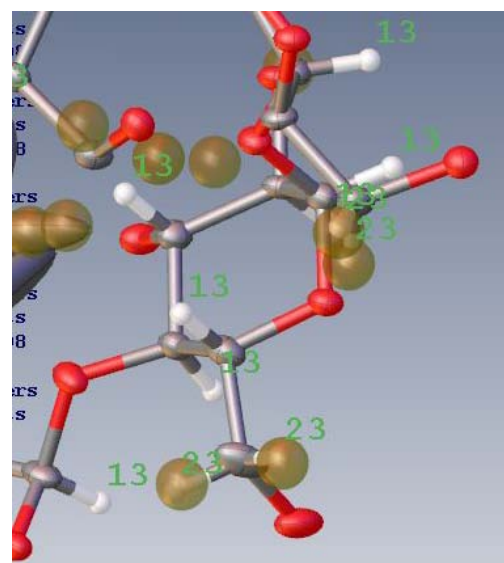


Figure 3.23: Methylene groups have been assigned.

3.8.2 Assignment of methylene groups

Methylene group has two hydrogens and two atomic bonds linked to non-hydrogen atoms.

In Fig. 3.23, the orange band of Fig. 3.20 [4] has been displayed by clicking Fig. 3.19 (b) [4].

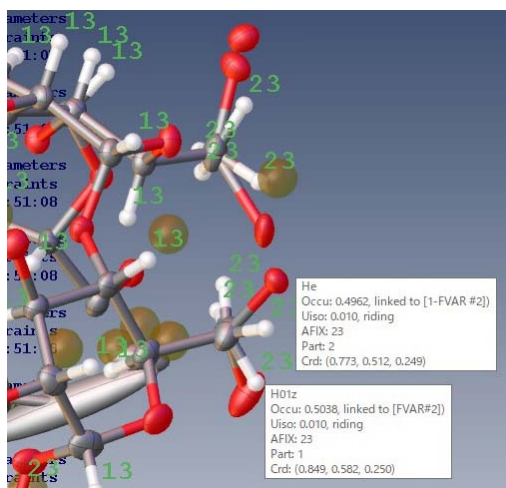


Figure 3.24: Hydrogens of disordered methylene group have been assigned.

[p.25] [4]. Here, carbons of methylene group have been clicked to assign them such that green labels '23' are displayed.

In Fig. 3.24, hydrogen atoms have been added to the disordered oxygens of methylene groups by clicking the parent atoms. Therefore, the carbons of the methylene groups have four hydrogens due to the disordered oxygens. By placing the mouse cursor on these hydrogens, labels can be shown as shown in Fig. 3.24 for several seconds. The same values of occupancy as the disordered oxygen have also been applied to these hydrogens.

After adding hydrogens to all methylene groups, the molecular structure can be refined about ten times by typing [Ctrl]+[R] or clicking 'Refine [3]' in Fig. 3.26 to show Fig. 3.25. As displayed on the upper right of Fig. 3.25 (a), the R-factor decreased to 6.08%. In Fig. 3.25 (b), hydrogens of hydroxy group and H₂O are found as Q peaks.

3.8.3 Assignment of hydroxy groups and H₂O

Hydrogens can be added to hydroxy groups (and H₂O) by replacing Q peaks with hydrogens more correctly than by clicking the icon of '[7]' in Fig. 3.19 (b) [p.25] to assign hydroxy groups since hydroxy groups and H₂O have high flexibility of rotation.

In Fig. 3.26, the refinement options have been

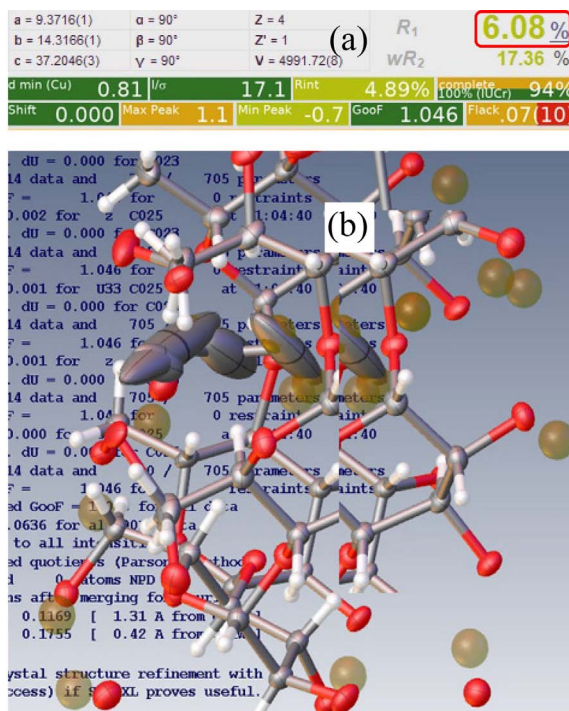


Figure 3.25: Refined with hydrogens of methine groups added

Figure 3.26: Refinement with hydrogens of hydroxy groups and H₂O added

displayed by clicking 'Work [2]' and then '↓ [4]' on the right of 'Refine [3]'. The Q peaks that are considered to be hydrogens can be clicked to assign them to hydrogen after clicking 'Toolbox Work [5]' and then '[6] H' in Fig. 3.26.

After assigning all hydrogens to hydroxy groups or H₂O, the molecular structure can be

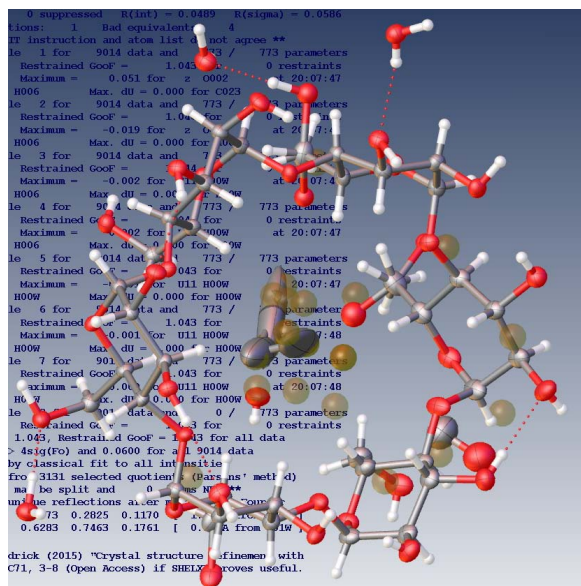


Figure 3.27: Refined with hydrogens of hydroxy groups and H₂O added

a = 9.3716(1)	$\alpha = 90^\circ$	Z = 4	R ₁	[1] 5.71 %
b = 14.3166(1)	$\beta = 90^\circ$	Z' = 1	wR ₂	16.00 %
c = 37.2046(3)	$\gamma = 90^\circ$	V = 4991.72(8)	d min (Cu)	0.81 μm
			R _{int}	17.1
			4.89%	completeness 94%
			100% (U _{cr})	
			Shift	0.000
			Max Peak	1.0
			Min Peak	-0.7
			Goof	1.052
			Flack	0.08(11)

Figure 3.29: Result of refinement

a = 9.3716(1)	$\alpha = 90^\circ$	Z = 4	R ₁	[1] 5.71 %
b = 14.3166(1)	$\beta = 90^\circ$	Z' = 1	wR ₂	16.00 %
c = 37.2046(3)	$\gamma = 90^\circ$	V = 4991.72(8)	d min (Cu)	0.81 μm
			R _{int}	17.1
			4.89%	completeness 94%
			100% (U _{cr})	
			Shift	0.000
			Max Peak	1.0
			Min Peak	-0.7
			Goof	1.049
			Flack	0.08(10)
Warning: 3 atoms may be split and 0 atoms NPD				
Home Work [2] View Tools Info				
Solve [3] Refine [3] Draw Report				
Program SheXL L.S. [4] Cycles 7 Peaks 20				
hkl file exp_663.hkl hkl: Sun Dec 15 13:39:12 2019				
Weight [5] .102 .102 2.49 2 [5] EXTI [5] 0.00022(14) ACTA				

Figure 3.30: Result of refinement with the extinction effect taken into account

Home	Work	View	Tools	Info [1]		
Recent Files						
Electron Density Peaks						
Refinement Indicators						
Bad Reflections [2]						
[3] OMIT	all reflections where [Error/esd] > than [4] 10			ClearOMITs		
Unsigned sorting by Error/esd (refine to update)						
[5]	H	K	L	Error/esd	d/Å	omit Edit...
	0	0	2	12.60	18.60	omit Edit...
	0	2	6	8.17	4.69	omit Edit...
	1	0	2	-6.51	8.37	omit Edit...
	1	4	2	6.28	3.29	omit Edit...
	1	0	5	-6.15	5.83	omit Edit...
[6]	H	K	L	Error/esd	d/Å	Omitted Edit...
	0	0	2	12.60	18.60	Omitted Edit...
	0	2	6	8.17	4.69	omit Edit...
	1	0	2	-6.51	8.37	omit Edit...
	1	4	2	6.28	3.29	omit Edit...
	1	0	5	-6.15	5.83	omit Edit...

Figure 3.28: Omitting bad reflections

refined about ten times by typing [Ctrl]+[R] or clicking ‘Refine [3]’ in Fig. 3.26 [p.27] to show Fig. 3.27. The R-factor has decreased to ‘[1] 5.71%’ as shown on the upper right of Fig. 3.26 [p.27]. This is the final molecular structure of α -cyclodextrin since further unfounded refinement should not be done.

3.9 Omitting bad reflections

By clicking ‘Info [1]’ in Fig. 3.28 and then ‘Bad Reflections [2]’, reflection indices whose discrepancy in structure factor by calculation and observation can be summarized. In Figs. 3.28 (a), it is shown that reflection indices whose values of [Error/esd] is larger than ‘10 [4]’ is ‘[5] 0 0 2 12.60’. ‘[3] OMIT’ can be clicked to change ‘omit’ on the rightmost of ‘[5] 0 0 2 12.60’ in Fig. 3.28 (a) to ‘Omitted’ on the rightmost of ‘[6] 0 0 2 12.60’ in Fig. 3.28 (b).

Then, the structure has been refined by typing [Ctrl]+[R] about ten times to show Fig. 3.29. In this case, the R-factor ‘[1] 5.71%’ has not been improved. However, this procedure is recommended to try since the R-factor can sometimes be improved by omitting bad reflections.

3.10 Consideration of extinction effect

In Fig. 3.30, ‘Work [2]’ and then ‘ \downarrow [4]’ on the right of ‘Refine [3]’ have been clicked to show the refinement options. ‘[5] EXTI’ can be checked to do refinement with the extinction effect taken into account.

The extinction is a dynamical diffraction ef-

fect that the $h k l$ -reflected X-ray intensities do not increase linearly due to $\bar{h} \bar{k} \bar{l}$ reflection. Since the R-factor is sometimes improved by checking '[5] EXTI', it is recommended to try to refine the structure with '[5] EXTI' checked. However, '[5] EXTI' should be unchecked when the R-factor increases. In the case of Fig. 3.30 the R-factor '[1] 5.71%' has not been improved.

This is the end of refinement of the molecular

structure of α -cyclodextrin

3.11 Creation of the report

The report can be created similarly to the case of sucrose. Refer to the description in §2.5 [p.13], please.

Appendix A

Reasonability of defining the reciprocal lattice

For many students working on crystallography, the first difficulty is understanding of reciprocal lattice. In spite that the Bragg condition written by (A.1) or (A.2) can easily be understood, why such strange ideas as reciprocal lattice and reciprocal space should we use? This chapter describes the equivalence of Bragg's reflection condition, Laue's reflection condition and Ewald construction (Reciprocal lattice node exists on the Ewald sphere), from which how reasonably the reciprocal lattice is defined can be understood.

Every space group of crystal has an extinction rule owing to its symmetry with which the crystal structure factor comes to be zero. However, it is neglected in the following description for simplicity.

A.1 Bragg's reflection condition

Figure A.1 shows Bragg's reflection condition. This figure is also found in high school text book. Bragg's reflection condition can relatively easily and intuitively referring to this figure. When atoms (or molecules) are arranged on a set of planes as shown in Fig. A.1. Optical path length of X-rays drawn as a gray line are longer than that drawn as a black line by $|\vec{ab}| + |\vec{bc}| (= 2d \sin \theta_B)$. When this length is an integral multiplication of the wavelength, these rays interfere constructively with each other. Therefore, reflection condition can be described as follows,

$$2d \sin \theta_B = n\lambda. \quad (\text{A.1})$$

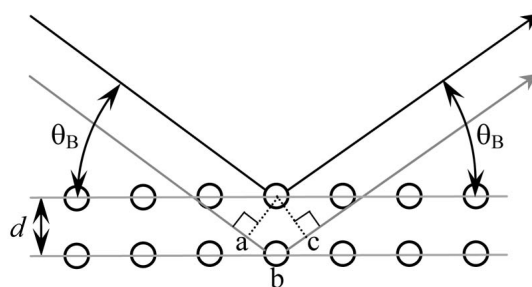


Figure A.1: Bragg's reflection condition.

By redefining lattice spacing d' to be $d' = d/n$, the following equation is also frequently used,

$$2d' \sin \theta_B = \lambda. \quad (\text{A.2})$$

Now, let us consider why the angle of incidence and emergence is identical. Is it evident since the Bragg plane works as a mirror plane? Then, why are the angles of incidence and emergence of a mirror identical? Sometimes, even a veteran of crystallography cannot answer to this question.

A.2 Laue's reflection condition

Laue's reflection condition was used to explain the phenomenon of X-ray diffraction when it was invented by Laue (Max Theodor Felix von Laue; 1879/10/9-1960/4/24) in 1912, which is described referring to Fig. A.2 as follows,

$$\begin{aligned} R_0B - AR_1 \\ = \overrightarrow{R_0R_1} \cdot \mathbf{s}_1 - \overrightarrow{R_0R_1} \cdot \mathbf{s}_0 = n_0\lambda. \end{aligned} \quad (\text{A.3})$$

Here, \mathbf{s}_0 and \mathbf{s}_1 are unit vectors in the direction of propagation of incident and reflected X-rays.

When R_0 and R_1 are equivalent lattice points, difference in optical path length between black and gray paths drawn in Fig. A.2 is given by (A.3). When this difference in path length is an integral multiplication of wavelength, X-rays scattered by lattice points R_0 and R_1 interfere constructively with each other.

Incidentally, since R_0 and R_1 are equivalent lattice point, there is a restriction as follows,

$$\overrightarrow{R_0R_1} = n_1\mathbf{a} + n_2\mathbf{b} + n_3\mathbf{c}, \quad (\text{A.4})$$

where, n_1 , n_2 and n_3 are arbitrary integers. \mathbf{a} , \mathbf{b} and \mathbf{c} are primitive translation vectors. That is to say the left hand side of (A.3) should be integral multiplication of wavelength for arbitrary integers n_1 , n_2 and n_3 . Lattice points R_0 and R_1 can move freely with a restriction that these are equivalent points. The value of left hand side of (A.3) is evidently positive when $\overrightarrow{R_0R_1} \cdot \mathbf{s}_1 > \overrightarrow{R_0R_1} \cdot \mathbf{s}_0$ and is negative when $\overrightarrow{R_0R_1} \cdot \mathbf{s}_1 < \overrightarrow{R_0R_1} \cdot \mathbf{s}_0$. Figure A.2 is drawn under an assumption of the latter case.

However, R_0 and R_1 can also be taken such that $\overrightarrow{R_0R_1} \cdot \mathbf{s}_1 = \overrightarrow{R_0R_1} \cdot \mathbf{s}_0$. In the following discussion in this paragraph, R_0 and R_1 are fixed such that $\overrightarrow{R_0R_1} \cdot \mathbf{s}_1 = \overrightarrow{R_0R_1} \cdot \mathbf{s}_0$. When R_0 , R_1 and optical paths drawn as black and gray lines are all on the drawing, there should be a plane perpendicular to the drawing that include those points and optical paths. When X-rays are scattered at any point on this plane under a condition that the angles of incidence and emergence are the same, the optical path length is always the same. This is also the reason for that the angle of incidence and emergence for a mirror is always identical.

In Bragg's reflection condition, under an implicit (the first and second dimensional) restriction that optical path length are always the same for a defined Bragg plane when the angle of incidence and emergence is identical, the third dimensional condition is given by (A.1) or (A.2). Behind the simple condition given by those equations, the above mentioned first and second dimensional restrictions are hidden.

Now, for description in the next section, the following equation is prepared by dividing the both sides of eq. (A.3) by the wavelength λ ,

$$\overrightarrow{R_0R_1} \cdot \left(\frac{\mathbf{s}_1}{\lambda} - \frac{\mathbf{s}_0}{\lambda} \right) = n_0. \quad (\text{A.5})$$

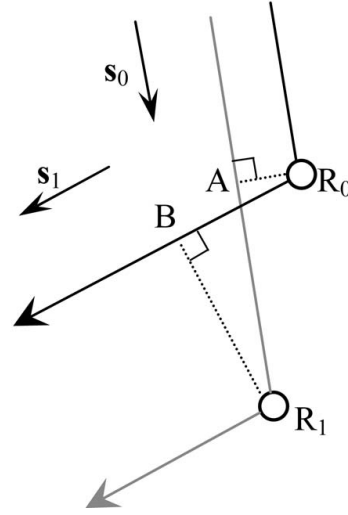


Figure A.2: Laue's reflection condition.

By substituting (A.4) into the above equation and considering that the wave vectors of incident and reflected X-rays are given by $\mathbf{K}_0 = \mathbf{s}_0/\lambda$ and $\mathbf{K}_1 = \mathbf{s}_1/\lambda$, the following equation can be obtained,

$$(n_1\mathbf{a} + n_2\mathbf{b} + n_3\mathbf{c}) \cdot (\mathbf{K}_1 - \mathbf{K}_0) = n_0. \quad (\text{A.6})$$

A.3 Ewald's reflection condition (Ewald construction)

A.3.1 Foundation of Ewald construction

Fig. A.3 [p.32] shows the situation that the origin O of reciprocal space and a reciprocal lattice node H_{hkl} simultaneously exist on the surface of Ewald sphere. Its center is the common initial point of wave vectors \mathbf{K}_0 and \mathbf{K}_1 .

In the description of Ewald construction, at first, reciprocal fundamental vectors \mathbf{a}^* , \mathbf{b}^* and \mathbf{c}^* are defined as follows:

$$\mathbf{a}^* = \frac{\mathbf{b} \times \mathbf{c}}{\mathbf{a} \cdot (\mathbf{b} \times \mathbf{c})}, \quad (\text{A.7a})$$

$$\mathbf{b}^* = \frac{\mathbf{c} \times \mathbf{a}}{\mathbf{a} \cdot (\mathbf{b} \times \mathbf{c})}, \quad (\text{A.7b})$$

$$\mathbf{c}^* = \frac{\mathbf{a} \times \mathbf{b}}{\mathbf{a} \cdot (\mathbf{b} \times \mathbf{c})}. \quad (\text{A.7c})$$

The denominator of (A.7), $\mathbf{a} \cdot (\mathbf{b} \times \mathbf{c})$ [= $\mathbf{b} \cdot (\mathbf{c} \times \mathbf{a}) = \mathbf{c} \cdot (\mathbf{a} \times \mathbf{b})$] is the volume of parallelepiped whose edges are \mathbf{a} , \mathbf{b} and \mathbf{c} . From

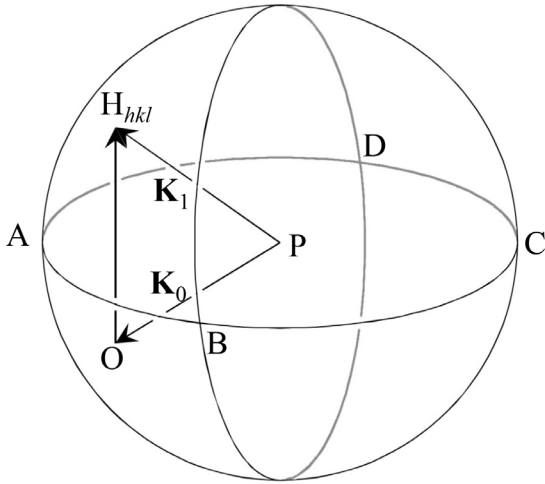


Figure A.3: Ewald sphere

the above definitions, the following equations are evident,

$$\mathbf{a} \cdot \mathbf{a}^* = 1, \quad (\text{A.8a})$$

$$\mathbf{b} \cdot \mathbf{b}^* = 1, \quad (\text{A.8b})$$

$$\mathbf{c} \cdot \mathbf{c}^* = 1. \quad (\text{A.8c})$$

Further, $\mathbf{b} \times \mathbf{c}$ is a vector that is perpendicular to both \mathbf{b} and \mathbf{c} and has a length of the area of parallelogram whose sides are \mathbf{b} and \mathbf{c} . Here, vectors \mathbf{b} , \mathbf{c} and $\mathbf{b} \times \mathbf{c}$ construct a right-handed system. Since the above is the same for $\mathbf{c} \times \mathbf{a}$ and $\mathbf{a} \times \mathbf{b}$, the following relations are also evident,

$$\mathbf{a} \cdot \mathbf{b}^* = \mathbf{a} \cdot \mathbf{c}^* = 0, \quad (\text{A.9a})$$

$$\mathbf{b} \cdot \mathbf{c}^* = \mathbf{b} \cdot \mathbf{a}^* = 0, \quad (\text{A.9b})$$

$$\mathbf{c} \cdot \mathbf{a}^* = \mathbf{c} \cdot \mathbf{b}^* = 0. \quad (\text{A.9c})$$

That is to say, \mathbf{a}^* , \mathbf{b}^* and \mathbf{c}^* have been defined such that (A.8) and (A.9) are satisfied.

A reflection vector giving $h k l$ reflection is defined in general as follows:

$$\overrightarrow{\text{OH}}_{hkl} = h\mathbf{a}^* + k\mathbf{b}^* + l\mathbf{c}^*. \quad (\text{A.10})$$

Here, O is the origin of reciprocal space. The Ewald sphere is a sphere whose center is P. The wave vector of the incident X-rays \mathbf{K}_0 is $\overrightarrow{\text{PO}}$. When a reciprocal lattice node H_{hkl} exists on the surface of the Ewald sphere, reflected X-rays whose wave vector \mathbf{K}_1 is $\overrightarrow{\text{OH}}_{hkl}$ are excited. Then, the following equation is satisfied,

$$\begin{aligned} \mathbf{K}_1 - \mathbf{K}_0 &= \overrightarrow{\text{OH}}_{hkl} \\ &= h\mathbf{a}^* + k\mathbf{b}^* + l\mathbf{c}^*. \end{aligned} \quad (\text{A.11})$$

Let us calculate the left-hand side of (A.6) [p.31] by substituting (A.11) into the second term of the left-hand side of (A.6) [p.31] and considering (A.8) and (A.9) as follows:

$$\begin{aligned} (n_x\mathbf{a} + n_y\mathbf{b} + n_z\mathbf{c}) \cdot (\mathbf{K}_1 - \mathbf{K}_0) \\ = (n_x\mathbf{a} + n_y\mathbf{b} + n_z\mathbf{c}) \cdot (h\mathbf{a}^* + k\mathbf{b}^* + l\mathbf{c}^*) \end{aligned} \quad (\text{A.12})$$

$$= n_x h + n_y k + n_z l. \quad (\text{A.13})$$

Since $n_x h + n_y k + n_z l$ is evidently an integer, Laue's reflection condition described by (A.3) [p.30], (A.5) [p.31] and (A.6) [p.31], is satisfied when the reciprocal lattice node H_{hkl} is on the surface of Ewald sphere. Therefore, Ewald's reflection condition is equivalent to Laue's reflection condition. Furthermore, Ewald's reflection condition is also equivalent to Bragg's reflection conditions, which is more clarified by the description in the next section A.3.2

Bragg's reflection condition can easily be understood by referring to Fig. A.1 [p.30]. Laue's reflection condition is more difficult than Bragg's reflection condition. However, it can also be understood by referring to Fig. A.2 [p.31]. The drawing of Fig. A.3 in reciprocal space was invented by Ewald. This way of drawing is extremely effective when considering various difficult problems in crystallography that cannot be understood by drawing figures as shown in Fig. A.1 [p.30] and /or Fig. A.2 [p.31] in real space. It is strongly recommended to use the Ewald construction by using Fig. A.3 by paying respect to Ewald (Paul Peter Ewald, 1888/1/23~1985/8/22).

A.3.2 Relation between reciprocal lattice vector and Bragg reflection plane

Reciprocal lattice vector is a vector whose direction is perpendicular to the Bragg plane and length is $1/d'$, where d' is the lattice spacing of the Bragg plane. These are verified in the following paragraphs.

By considering $n_0 = n_x h + n_y k + n_z l$, (A.10) and (A.12)=(A.13), the following equation is obtained.

$$\overrightarrow{\text{OH}}_{hkl} \cdot (n_x\mathbf{a} + n_y\mathbf{b} + n_z\mathbf{c}) = n_0. \quad (\text{A.14})$$

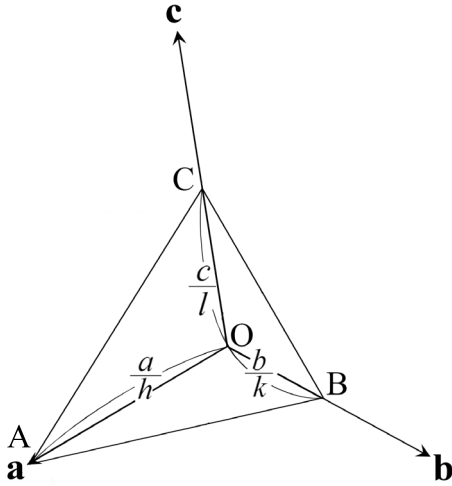


Figure A.4: Drawing of Miller and Miller indices

By multiplying $1/|\overrightarrow{OH_{hkl}}|$ to the both sides of the above equation, the following equation is obtained,

$$\frac{\overrightarrow{OH_{hkl}}}{|\overrightarrow{OH_{hkl}}|} \cdot (n_x \mathbf{a} + n_y \mathbf{b} + n_z \mathbf{c}) = \frac{n_0}{|\overrightarrow{OH_{hkl}}|}. \quad (\text{A.15})$$

A plane is described in general as follows:

$$\begin{aligned} & [\text{Unit normal vector}] \cdot [\text{Location vector}] \\ & = [\text{Distance from the origin}]. \end{aligned} \quad (\text{A.16})$$

Therefore, $n_0 \in \{ \dots, -2, -1, 0, 1, 2, \dots \}$ in (A.15) means that location vector $n_x \mathbf{a} + n_y \mathbf{b} + n_z \mathbf{c}$ is on Bragg planes piled up with a spacing of $d' (= 1/|\overrightarrow{OH_{hkl}}|)$, which reveals that the reciprocal lattice vector $\overrightarrow{OH_{hkl}}$ is the normal vector of Bragg plane whose length is $1/d'$.

A.4 Drawing of Miller and Miller indices

Fig. A.4 shows the relation between the Miller indices and the Bragg plane and is found in almost all text books describing the crystallography. This way of drawing was invented by Miller (William Hallows Miller; 1801/4/6-1880/5/20). However, it should be noted that

he was a mineralogist of the 19th century before X-rays and X-ray diffraction were invented. Figs. A.1[p.30] and A.4 are found in many text books. However, it cannot be recommended that the students and researchers attempt to understand the X-ray diffraction phenomena only by referring to Figs. A.1[p.30] and A.4.

Points A, B and C in Fig. A.4 exist on \mathbf{a} , \mathbf{b} and \mathbf{c} axes, respectively. Distances of them from the origin O are a/h , b/k and c/l . Miller invented that \mathbf{a} , \mathbf{b} and \mathbf{c} axes can be defined such that all facets of crystals are drawn as shown in Fig. A.4 with small integers h , k and l .

When $h = 0$, distance of A from O is infinite and then the plane ABC is parallel to \mathbf{a} . This is the case for k , B and \mathbf{b} and for l , C and \mathbf{c} .

h , k and l are indices of reciprocal lattice nodes, which was clarified several decades after Miller's invention. ABC is a plane whose direction is parallel to the Bragg plane and distance from O is d' . These are confirmed in the following description.

By referring to Fig. A.4, $\overrightarrow{AB} = -\mathbf{a}/h + \mathbf{b}/k$ and then $\overrightarrow{AB} \cdot \overrightarrow{OH_{hkl}}$ is calculated as follows:

$$\begin{aligned} \overrightarrow{AB} \cdot \overrightarrow{OH_{hkl}} &= (-\mathbf{a}/h + \mathbf{a}/k) \cdot (h\mathbf{a}^* + k\mathbf{b}^* + l\mathbf{c}^*) \\ &= -1 + 1 \\ &= 0. \end{aligned} \quad (\text{A.17})$$

Therefore, line AB is confirmed to be perpendicular to $\overrightarrow{OH_{hkl}}$. Similarly, lines BC and CA are confirmed to be perpendicular to $\overrightarrow{OH_{hkl}}$. Further, from this, the distance of ABC from the origin O can be obtained from scalar product between the unit normal vector of plane ABC and vector \overrightarrow{OA} , \overrightarrow{OB} or \overrightarrow{OC} as follows:

$$\begin{aligned} & \overrightarrow{OA} \cdot \overrightarrow{OH_{hkl}} / |\overrightarrow{OH_{hkl}}| \\ &= \frac{\mathbf{a}}{h} (h\mathbf{a}^* + k\mathbf{b}^* + l\mathbf{c}^*) / |\overrightarrow{OH_{hkl}}| \\ &= 1 / |\overrightarrow{OH_{hkl}}| \\ &= d' \end{aligned} \quad (\text{A.18})$$

As described above, the explanation of Fig. A.4 needs complex descriptions. It cannot be recommended to understand the phenomena of X-ray diffraction only referring to the drawing of Miller as shown in Fig. A.4.

Appendix B

Determination of space group from extinction rule

==> general reflections sorted into even/odd parity classes

eee			eoo			ooo		
totl	obsd	<I/sig>	totl	obsd	<I/sig>	totl	obsd	<I/sig>
205	196	30.0	253	240	29.2	289	272	32.1
[1]								
eoo			ooo			ooo		
370	354	38.4	337	322	40.5	419	392	40.3
ooo			ooo			ooo		
318	297	33.6	355	343	38.6			

==> Special reflections sorted into various classes
 A * indicates a potential systematic absence and is used if the average I/sig(I) for a particular class is less than 3.5.

ee			eo			
totl	obsd	<I/sig>	totl	obsd	<I/sig>	
hhl refl	27	24	48.5	36	35	58.0
h-hl refl	30	28	49.2	37	35	55.7
OkI zone	89	80	43.2	110	106	54.0
h0l zone	34	31	43.8	40	11	2.2*
hk0 zone	62	57	39.1	68	65	53.8
oe			oo			
hhl refl	40	39	45.4	47	44	68.4
h-hl refl	40	38	48.0	44	40	66.9
OkI zone	97	94	53.9	109	103	48.9
h0l zone	36	36	73.1	43	13	2.5*
hk0 zone	71	64	46.7	74	72	46.5

e			o			
totl	obsd	<I/sig>	totl	obsd	<I/sig>	% of o/e
hhh line	2	2	31.3	7	5	71.6
hh0 zone	7	7	42.2	9	9	98.6
Ok0 line	17	17	74.6	16	2	1.7*
00l line	10	8	102.3	9	1	2.4*
h00 line	3	3	95.0	6	6	38.3
						40.3

Figure B.1: Content of 'process.out' (#1). [Taurine; monoclinic $P2_1/c$ (#14)].

One of the most important process in the crystal structure analysis is determination of space group. CrystalStructure 4.1 determines the space group automatically as shown in Fig. B.3.

In this chapter, how the computer determines the space group, is described. When the computer failed to determine the space group correctly, it should be determined manually referring to the description of this chapter.

Figs. B.1, B.2 and B.3 show contents of 'process.out' displayed by clicking 'View output file' button in Fig. 2.12 of Part2a manual. In this file, information about the extinction rule based

==> reflections sorted for identifying 4n type conditions
 a and b represent h, k, or l

a+b=4n			a+b not equal 4n			
totl	obsd	<I/sig>	totl	obsd	<I/sig>	
OkI zone	106	102	49.6	299	281	50.1
h0l zone	37	20	18.2	116	71	30.8
hk0 zone	69	66	38.9	206	192	48.8
a=4n			a not equal 4n			
Ok0 line	8	8	77.5	25	11	28.2
00l zone	4	2	60.2	15	7	54.3
h00 zone	1	1	91.3	8	8	41.4
2h+l=4n			2h+l not equal 4n			
hhl refl	34	32	47.5	116	110	59.9

==> reflections sorted for identifying 3n and 6n type conditions

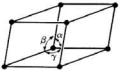
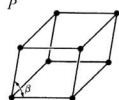
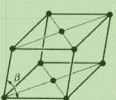
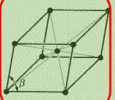
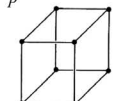
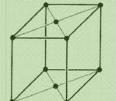


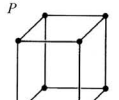
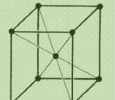
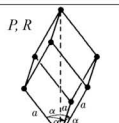
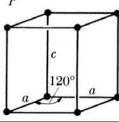
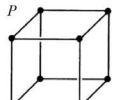


h+l=3n; l odd			h+l=3n			h+l not equal 3n			
totl	obsd	<I/sig>	totl	obsd	<I/sig>	totl	obsd	<I/sig>	
h-h0l	26	24	54.1	54	52	64.6	97	89	51.8
-h+l=3n; l even			-h+l=3n			-h+l not equal 3n			
h-h0l	28	22	62.7	49	43	55.6	102	98	56.7
l=3n			l not equal 3n						
000l line	7	2	32.5	12	7	67.7			
l=6n			l not equal 6n						
000l line	2	2	185.7	17	7	47.2			

Figure B.2: Content of 'process.out' (#2). [Taurine; monoclinic $P2_1/c$ (#14)]

on which the space group can be determined, are summarized.

Information about extinctions of reflections whose three, two or one indices are not zero, are summarized on parts [1], [2, 3] and [4], respectively, of Fig. B.1. For example, 'eoo' found on the upper part of [1] in Fig. B.1 means that indices of hkl are even, even and odd. 'totl' and 'obsd' are numbers of total and observed reflections. $\langle I/\sigma \rangle$ are mean values of I/σ , where I is observed intensity of reflected X-rays and σ is standard deviation of background. Since values of 'obsd' and $\langle I/\sigma \rangle$ are sufficiently large, there is no extinction for three nonzero hkl . On parts [2] and [3] in Fig. B.1, $h0l$ reflections are

Table B.1: 14 Bravais lattices and ‘Face-centered monoclinic’. Refer to the last paragraph of §B.2 [p.37], please about why ‘Face-centered monoclinic’ is added.

Crystal system Laue group (No. of space group)	Axial distances (a, b, c) Axial angles (α, β, γ)	Primitive lattice (P, R)	Base-centered lattice (A, B, C)	Body-centered lattice (I)	Face-centered lattice (F)
Triclinic $\bar{1}$ (#1, #2)	$a \neq b \neq c$ $\alpha \neq \beta \neq \gamma$				
Monoclinic $2/m$ (#3 ~#15)	$a \neq b \neq c$ two of α, β, γ $= 90^\circ$, one $\neq 90^\circ$				
Orthorhombic mmm (#16 ~#74)	$a \neq b \neq c$ $\alpha = \beta = \gamma$ $= 90^\circ$				
Tetragonal $4/m$ (#75 ~#88), $4/mmm$ (#89 ~#142)	Two of a, b, c are the same. One of them is different. $\alpha = \beta = \gamma$ $= 90^\circ$				
Trigonal $\bar{3}$ (#143 ~#148), $\bar{3}m$ (#149 ~#167)	$a = b = c$ $\alpha = \beta = \gamma$ $\neq 90^\circ$				
Hexagonal $6/m$ (#168 ~#176) $6/mmm$ (#177 ~#194)	a and b are the same. c is different. $\alpha = \beta = 90^\circ$ $\gamma = 120^\circ$				
Cubic $m\bar{3}$ (#195 ~#206) $m\bar{3}m$ (#207 ~#230)	$a = b = c$, $\alpha = \beta = \gamma$ $= 90^\circ$				

o/e' are extremely small. In parts [5] and [6] in

Space group # 14 setting # 1
The selected space group symbol is: $P2_1/c$

Figure B.3: Content of ‘process.out’ (#3) [Taurine; monoclinic $P2_1/c$ (#14)]. [setting #1] corresponds to ‘[1] CELL CHOICE 1’ in Fig. B.5.

recognized to distinguish since value of $\langle I/\text{sig} \rangle$ is extremely small when l is odd. This is indicated by an ‘*’ mark. Similarly, in part [4] in Fig. B.1, $0k0$ and $00l$ reflections are recognized to distinguish when k is odd and l is odd, respectively since values of $\langle I/\text{sig} \rangle$ and ‘% of

Reflection conditions

General:

$$h0l : l = 2n$$

$$0k0 : k = 2n$$

$$00l : l = 2n$$

Figure B.4: Reflection condition of $P2_1/c$ (#14) described in *International Tables for Crystallography* (2006) Vol.A. $0k0$ reflections when k is odd and, $h0l$ and $00l$ reflections when l is odd, extinguish.

Fig. B.2, information about reflection indices when indices or summation of them are

Table B.2: Symmetric elements (planes). Protein crystals do not have these symmetric elements absolutely.

Name of symmetric plane	Symbol	Graphic symbol (perpendicular to the space)	Graphic symbol (parallel to the space)
Mirror plane	m	—	
Axial glide plane	a, b or c	----- (Glide parallel to the space)	
Axial glide plane	a, b or c (Glide perpendicular to the space)	
Double glide plane	e	
Diagonal glide plane	n	-----	
Diamond glide plane	d	-----	

divided by 4, by 3 and by 6, from which existence of four-, three- and six-fold screw axes can be discussed.

Fig. B.3 [p.35] shows that the space group of taurine crystal has been determined to be $P2_1/c(\#14)$.

Fig. B.4 shows reflection condition of $P2_1/c(\#14)$ described in *International Tables for Crystallography* (2006) Vol.A. The information described in Figs. B.1 [p.34] and B.2 [p.34] coincides with the condition in Fig. B.4 [p.35], from which the space group has been determined to be $P2_1/c(\#14)$.

In the following description, how the extinction of reflections are caused by symmetries of crystals depending on the space group, is explained.

B.1 Symmetric elements of crystal derived based on the group theory

Who showed the importance of group theory to determine the crystal structure for the first time was Shoji Nishikawa (1884/12/5~1952/1/5). Wyckoff (R. W. G. Wyckoff; 1897/8/9~1994/11/3)

Table B.3: Symmetric elements of crystal (axes and point).

Symmetric axis or center	Symbol	Graphic symbol (perpendicular to the space)	Graphic symbol (parallel to the space)
-	1		
Two-fold rotation axis	2	⦶	⦶
2 ₁ screw axis	2 ₁	⦶	⦶
Three-fold rotation axis	3	⦶	
3 ₁ screw axis	3 ₁	⦶	
3 ₂ screw axis	3 ₂	⦶	
Four-fold rotation axis	4	⦶	⦶
4 ₁ screw axis	4 ₁	⦶	⦶
4 ₂ screw axis	4 ₂	⦶	⦶
4 ₃ screw axis	4 ₃	⦶	⦶
Six-fold rotation axis	6	⦶	
6 ₁ screw axis	6 ₁	⦶	
6 ₂ screw axis	6 ₂	⦶	
6 ₃ screw axis	6 ₃	⦶	
6 ₄ screw axis	6 ₄	⦶	
6 ₅ screw axis	6 ₅	⦶	
Symmetry center	$\bar{1}$	⦶	
Three-fold rotatory inversion axis	$\bar{3}$	⦶	
Four-fold rotatory inversion axis	$\bar{4}$	⦶	⦶
Six-fold rotatory inversion axis	$\bar{6}$	⦶	

who was strongly influenced by Nishikawa, systemized and established the space group theory that is widespread today and summarized in *International Tables for Crystallography* (2006) Vol.A.

As shown in Table B.1 [p.35], crystals are categorized into seven crystal systems depending on their shapes of unit cells. Further, there are several complex lattices whose backgrounds in Table B.1 [p.35] are green, other than primitive cells. Fourteen kinds of lattice except for ‘body-centered monoclinic lattice’ are called Bravais lattice.

‘Body-centered monoclinic lattice’ was added by the present author’s own judgment. The reason is that base-centered monoclinic lattice can sometimes change to body-centered lattice without changing the symmetry of monoclinic lattice or changing volume of unit cell by reselecting axes of unit cell.

In the first column of Table B.1 [p.35], Laue groups and ranges of space group number are summarized. Laue group is determined by symmetry of reciprocal lattice of crystals.

It has been clarified that crystals can be categorized into 230 space groups depending on the symmetric elements as shown in Tables. B.1 [p.35], B.2 and B.3.

What is important to determine the space group is the extinction rule, about which the

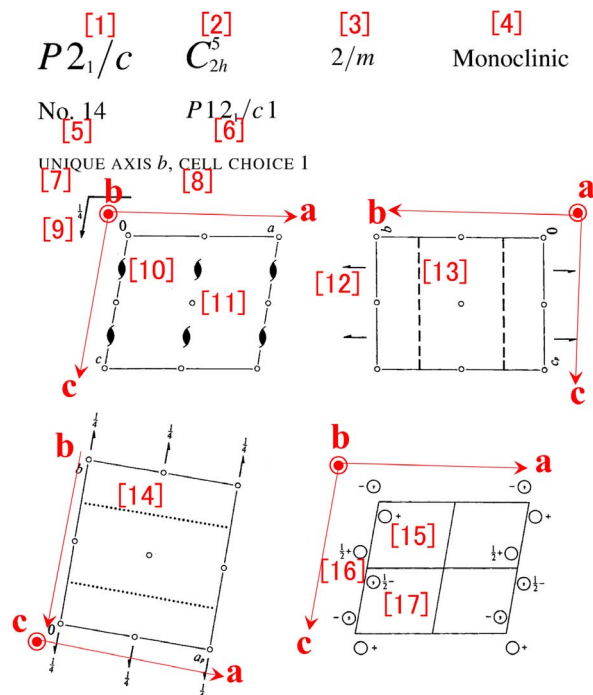


Figure B.5: Drawings for space group $P2_1/c$ (#14) in *International Tables for Crystallography* (2006) Vol.A. Protein crystals do not belong to this space group absolutely.

information can be extracted by referring to descriptions in ‘process.out’ as shown in Figs. B.1 [p.34] and B.2 [p.34]. It can be viewed by clicking ‘View output file’ button in Fig. 2.21 of Part 2a manual.

B.2 Symbols of space groups

Fig. B.5 is a diagram on the first two pages showing symmetric elements of crystal group $P12_1/c1$ in *International Tables for Crystallography* (2006) Vol.A, Chapter 7. Marks [1]-[17] are as follows; [1]: Hermann-Mouguin notation, [2]: Schönflies notation, [3]: Laue group, [4]: crystal system, [5]: ordinal number of space group, [6]: Hermann-Mouguin full notation, [7]: unique axis, [8]: cell choice, [9]: graphic symbol of c glide plane, [10]: graphic symbol of 2₁ screw axis, [11]: graphic symbol of symmetric center, [12]: graphic symbol of 2₁ screw axis, [13]: graphic symbol of c glide plane, [14]: graphic symbol of c glide plane, [15]: position of atom, [16]: position of atom (an image due to 2₁ screw axis), [17]: position of atom (an image due to 2₁ screw axis).

Table B.4: Extinctions owing to complex lattice.

Name of lattice	Symbol	Reflection condition(not extinct)	Example
A base-centered	<i>A</i>	$hkl : k + l = 2n$	<i>A</i> 12/ <i>n</i> 1 (#15)
B base-centered	<i>B</i>	$hkl : h + l = 2n$	<i>B</i> 2/ <i>n</i> 11 (#15)
C base-centered	<i>C</i>	$hkl : h + k = 2n$	<i>C</i> 12/ <i>c</i> 1 (#15)
Body-centered	<i>I</i>	$hkl : h + k + l = 2n$	<i>I</i> 2/ <i>b</i> 11 (#15)
Face-centered	<i>F</i>	$hkl : h + k, h + l, k + l = 2n$	

Table B.5: Extinction rules owing to glide planes. Protein crystals do not have glide plane absolutely.

Name of glide plane (Symbol)	Normal to	Reflection condition (not extinct)	Example
Axial glide plane (<i>a</i>)	b	$h0l : h = 2n$	<i>P</i> 12 ₁ / <i>a</i> 1 (#14)
Axial glide plane (<i>a</i>)	c	$hk0 : h = 2n$	<i>P</i> 112 ₁ / <i>a</i> (#14)
Axial glide plane (<i>b</i>)	a	$0kl : k = 2n$	<i>P</i> 2 ₁ / <i>b</i> 11 (#14)
Axial glide plane (<i>b</i>)	c	$hk0 : k = 2n$	<i>P</i> 112 ₁ / <i>b</i> (#14)
Axial glide plane (<i>c</i>)	a	$0kl : l = 2n$	<i>P</i> 2 ₁ / <i>c</i> 11 (#14)
Axial glide plane (<i>c</i>)	b	$h0l : l = 2n$	<i>P</i> 12 ₁ / <i>c</i> 1(#14) <i>C</i> 12/ <i>c</i> 1 (#15)
Double glide plane (<i>e</i>)	a	$hkl : k + l = 2n$	
Double glide plane (<i>e</i>)	b	$hkl : h + l = 2n$	
Double glide plane (<i>e</i>)	c	$hkl : h + k = 2n$	
Diagonal glide plane (<i>n</i>)	a	$0kl : k + l = 2n$	<i>B</i> 2/ <i>n</i> 11 (#15)
Diagonal glide plane (<i>n</i>)	b	$h0l : h + l = 2n$	<i>C</i> 12/ <i>c</i> 1 (#15)
Diagonal glide plane (<i>n</i>)	c	$hk0 : h + k = 2n$	<i>P</i> 112 ₁ / <i>n</i> (#14)

due to *c* glide plane).

‘[8] CELL CHOICE 1’ corresponds to ‘setting #1’ in Fig. B.3 [p.35]. ‘ $\frac{1}{4}$ ’ described near [9] is the height of *c* glide plane. About graphic symbols of *c* glide plane [9], [13] and [14], refer to Table B.2 [p.36], please. About graphic symbols of 2₁ screw axis [10] and [12], refer to Table B.3 [p.37]. Atoms at positions [16] and [17] are images of atom at [15] by symmetric operations due to 2₁ screw axis and *c* glide plane, respectively. ‘ $\frac{1}{2}+$ ’ near [16] and ‘ $\frac{1}{2}-$ ’ near [17] means that locations of atoms at [16] and [17] are $-x\mathbf{a} + (\frac{1}{2} + y)\mathbf{b} + (\frac{1}{2} - z)\mathbf{c}$ and $x\mathbf{a} + (\frac{1}{2} - y)\mathbf{b} + (\frac{1}{2} + z)\mathbf{c}$, respectively when that of [15] is $x\mathbf{a} + y\mathbf{b} + z\mathbf{c}$. Comma (,) in ‘○’ at [17] means that this atom (or molecule) is an enantiomer of those at [15] and [16].

Initial character of Hermann-Mouguin notation is *P* (or *R* partially for trigonal system) for primitive lattice, *A*, *B* or *C* for base-centered lattice, *I* for body-centered lattice or *F* for face-centered lattice. In many cases of base-centered lattice, *C* is mainly used for H-M notations. However, there are four exceptions,

Table B.6: Extinction owing to screw axes.

Name of screw axis	Direction	Reflection condition (not extinct)	Example
2 ₁ screw axis	a	$h00 : h = 2n$	<i>P</i> 2 ₁ 2 ₁ 2 ₁ (#19) <i>P</i> 12 ₁ 1 (#4) <i>P</i> 12 ₁ / <i>c</i> 1 (#14) <i>C</i> 12/ <i>c</i> 1 (#15) <i>P</i> 2 ₁ 2 ₁ 2 ₁ (#19)
2 ₁ screw axis	b	$0k0 : k = 2n$	<i>P</i> 2 ₁ 2 ₁ 2 ₁ (#19)
2 ₁ screw axis	c	$00l : l = 2n$	<i>P</i> 2 ₁ 2 ₁ 2 ₁ (#19)
3 ₁ screw axis	c	$00l : l = 3n$	
3 ₂ screw axis	c	$00l : l = 3n$	
4 ₁ screw axis	c	$00l : l = 4n$	
4 ₂ screw axis	c	$00l : l = 2n$	
4 ₃ screw axis	c	$00l : l = 4n$	
6 ₁ screw axis	c	$00l : l = 6n$	
6 ₂ screw axis	c	$00l : l = 3n$	
6 ₃ screw axis	c	$00l : l = 2n$	
6 ₄ screw axis	c	$00l : l = 3n$	
6 ₅ screw axis	c	$00l : l = 6n$	

i.e. *Amm*2(#38), *Abm*2(#39), *Ama*2(#40) and *Aba*2(#41).

There are nine H-M full notations, i.e. *P*12₁/*c*1, *P*12₁/*n*1, *P*12₁/*a*1, *P*112₁/*a*, *P*112₁/*n*, *P*112₁/*b*, *P*2₁/*b*11, *P*2₁/*n*11, *P*2₁/*c*11 for *P*2₁/*c* due to arbitrariness to take axes. There are plural H-M full notations for an H-M notation in general. In some cases, however, there is only one H-M full notation, e.g. *P*2₁2₁2₁ (orthorhombic #19) since it has an identical symmetric element all in the directions of *a*, *b* and *c* axes.

In the case of *C*2/*c*, one of H-M full notation is *I*12/*a*1 when changing the choice of unit cell axes. This is the reason for ‘body-centered monoclinic lattice’ is added in Table B.1 [p.35].

B.3 How to read extinction rules

In this section, how to determine the space group by reading ‘process.out’ as shown in Figs. B.1 [p.34] and B.2 [p.34] and comparing them with *International Tables for Crystallography* (2006) Vol.A, Chapter 3.1, is described. When the space group were determined not correctly, it should be redetermined referring to the following description.

Table B.7 shows a part of *International Ta-*

Table B.7: *International Tables for Crystallography* (2006) Vol.A, A part of *International Tables for Crystallography* (2006) Vol.A, Chapter 3.1.

MONOCLINIC, Laue class $2/m$

Unique axis b				Laue class $1\ 2/m\ 1$			
Reflection condition				Point group			
hkl	$h0l$	$h00\ 00l$	$0k0$	Extinction symbol	2	m	$2/m$
			k	$P1-1$	$P121$ (3)	$P1m1$ (6)	$P1\ 2/m\ 1$ (10)
				$P12_11$	$P12_11$ (4)		$P1\ 2_1/m\ 1$ (11)
				$P1a1$		$P1a1$ (7)	$P1\ 2/a\ 1$ (13)
[1]	h	k		$P1\ 2_1/a\ 1$			$P1\ 2_1/a\ 1$ (14)
	l			$P1c1$		$P1c1$ (7)	$P1\ 2/c\ 1$ (13)
[2]	l	k		$P1\ 2_1/c\ 1$			$P1\ 2_1/c\ 1$ (14)
	$h+l$			$P1n1$		$P1n1$ (7)	$P1\ 2/n\ 1$ (13)
[3]	$h+l$	k		$P1\ 2_1/n\ 1$			$P1\ 2_1/n\ 1$ (14)
$h+k$	h	k		$C1-1$	$C121$ (5)	$C1m1$ (8)	$C1\ 2/m\ 1$ (12)
$h+k$	h, l	k		$C1c1$		$C1c1$ (9)	$C1\ 2/c\ 1$ (15)
$k+l$	l	k		$A1-1$	$A121$ (5)	$A1m1$ (8)	$A1\ 2/m\ 1$ (12)
$k+l$	h, l	k		$A1n1$		$A1n1$ (9)	$A1\ 2/n\ 1$ (15)
$h+k+l$	$h+l$	k		$I1-1$	$I121$ (5)	$I1m1$ (8)	$I1\ 2/m\ 1$ (12)
$h+k+l$	h, l	k		$I1a1$		$I1a1$ (9)	$I1\ 2/a\ 1$ (15)

bles for *Crystallography* (2006) Vol.A, Chapter 3.1. Here, relations between the extinction rule and space group, are summarized. You can refer to pdf version of *International Tables for Crystallography* (2006) Vol.A, Chapter 3.1 that is placed on the desktop of computers.

In part [1] of Fig. B.1 [p.34] reflection conditions for hkl all of which are not zero, is described. Since no extinction can be found, the first column of Table B.7 should be empty. $h+k$, $k+l$ and $h+k+l$ in this column means that reflection indices that satisfies $h+k=2n$, $k+l=2n$ and $h+k+l=2n$ do not distinguish. In first, second and third column in Table B.7, ‘ $=2n$ ’ is omitted.

In the case of Fig. B.1 [p.34], $0k0$ and $00l$ reflections distinguish when k is odd and when l is odd, respectively, which corresponds to [1], [2] and [3] rows in Table B.7. Therefore, H-M full notation of the space group of taurine is $P12_1/a1$, $P12_1/c1$ or $P12_1/n1$. These all belong to $P2_1/c$ (#14).

For redesignating space group in CrystalStructure 4.1, ‘Space Group’ Menu window as shown in Fig. B.6 [p.39] can be opened by clicking ‘Space Group’ from ‘Parameters’ menu. Since b axis is usually taken as the main axis in the case of monoclinic crystal system, $P12_1/c1$ should be selected. Then, click ‘Apply’ and ‘OK’ in this order, please.

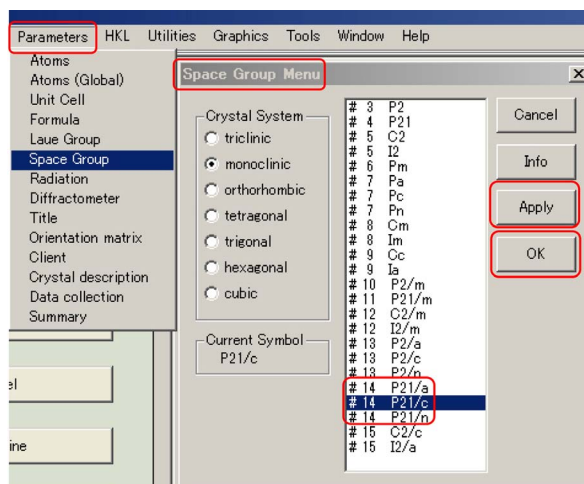


Figure B.6: Redesignation of space group in CrystalStructure 4.1. (in the case of small molecular-weight crystal).

B.4 Examples of extinction rules due to combinations of symmetric elements

In this section, several examples are described, in which the extinction rules are given by combinations of symmetric elements as summarized in Tables B.4 [p.38], B.5 [p.38] and B.6.

In cases of small molecular-weight organic crystals, frequently found space groups can be listed up in order of decreasing as follows, $P2_1/c$ (#14), $P\bar{1}$ (#2), $C2/c$ (#15), $P2_12_12_1$ (#19), $P2_1$ (#4). As many as 80% of small molecular weight organic crystals are occupied by those with space groups that belong to the above five.

In the cases of protein crystals, however, Hermann-Morguin notations of their space group do not have symbols of $\bar{1}$ (symmetric center), m (mirror plane), a , b , c , d , e and n (glide planes) absolutely since they need both optical enantiomer molecules in spite that protein molecules consist of only L amino acids but not of D amino acids. (L and D amino acids are optical enantiomer with each other). Also in the cases of small molecular-weight crystals, when they consist of chiral

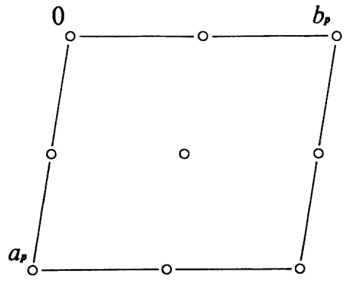


Figure B.7: Drawing for $P\bar{1}(\#2)$ in *International Tables for Crystallography* (2006) Vol.A. Since this space group has symmetric center, protein crystals do not belong to it. The phase problem is simple (0 or π (180°)).

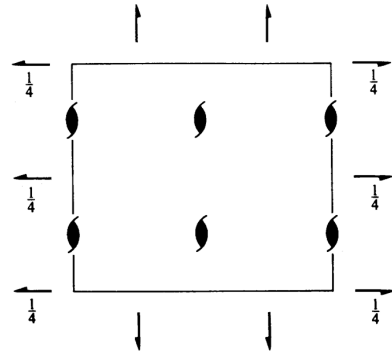


Figure B.9: *International Tables for Crystallography* (2006) Vol.A $P2_12_12_1(\#19)$.

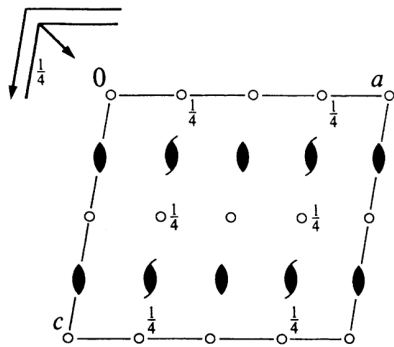


Figure B.8: Drawing for $C12/c1[C2/c](\#15)$ in *International Tables for Crystallography* (2006) Vol.A. Protein crystals do not belong to this space group absolutely since it has glide plane.

molecules, H-M notations of them do not have $\bar{1}, m, a, b, c, d, e$ and n . In the cases of racemic crystals, these symbols are frequently included in their H-M notations.

Read the following description, please by referring Tables B.4 [p.38], B.5 [p.38] and B.6.

It can be read from Fig. B.5 [p.37] that space group $P2_1/c$ ($P12_1/c1$) has c glide plane and 2_1 screw axis in the direction of b . Reflection conditions due to these symmetric elements can be read from Tables B.5 [p.38] and B.6.

Reflection conditions are described in *International Tables for Crystallography* (2006) Vol.A dividing three cases in which one, two and three indices of hkl are not zero. Following this rule, the reflection conditions due to

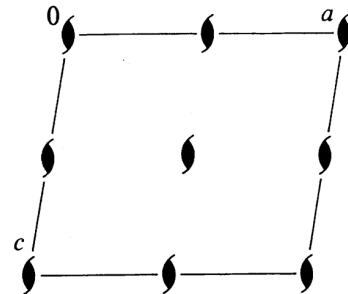


Figure B.10: *International Tables for Crystallography* (2006) Vol.A $P12_11[P2_1](\#4)$.

c glide plane and 2_1 screw axis are described as follows,

$$\begin{aligned} h0l : & \quad l = 2n, \\ 0k0 : & \quad k = 2n, \\ 00l : & \quad l = 2n. \end{aligned}$$

This is found as shown in Fig. B.4 [p.35] in *International Tables for Crystallography* (2006) Vol.A.

Symmetric element that space group $P\bar{1}(\#2)$ has, is only symmetric center. Therefore, there is no extinction. Protein crystals and chiral crystals do not belong to this space group, absolutely.

However, the phase problem is extremely simple (0 or π (180°)). Therefore, the molecular structure can be obtained frequently even for a crystal with low quality.

Since the initial character of $C12/c1$ is C , it is base-centered lattice. Since there are symmetric centers indicated by small open circles, the phase problem is very simple (0 or π (180°)).

Then, the molecular structure can be solved with high possibility.

Due to arbitrariness to take axes, there are three kinds of base-centered lattice, i.e. *A* base-centered, *B* base-centered and *C* base-centered lattice. However, let us focus the discussion on *C* base-centered lattice, here. The reflection condition shown in Table B.4 [p.38] can be written down dividing it into three cases in which one, two and three indices are not zero, as follows, $[hkl : h + k = 2n]$, $[hk0 : h + k = 2n]$, $[h0l : h = 2n]$, $[0kl : k = 2n]$, $[h00 : h = 2n]$, $[0k0 : k = 2n]$.

Referring to Fig. B.8[p.40], we can understand the existence of *c* glide plane, *n* glide plane and 2_1 screw axis that are perpendicular to **b** axis. The reflection condition due to *c* glide plane and *n* glide plane perpendicular to *b* axis can be read to be $[h0l : h, l = 2n]$. Further, that due to 2_1 screw axis can be read to be $[0k0 : k = 2n]$.

The logical product of the above conditions can be written down as follows,

$$\begin{array}{ll} hkl : & h + k = 2n, \\ h0l : & h, l = 2n, \\ 0kl : & k = 2n, \\ hk0 : & h + k = 2n, \\ 0k0 : & k = 2n, \\ h00 : & h = 2n, \\ 00l : & l = 2n. \end{array}$$

B.4.1 Orthorhombic $P2_12_12_1$ (#19)

It is evident from Fig. B.9 that $P2_12_12_1$ (#19) has 2_1 screw axes all in the directions of *a*, *b* and *c* axes. Therefore, referring to Table B.6 [p.38], the reflection condition is given as follows,

$$\begin{array}{ll} h00 : & h = 2n, \\ 0k0 : & k = 2n, \\ 00l : & l = 2n. \end{array}$$

B.4.2 Monoclinic $P12_11$ [$P2_1$ (#4)]

There are three H-M full notations for space group $P2_1$ (#4). Here, the description is given for $P12_11$.

Space group $P12_11$ has 2_1 screw axis as shown in Fig. B.10. Therefore, as described in Table

B.6 [p.38], it has a reflection condition as follows,

$$0k0 : \quad k = 2n.$$

B.5 Mathematical proofs of extinction rules

When the reader has time, refer to this chapter, please.

The extinction of reflection is caused by the existence of complex latticeC glide plane and screw axis whose background color is green in Tables B.1[p.35], B.2[p.36] and B.3[p.37]. To the contrary, only the above three symmetric elements give the extinction. However, protein crystals do not have glide plane absolutely. In this chapter, mathematical proofs of extinction due to the above symmetric elements are described.

For later description, let us note the definition of crystal structure factor, F_{hkl} for *hkl* reflection given as follows,

$$\begin{aligned} F_{hkl} &= \int_{\text{cell}} \rho(\mathbf{r}) \exp[-i2\pi(\mathbf{h} \cdot \mathbf{r})] dv. \\ &= \int_{\text{cell}} \rho(\mathbf{r}) \exp[-i2\pi(hx + ky + lz)] dv. \end{aligned} \tag{B.1}$$

Here, $\int_{\text{cell}} dv$ is a volume integral over a unit cell, $\rho(\mathbf{r})$ is electron density at location **r** ($= x\mathbf{a} + y\mathbf{b} + z\mathbf{c}$), and **h** ($= h\mathbf{a}^* + k\mathbf{b}^* + l\mathbf{c}^*$) is a reciprocal lattice vector giving *h k l* reflection. With regard to reciprocal lattice, refer to Appendix A [p.30], please.

Symmetry element that makes *N* equivalent points can be described as follows,

$$\rho[T^{(i)}(\mathbf{r})] = \rho[T^{(0)}(\mathbf{r})], \quad i \in \{0, 1, \dots, N-1\}.$$

Since F_{hkl} is zero when the *N* integral elements,

$$\sum_{i=0}^{N-1} \rho[T^{(0)}(\mathbf{r})] \exp[-i2\pi\mathbf{h} \cdot T^{(i)}(\mathbf{r})] = 0$$

That is to say,

$$\sum_{i=0}^{N-1} \exp[-i2\pi\mathbf{h} \cdot T^{(i)}(\mathbf{r})] = 0 \tag{B.2}$$

B.5.1 Extinction rules due to complex lattice

Table B.4 [p.38] summarizes the extinction rules due to complex lattice. In the following description, mathematical proofs for those due to base-centered, body-centered and face-centered lattice are given.

B.5.1.1 Extinction due to base-centered lattice

Symmetry of C base-centered lattice is described as follows,

$$\rho[T_C^{(i)}(\mathbf{r})] = \rho[T_C^{(0)}(\mathbf{r})], \quad i \in \{0, 1\}.$$

$$T_C^{(0)}(\mathbf{r}) = x\mathbf{a} + y\mathbf{b} + z\mathbf{c},$$

$$T_C^{(1)}(\mathbf{r}) = \left(x + \frac{1}{2}\right)\mathbf{a} + \left(y + \frac{1}{2}\right)\mathbf{b} + z\mathbf{c}.$$

The extinction condition is described similarly to (B.2) as follows:

$$\sum_{i=0}^1 \exp[-i2\pi\mathbf{h} \cdot T_C^{(i)}(\mathbf{r})] = 0. \quad (\text{B.3})$$

Here, mathematical convenience to calculate \sum in (B.3), let us define $f_C(\mathbf{h}, \mathbf{r})$ as follows,

$$\begin{aligned} f_C(\mathbf{h}, \mathbf{r}) &= \exp\{-i2\pi[h(x + \frac{1}{4}) + k(y + \frac{1}{4}) + lz]\}. \end{aligned}$$

Therefore, the extinction condition is described as follows,

$$\begin{aligned} f_C(\mathbf{h}, \mathbf{r}) &\times \{\exp[-i\frac{\pi}{2}(h+k)] + \exp[+i\frac{\pi}{2}(h+k)]\} \\ &= 2f_C(\mathbf{h}, \mathbf{r}) \cos[\frac{\pi}{2}(h+k)] = 0. \end{aligned}$$

Since $f_C(\mathbf{h}, \mathbf{r})$ is not zero in general, the extinction condition is given by

$$\cos[\frac{\pi}{2}(h+k)] = 0.$$

Since the above equation is satisfied when $h+k$ is odd, the reflection condition (not extinct) as shown in Table B.4 [p.38] is given by

$$hkl : \quad @h + k = 2n$$

Here, l is an arbitrary integer.

Reflection conditions for A and B base-centered lattice can be derived similarly to the above description.

B.5.1.2 Extinction due to body-centered lattice

Symmetry of body-centered lattice is described as follows,

$$\rho[T_I^{(i)}(\mathbf{r})] = \rho[T_I^{(0)}(\mathbf{r})], \quad i \in \{0, 1\}.$$

$$T_I^{(0)}(\mathbf{r}) = x\mathbf{a} + y\mathbf{b} + z\mathbf{c},$$

$$T_I^{(1)}(\mathbf{r}) = \left(x + \frac{1}{2}\right)\mathbf{a}$$

$$+ \left(y + \frac{1}{2}\right)\mathbf{b}$$

$$+ \left(z + \frac{1}{2}\right)\mathbf{c}.$$

The extinction condition is described similarly to (B.2) [p.41] as follows,

$$\sum_{i=0}^1 \exp[-i2\pi\mathbf{h} \cdot T_I^{(i)}(\mathbf{r})] = 0. \quad (\text{B.4})$$

For convenience for calculation of \sum in (B.4), let $f_I(\mathbf{h}, \mathbf{r})$ be defined as follows,

$$\begin{aligned} f_I(\mathbf{h}, \mathbf{r}) &= \exp\{-i2\pi[h(x + \frac{1}{4}) \\ &\quad + k(y + \frac{1}{4}) \\ &\quad + l(z + \frac{1}{4})]\}. \end{aligned}$$

Therefore, the extinction condition is given as follows,

$$\begin{aligned} f_I(\mathbf{h}, \mathbf{r}) &\times \\ &\{\exp[-i\frac{\pi}{2}(h+k+l)] \\ &+ \exp[+i\frac{\pi}{2}(h+k+l)]\} \\ &= 2f_I(\mathbf{h}, \mathbf{r}) \cos[\frac{\pi}{2}(h+k+l)] = 0. \end{aligned}$$

Since $f_I(\mathbf{h}, \mathbf{r})$ is not zero in general, the extinction condition is given by

$$\cos[\frac{\pi}{2}(h+k+l)] = 0.$$

Since the above equation is satisfied when $h+k+l$ is odd, the reflection condition (not extinct) as shown in Table B.4 [p.38], is given as follows,

$$hkl : \quad h + k + l = 2n$$

B.5.1.3 Extinction due to face-centered lattice

Symmetry of face-centered lattice is described as follows,

$$\begin{aligned}\rho[T_F^{(i)}(\mathbf{r})] &= \rho[T_F^{(0)}(\mathbf{r})], \quad i \in \{0, 1, 2, 3\}. \\ T_F^{(0)}(\mathbf{r}) &= x\mathbf{a} + y\mathbf{b} + z\mathbf{c}, \\ T_F^{(1)}(\mathbf{r}) &= x\mathbf{a} + (y + \frac{1}{2})\mathbf{b} + (z + \frac{1}{2})\mathbf{c}, \\ T_F^{(2)}(\mathbf{r}) &= (x + \frac{1}{2})\mathbf{a} + y\mathbf{b} + (z + \frac{1}{2})\mathbf{c}, \\ T_F^{(3)}(\mathbf{r}) &= (x + \frac{1}{2})\mathbf{a} + (y + \frac{1}{2})\mathbf{b} + z\mathbf{c}.\end{aligned}$$

The extinction condition is described similarly to (B.2) [p.41] by the following equation,

$$\sum_{i=0}^3 \exp[-i2\pi\mathbf{h} \cdot T_F^{(i)}(\mathbf{r})] = 0. \quad (\text{B.5})$$

Here, for mathematical convenience to calculate \sum in (B.5), let us define $f_F(\mathbf{h}, \mathbf{r})$ as follows,

$$\begin{aligned}f_F(\mathbf{h}, \mathbf{r}) &= \exp\{-i2\pi[h(x + \frac{1}{4}) \\ &\quad + k(y + \frac{1}{4}) \\ &\quad + l(z + \frac{1}{4})]\}.\end{aligned}$$

Therefore, the extinction condition is given as follows,

$$\begin{aligned}& f_F(\mathbf{h}, \mathbf{r}) \{ \exp[-i\frac{\pi}{2}(-h - k - l)] \\ & \quad + \exp[-i\frac{\pi}{2}(-h + k + l)] \\ & \quad + \exp[-i\frac{\pi}{2}(+h - k + l)] \\ & \quad + \exp[-i\frac{\pi}{2}(+h + k - l)] \} \quad (\text{B.6}) \\ &= 2f_F(\mathbf{h}, \mathbf{r}) \{ \exp(+i\frac{\pi}{2}h) \cos[\frac{\pi}{2}(k + l)] \\ & \quad + \exp(-i\frac{\pi}{2}h) \cos[\frac{\pi}{2}(k - l)] \} = 0. \quad (\text{B.7})\end{aligned}$$

Since $f_F(\mathbf{h}, \mathbf{r})$ is not zero in general, the extinction condition is represented as follows,

$$\begin{aligned}\cos[\frac{\pi}{2}(k + l)] &= 0, \\ \cos[\frac{\pi}{2}(k - l)] &= 0.\end{aligned}$$

[[$(k + l$ is even) and $(k - l$ is even)] is identical to [(both k and l are even) or (both k and l are odd)] i.e. $k + l = 2n$. Here, h is an arbitrary integer. Since (B.6) is symmetrical for h, k and l , equations similar to (B.7) can be derived also for $h + k, h - k$ and $h + l, h - l$. Then, The reflection condition (not distinguishing) as shown in Table B.4 [p.38] is given by

$$\begin{aligned}hkl : \quad h + k &= 2n, \\ hkl : \quad h + l &= 2n, \\ hkl : \quad l + k &= 2n.\end{aligned}$$

That is to say, reflection distinguishes when even and odd integers are mixed in h, k and l .

B.5.2 Extinction owing to glide axes

In cases of protein crystals, they do not have glide axis absolutely since they consist of only L amino acids but of not D amino acids (optical isomers of L amino acids).

B.5.2.1 Extinction due to axial glide plane

Symmetry due to c glide plane perpendicular to \mathbf{b} axis whose height is $\frac{1}{4}\mathbf{b}$, is given by

$$\begin{aligned}\rho[T_{Bc}^{(i)}(\mathbf{r})] &= \rho[T_{Bc}^{(0)}(\mathbf{r})], \quad i \in \{0, 1\}. \\ T_{Bc}^{(0)}(\mathbf{r}) &= x\mathbf{a} + y\mathbf{b} + z\mathbf{c}, \\ T_{Bc}^{(1)}(\mathbf{r}) &= x\mathbf{a} + (\frac{1}{2} - y)\mathbf{b} + (\frac{1}{2} + z)\mathbf{c},\end{aligned}$$

Similarly to (B.2) [p.41], the extinction condition is given by

$$\sum_{i=0}^1 \exp[-i2\pi\mathbf{h} \cdot T_{Bc}^{(i)}(\mathbf{r})] = 0. \quad (\text{B.8})$$

Here, for mathematical convenience to calculate \sum in (B.8) [p.43], let us define $f_{Bc}(\mathbf{h}, \mathbf{r})$ as follows,

$$f_{Bc}(\mathbf{h}, \mathbf{r}) = \exp\{-i2\pi[hx + k\frac{1}{4} + l(\frac{1}{4} + z)]\}.$$

$$\begin{aligned}& f_{Bc}(\mathbf{h}, \mathbf{r}) \times \\ & \quad \left\{ \exp\{+i2\pi[k(\frac{1}{4} - y) + l\frac{1}{4}]\} \right. \\ & \quad \left. + \exp\{-i2\pi[k(\frac{1}{4} - y) + l\frac{1}{4}]\} \right\} \\ &= 2f_{Bc}(\mathbf{h}, \mathbf{r}) \cos\{\frac{\pi}{2}[k(1 - 4y) + l]\} = 0.\end{aligned}$$

Since $f_F(\mathbf{h}, \mathbf{r})$ is not zero in general, reflections distinguish when the term of $\cos\{ \}$ is zero, i.e. when h is arbitrary, $k = 0$ and l is odd, the reflection condition as shown in Table B.5 [p.38] is given by

$$h0l : \quad l = 2n$$

B.5.2.2 Extinction due to double glide plane (e glide plane)

Therefore, Symmetry due to double glide plane (e glide plane) whose height is zero, is described as follows,

$$\begin{aligned} \rho[T_{Be}^{(i)}(\mathbf{r})] &= \rho[T_{Be}^{(0)}(\mathbf{r})], \quad i \in \{0, 1, 2, 3\}. \\ T_{Be}^{(0)}(\mathbf{r}) &= x\mathbf{a} + y\mathbf{b} + z\mathbf{c}, \\ T_{Be}^{(1)}(\mathbf{r}) &= (x + \frac{1}{2})\mathbf{a} - y\mathbf{b} + z\mathbf{c}, \\ T_{Be}^{(2)}(\mathbf{r}) &= x\mathbf{a} - y\mathbf{b} + (z + \frac{1}{2})\mathbf{c}, \\ T_{Be}^{(3)}(\mathbf{r}) &= (x + \frac{1}{2})\mathbf{a} + y\mathbf{b} + (z + \frac{1}{2})\mathbf{c}, \end{aligned}$$

Similarly to (B.2) [p.41], the extinction rule is described by

$$\sum_{i=0}^3 \exp[-i2\pi\mathbf{h} \cdot T_{Be}^{(i)}(\mathbf{r})] = 0. \quad (\text{B.9})$$

Here, for mathematical convenience to calculate \sum in (B.9), let us define $f_{Be}(\mathbf{h}, \mathbf{r})$ as follows,

$$f_{Be}(\mathbf{h}, \mathbf{r}) = \exp\{-i2\pi[h(\frac{1}{4} + x) + l(\frac{1}{4} + z)]\}.$$

Therefore, the extinction condition can be described as follows,

$$\begin{aligned} f_{Be}(\mathbf{h}, \mathbf{r}) \times \\ \left\{ \exp\{-i2\pi[-h\frac{1}{4} + ky - l\frac{1}{4}]\} \right. \\ + \exp\{-i2\pi[+h\frac{1}{4} - ky - l\frac{1}{4}]\} \\ + \exp\{-i2\pi[-h\frac{1}{4} - ky + l\frac{1}{4}]\} \\ \left. + \exp\{-i2\pi[+h\frac{1}{4} + ky + l\frac{1}{4}]\} \right\} \\ = 2f_{Be}(\mathbf{h}, \mathbf{r}) \times \\ \left\{ \exp(-i2\pi ky) \cos[\frac{\pi}{2}(h + l)] \right. \\ \left. + \exp(+i2\pi ky) \cos[\frac{\pi}{2}(h - l)] \right\} = 0. \end{aligned}$$

Since $f_{Be}(\mathbf{h}, \mathbf{r})$ and $\exp(\pm i2\pi ky)$ are not zero in general, the above extinction condition is satisfied when $\cos[\frac{\pi}{2}(h + l)] = 0 \cos[\frac{\pi}{2}(h - l)] = 0$. hkl reflections distinguish when both $h + l$ and $h - l$ are odd, i.e. when k is arbitrary and $[(h, k \text{ are odd}) \text{ or } (h, k \text{ are even})]$. The reflection condition (not extinct) is given by

$$hkl : \quad h + l = 2n$$

With regard to other double glide planes, extinction rules as shown in Table B.5 [p.38] can be derived in a similar way.

B.5.2.3 Extinction due to diagonal glide plane

Symmetry due to diagonal glide plane (n glide plane) whose height is zero, is described as follows,

$$\begin{aligned} \rho[T_{Bn}^{(i)}(\mathbf{r})] &= \rho[T_{Bn}^{(0)}(\mathbf{r})], \quad i \in \{0, 1\}. \\ T_{Bn}^{(0)}(\mathbf{r}) &= x\mathbf{a} + y\mathbf{b} + z\mathbf{c}, \\ T_{Bn}^{(1)}(\mathbf{r}) &= (\frac{1}{2} + x)\mathbf{a} - y\mathbf{b} + (\frac{1}{2} + z)\mathbf{c}, \end{aligned}$$

The extinction condition is described similarly to (B.2) [p.41] as follows,

$$\sum_{i=0}^1 \exp[-i2\pi\mathbf{h} \cdot T_{Bn}^{(i)}(\mathbf{r})] = 0. \quad (\text{B.10})$$

Here, mathematical convenience to calculate \sum in (B.10), let us define $f_{Bn}(\mathbf{h}, \mathbf{r})$ as follows,

$$f_{Bn}(\mathbf{h}, \mathbf{r}) = \exp\{-i2\pi[h(\frac{1}{4} + x) + l(\frac{1}{4} + z)]\}.$$

Therefore, the extinction condition is described as follows,

$$\begin{aligned} f_{Bn}(\mathbf{h}, \mathbf{r}) \times \\ \left\{ \exp\{-i2\pi[-h\frac{1}{4} + ky - l\frac{1}{4}]\} \right. \\ \left. + \exp\{-i2\pi[h\frac{1}{4} - ky + l\frac{1}{4}]\} \right\} \\ = 2f_{Bn}(\mathbf{h}, \mathbf{r}) \cos\left\{\frac{\pi}{2}[4ky - (h + l)]\right\} = 0. \end{aligned}$$

Since $f_{Bn}(\mathbf{h}, \mathbf{r})$ is not zero in general, hkl reflections distinguish when the term of $\cos\{ \}$ is zero. Therefore, the reflection condition (not extinct) is described as follows,

$$h0l : \quad h + l = 2n$$

With regard to other orthogonal glide plane, reflection conditions as summarized in Table B.5 [p.38] can be derived.

B.5.3 Extinction due to screw axes tion,

Table B.6 [p.38] summarizes extinction rules due to p_q screw axes. Here $p \in \{2, 3, 4, 6\}$ and $q \in \{1, \dots, p-1\}$, p_q screw axis makes p equivalent points such that they translate by $q\mathbf{c}/p$, ($q\mathbf{a}/p$ or $q\mathbf{b}/p$) when rotated by $2\pi/p$ around the axis. As summarized in Table B.6 [p.38], reflection condition $[00l : l = 2n]$ is given by 2_1 , 4_2 and 6_3 screw axes since they make layers of atoms (molecules) whose spacing is c , (a or b).

Similarly, reflection conditions $[000l : l = 3n]$ for 3_1 , 3_2 , 6_2 , 6_4 screw axes, $[00l : l = 4n]$ for 4_1 , 4_3 screw axes and $[000l : l = 6n]$ for 6_1 , 6_5 screw axes can be derived. For mathematical proof of reflection conditions for three- and six-fold screw axes, refer to Appendix C [p.48], please.

In the following description, mathematical proofs of extinction rules due to 2_1 , 4_1 and 4_2 screw axes.

B.5.3.1 Extinction due to 2_1 screw axis

Symmetry of 2_1 screw axis in the direction of \mathbf{c} located at $\frac{1}{2}\mathbf{a} + \frac{1}{2}\mathbf{b}$, is described as follows,

$$\begin{aligned} \rho[T_{2_1}^{(i)}(\mathbf{r})] &= \rho[T_{2_1}^{(0)}(\mathbf{r})], \quad i \in \{0, 1\}. \\ T_{2_1}^{(0)}(\mathbf{r}) &= \left(\frac{1}{2} + x\right)\mathbf{a} + \left(\frac{1}{2} + y\right)\mathbf{b} + z\mathbf{c}, \\ T_{2_1}^{(1)}(\mathbf{r}) &= \left(\frac{1}{2} - x\right)\mathbf{a} + \left(\frac{1}{2} - y\right)\mathbf{b} + \left(\frac{1}{2} + z\right)\mathbf{c}. \end{aligned}$$

The extinction condition is described similarly to (B.2) [p.41] as follows,

$$\sum_{i=0}^1 \exp[-i2\pi\mathbf{h} \cdot T_{2_1}^{(i)}(\mathbf{r})] = 0. \quad (\text{B.11})$$

Here, for mathematical convenience to calculate \sum of (B.11), let us define $f_{2_1}(\mathbf{h}, \mathbf{r})$ as follows,

$$f_{2_1}(\mathbf{h}, \mathbf{r}) = \exp\left\{-i2\pi\left[h\frac{1}{2} + k\frac{1}{2} + l\left(\frac{1}{4} + z\right)\right]\right\}.$$

Therefore, summation in (B.11) can be deformed to give the following extinction condi-

$$\begin{aligned} &f_{2_1}(\mathbf{h}, \mathbf{r}) \times \\ &\left\{ \exp\left\{-i2\pi\left[hx + ky - l\frac{1}{4}\right]\right\} \right. \\ &\left. + \exp\left\{-i2\pi\left[-hx - ky + l\frac{1}{4}\right]\right\} \right\} \\ &= f_{2_1}(\mathbf{h}, \mathbf{r}) \times \\ &\cos\left\{\frac{\pi}{2}[4(hx + ky) - l]\right\} = 0. \end{aligned}$$

Since term of $\cos\{ \}$ is zero when $h, k = 0$ and l is odd, the reflection condition (not extinct) is given by

$$00l : l = 2n.$$

Similarly, the reflection conditions due to \mathbf{c} and \mathbf{a} screw axes can be obtained as summarized in Table B.6 [p.38].

B.5.3.2 Extinction due to 4_1 screw axis

Symmetry due to 4_1 screw axis that is located at the origin, can be described as follows,

$$\begin{aligned} \rho[T_{4_1}^{(i)}(\mathbf{r})] &= \rho[T_{4_1}^{(0)}(\mathbf{r})], \quad i \in \{0, 1, 2, 3\}. \\ T_{4_1}^{(0)}(\mathbf{r}) &= +x\mathbf{a} + y\mathbf{b} + \frac{1}{8}\mathbf{c}, \\ T_{4_1}^{(1)}(\mathbf{r}) &= -y\mathbf{a} + x\mathbf{b} + \frac{3}{8}\mathbf{c}, \\ T_{4_1}^{(2)}(\mathbf{r}) &= -x\mathbf{a} - y\mathbf{b} + \frac{5}{8}\mathbf{c}, \\ T_{4_1}^{(3)}(\mathbf{r}) &= +y\mathbf{a} - x\mathbf{b} + \frac{7}{8}\mathbf{c}. \end{aligned}$$

Here, the extinction condition is described similarly to (B.2) [p.41] as follows,

$$\sum_{i=0}^3 \exp[-i2\pi\mathbf{h} \cdot T_{4_1}^{(i)}(\mathbf{r})] = 0. \quad (\text{B.12})$$

Here, let us define $f_{4_1}(\mathbf{h}, \mathbf{r})$ as follows,

$$f_{4_1}(\mathbf{h}, \mathbf{r}) = \exp(-i2\pi l \frac{1}{2}).$$

Therefore, summation in (B.12) can be deformed to give the following extinction condi-

tion,

$$\begin{aligned}
& f_{4_1}(\mathbf{h}, \mathbf{r}) \times \\
& \left\{ \exp[-i2\pi(+hx + ky - l\frac{3}{8})] \right. \\
& + \exp[-i2\pi(-hy + kx - l\frac{1}{8})] \\
& + \exp[-i2\pi(-hx - ky + l\frac{1}{8})] \\
& \left. + \exp[-i2\pi(+hy - kx + l\frac{3}{8})] \right\} \\
& = 2f_{4_1}(\mathbf{h}, \mathbf{r}) \times \\
& \left\{ \exp(+i2\pi l\frac{1}{8}) \cos\left\{\frac{\pi}{2}[4(hx + ky) - l]\right\} \right. \\
& \left. + \exp(-i2\pi l\frac{1}{8}) \cos\left\{\frac{\pi}{2}[4(hy - kx) + l]\right\} \right\} \\
& = 0.
\end{aligned}$$

When $h, k = 0$ and l is even, $\cos\{ \}$ in the first and second terms of the above equation have an identical value (1 or -1). Under an assumption that this condition is satisfied, let us discuss the condition that the above equation gives value of zero as follows,

$$\begin{aligned}
& \exp(-i2\pi l\frac{1}{8}) + \exp(-i2\pi l\frac{1}{8}) \\
& = 2 \cos\left(\frac{\pi}{2} \cdot \frac{l}{2}\right) = 0.
\end{aligned}$$

The above equation means that reflections distinguish when $l/2$ is odd. Therefore, the reflection condition (not extinct) can be described as follows,

$$00l : l = 4n.$$

Similarly, reflection condition due to 4_3 screw axis can be obtained.

B.5.3.3 Extinction due to 4_2 screw axis

Symmetry due to 4_2 screw axis at the origin can be describes as follows,

$$\begin{aligned}
\rho[T_{4_2}^{(i)}(\mathbf{r})] &= \rho[T_{4_2}^{(0)}(\mathbf{r})], \quad i \in \{0, 1, 2, 3\}. \\
T_{4_2}^{(0)}(\mathbf{r}) &= +x\mathbf{a} + y\mathbf{b} + \frac{1}{4}\mathbf{c}, \\
T_{4_2}^{(1)}(\mathbf{r}) &= -y\mathbf{a} + x\mathbf{b} + \frac{3}{4}\mathbf{c}, \\
T_{4_2}^{(2)}(\mathbf{r}) &= -x\mathbf{a} - y\mathbf{b} + \frac{1}{4}\mathbf{c}, \\
T_{4_2}^{(3)}(\mathbf{r}) &= +y\mathbf{a} - x\mathbf{b} + \frac{3}{4}\mathbf{c}.
\end{aligned}$$

A point translates by $\frac{2}{4}\mathbf{c}$ when rotating by $\frac{2\pi}{4}$ around the axis. Here, note that the heights of $T_{4_2}^{(2)}(\mathbf{r})$ and $T_{4_2}^{(3)}(\mathbf{r})$ are $\frac{5}{4}\mathbf{c}$ and $\frac{7}{4}\mathbf{c}$ which are equivalent to $\frac{1}{4}\mathbf{c}$, $\frac{3}{4}\mathbf{c}$ due to translation symmetry of unit cell.

The, the extinction condition is described similarly to (B.2) [p.41] as follows,

$$\sum_{i=0}^3 \exp[-i2\pi\mathbf{h} \cdot T_{4_2}^{(i)}] = 0. \quad (\text{B.13})$$

Here, for mathematical convenience to calculate \sum in (B.13), let $f_{4_2}(\mathbf{h}, \mathbf{r})$ be dined as follows,

$$f_{4_2}(\mathbf{h}, \mathbf{r}) = \exp[-i2\pi(l\frac{1}{2})].$$

$f_{4_2}(\mathbf{h}, \mathbf{r})$ Therefore, deforming the \sum in (B.13), the extinction condition can be obtained as follows,

$$\begin{aligned}
& f_{4_2}(\mathbf{h}, \mathbf{r}) \times \\
& \left\{ \exp[-i2\pi(+hx + ky - l\frac{1}{4})] \right. \\
& + \exp[-i2\pi(-ky + hx + l\frac{1}{4})] \\
& + \exp[-i2\pi(-hx - ky - l\frac{1}{4})] \\
& \left. + \exp[-i2\pi(+kx - hy + l\frac{1}{4})] \right\}
\end{aligned}$$

$$\begin{aligned}
&= 2f_{4_2}(\mathbf{h}, \mathbf{r}) \times \\
&\left\{ \exp(+i2\pi l \frac{1}{4}) \cos[2\pi(hx + ky)] \right. \\
&\left. + \exp(-i2\pi l \frac{1}{4}) \cos[2\pi(kx - hy)] \right\} \\
&= 0.
\end{aligned}$$

The above extinction can be discussed when the content of $\cos[]$ is zero. Under the assumption that the above condition is satisfied, the above equation can be further deformed as follows,

$$\begin{aligned}
&\exp(-i2\pi l \frac{1}{4}) + \exp(+i2\pi l \frac{1}{4}) \\
&= 2 \cos(\frac{\pi}{2}l) = 0.
\end{aligned}$$

Therefore, the reflection condition (not extinct) can be described as follows,

$$00l : l = 2n.$$

Reflection condition due to 6_3 screw axis is the same as the above description. With regard to this, refer to §C.2.5 [p.53] in Appendix C, please.

Appendix C

Reflection indices and extinction rules in the cases of trigonal and hexagonal crystals

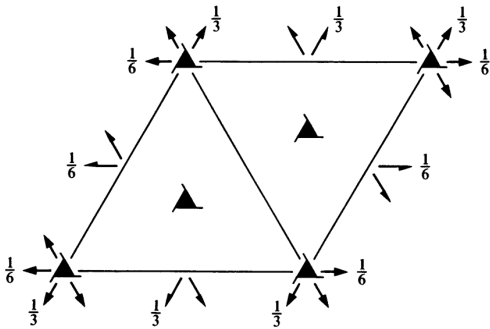


Figure C.1: *International Tables for Crystallography* (2006) Vol.A, Symmetric elements. $P3_121$ (#152).

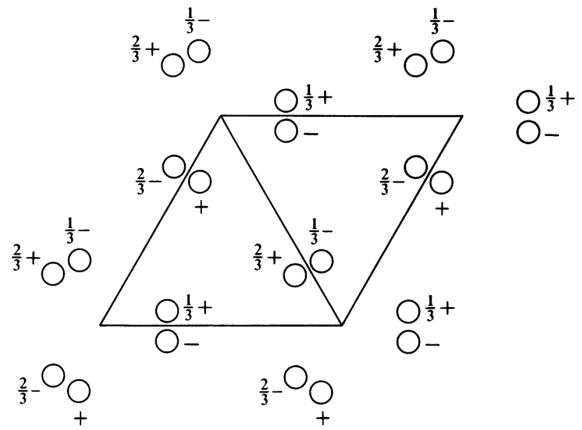


Figure C.2: *International Tables for Crystallography* (2006) Vol.A, Positions of atoms. $P3_121$ (#152).

Read this chapter when the reader has time, please.

In cases of trigonal and hexagonal crystal system, reflection vectors are usually indexed by four integers, $h k i l$ ($h + k + i = 0$). This chapter describes the reasonableness of this way of indexing and the extinction rules due to three- and six-fold screw axes.

C.1 Cases of trigonal system

C.1.1 Diagram shown in *International Tables for Crystallography* (2006) Vol.A

Fig. C.1 is a diagram in *International Tables for Crystallography* (2006) Vol.A that

shows symmetric elements of space group $P3_121$ (#152). Fig. C.2 shows atomic coordinates of $P3_121$ (#152).

The unit cell is usually taken to be a rhombus that consists of two regular triangles as shown in Figs. C.1 and C.2. Space group $P3_121$ (#152) has three-fold screw axis in the direction of c axis and two-fold screw axis perpendicular to c axis. However, in the case of trigonal system, there is no extinction due to the two-fold screw axis. About this, refer to the description in §C.1.4 [p.50], please.

C.1.2 Real and reciprocal coordinates

Fig. C.3 shows real and reciprocal primitive translation vectors in the cases of trigonal and hexagonal crystal system.

\mathbf{a} , \mathbf{b} and \mathbf{c} axes are usually taken such that the angle spanned by \mathbf{a} and \mathbf{b} axes is 120° and \mathbf{c} is parallel to three-fold rotation or screw axis. There are three way of taking \mathbf{a} and \mathbf{b} axes as shown in Fig. C.3 i.e. combinations of \mathbf{a}_0 and \mathbf{b}_0 axes, \mathbf{a}_1 and \mathbf{b}_1 axes and \mathbf{a}_2 and \mathbf{b}_2 axes.

reciprocal primitive vectors are defined as follows:

$$\begin{aligned}\mathbf{a}^* &= \frac{\mathbf{b} \times \mathbf{c}}{\mathbf{a} \cdot (\mathbf{b} \times \mathbf{c})}, \\ \mathbf{b}^* &= \frac{\mathbf{c} \times \mathbf{a}}{\mathbf{a} \cdot (\mathbf{b} \times \mathbf{c})}, \\ \mathbf{c}^* &= \frac{\mathbf{a} \times \mathbf{b}}{\mathbf{a} \cdot (\mathbf{b} \times \mathbf{c})}.\end{aligned}$$

About the reasonableness of the above definition, refer to Appendix A [p.30], please.

By following the above definition, in Fig. C.3, real (black) and reciprocal (gray) primitive translation vectors are drawn. Referring to this figure, the following relations can easily be understood,

$$\begin{aligned}\mathbf{a}_0^* &= -\mathbf{b}_1^* \\ &= -\mathbf{a}_2^* + \mathbf{b}_2^*, \\ \mathbf{b}_0^* &= \mathbf{a}_1^* - \mathbf{b}_1^* \\ &= -\mathbf{a}_2^*.\end{aligned}$$

From the above relations, reciprocal lattice vector $h\mathbf{a}_0^* + k\mathbf{b}_0^* + l\mathbf{c}^*$ can also be represented as follows:

$$\begin{aligned}h\mathbf{a}_0^* + k\mathbf{b}_0^* + l\mathbf{c}^* \\ &= k\mathbf{a}_1^* + i\mathbf{b}_1^* + l\mathbf{c}^* \\ &= i\mathbf{a}_2^* + h\mathbf{b}_2^* + l\mathbf{c}^*,\end{aligned}$$

where, $h + k + i = 0$.

By using four indices h , k , i and l ($h + k + i = 0$) to describe reflections, we can easily understand the equivalence of reflections due to three-fold symmetry. For example, a reflection described as $1\ 1\ 1\ 0$ by using $\mathbf{a}_0^*-\mathbf{b}_0^*-\mathbf{c}^*$ coordinate system is equivalent to $1\ \bar{2}\ 0$ by $\mathbf{a}_1^*-\mathbf{b}_1^*-\mathbf{c}^*$ system and also to $\bar{2}\ 1\ 0$ by $\mathbf{a}_2^*-\mathbf{b}_2^*-\mathbf{c}^*$ system. This reflection $1\ 1\ \bar{2}\ 0$ described using four indices can easily be understood to be equivalent to $1\ \bar{2}\ 1\ 0$ and $\bar{2}\ 1\ 1\ 0$.

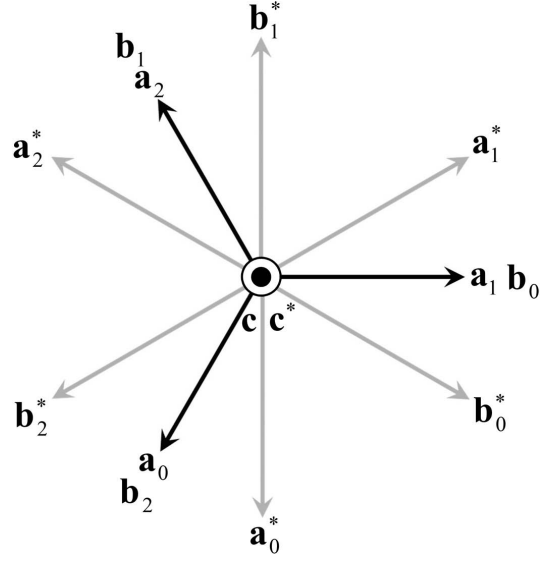


Figure C.3: Real (black) and reciprocal (gray) primitive translation vectors.

C.1.3 Derivation of extinction rule due to 3_1 screw axis

Similarly to the description in Appendix B §B.5 [p.41], the extinction due to 3_1 screw axis can be derived as follows.

Symmetry due to 3_1 screw axis at the origin is described as follows:

$$\begin{aligned}\rho[T_{3_1}^{(i)}(\mathbf{r})] &= \rho[T_{3_1}^{(0)}(\mathbf{r})], \quad i \in \{0, 1, 2\}. \\ T_{3_1}^{(0)}(\mathbf{r}) &= x\mathbf{a}_0 + y\mathbf{b}_0 + z\mathbf{c}, \\ T_{3_1}^{(1)}(\mathbf{r}) &= x\mathbf{a}_1 + y\mathbf{b}_1 + \left(\frac{1}{3} + z\right)\mathbf{c}, \\ T_{3_1}^{(2)}(\mathbf{r}) &= x\mathbf{a}_2 + y\mathbf{b}_2 + \left(\frac{2}{3} + z\right)\mathbf{c}.\end{aligned}\quad (\text{C.1})$$

On the other hand, referring to Fig. C.3, the following relations are evident.

$$\begin{aligned}\mathbf{a}_1 &= \mathbf{b}_0, \\ \mathbf{b}_1 &= -\mathbf{a}_0 - \mathbf{b}_0, \\ \mathbf{a}_2 &= -\mathbf{a}_0 - \mathbf{b}_0, \\ \mathbf{b}_2 &= \mathbf{a}_0,\end{aligned}$$

Substituting the above equation into (C.1),

$$\begin{aligned}\rho[T_{3_1}^{(i)}(\mathbf{r})] &= \rho[T_{3_1}^{(0)}(\mathbf{r})], \quad i \in \{0, 1, 2\}. \\ T_{3_1}^{(0)}(\mathbf{r}) &= x\mathbf{a}_0 + y\mathbf{b}_0 + z\mathbf{c}, \\ T_{3_1}^{(1)}(\mathbf{r}) &= -y\mathbf{a}_0 + (x - y)\mathbf{b}_0 + \left(\frac{1}{3} + z\right)\mathbf{c}, \\ T_{3_1}^{(2)}(\mathbf{r}) &= (-x + y)\mathbf{a}_0 - x\mathbf{b}_0 + \left(\frac{2}{3} + z\right)\mathbf{c}.\end{aligned}$$

The extinction condition can be described similarly to (B.2) [p.41] as follows:

$$\sum_{i=0}^2 \exp[-i2\pi \mathbf{h} \cdot T_{3_1}^{(i)}(\mathbf{r})] = 0. \quad (\text{C.2})$$

Here, for mathematical convenience to calculate \sum of (C.2), let us define $f_{3_1}(\mathbf{h}, \mathbf{r})$ as follows:

$$f_{3_1}(\mathbf{h}, \mathbf{r}) = \exp[-i2\pi(lz)].$$

Therefore, (C.2) can be deformed as follows:

$$\begin{aligned} & f_{3_1}(\mathbf{h}, \mathbf{r}) \times \\ & \left\{ \exp\{-i2\pi[hx + ky]\} \right. \\ & + \exp\{-i2\pi[-hy + k(x - y) + l\frac{1}{3}]\} \\ & \left. + \exp\{-i2\pi[+h(-x + y) - kx + l\frac{2}{3}]\} \right\} = 0. \end{aligned}$$

Since terms $[hx + ky]$, $[-hy + k(x - y)]$ and $[h(-x + y) - kx]$ in $\exp\{\}$ of the above equation depend on value of x and y , the extinction can be discussed only when $h = k = l = 0$. Under this condition, the extinction condition can be described as follows:

$$1 + \exp(-i2\pi l \frac{1}{3}) + \exp(-i2\pi l \frac{2}{3}) = 0.$$

The second and third terms of on the left-hand side of the above equation are 1 and 1 not giving extinction when $l = 3n$, $\exp(-i2\pi \frac{1}{3})$ and $\exp(-i2\pi \frac{2}{3})$ giving extinction and $\exp(-i2\pi \frac{2}{3})$ and $\exp(-i2\pi \frac{1}{3})$ giving extinction. Therefore, the reflection condition can be described as follows:

$$000l : \quad l = 3n.$$

With similar consideration, the same reflection condition for 3_2 can be derived.

C.1.4 On the absence of extinction due to 2_1 screw axis perpendicular to \mathbf{c} .

In Fig. C.1 [p.48], there are 2_1 screw axes perpendicular to \mathbf{c} at positions of $x = \frac{1}{2}$ and $y = \frac{1}{2}$. However, these 2_1 screw axes cause no extinction. The reason is that the angle spanned by \mathbf{a} and \mathbf{a}^* and that spanned by \mathbf{b} and \mathbf{b}^* are not zero (not parallel). About this, refer to the following description, please.

Symmetric operation due to rotation around \mathbf{a}_0 is represented by movement of point on a plane perpendicular to \mathbf{a}_0 . Referring to Fig. C.3, reciprocal vectors perpendicular to \mathbf{a}_0 are \mathbf{c}_0^* and \mathbf{b}_0^* . A real vector parallel to \mathbf{b}_0^* is represented by a linear combination of \mathbf{a}_0 and \mathbf{b}_0 , as $\frac{1}{2}\mathbf{a}_0 + \mathbf{b}_0$. Therefore, Symmetry due to 2_1 screw axis in the direction of \mathbf{a}_0 located at $(y, z) = \frac{1}{2}, \frac{1}{3}$ is represented as follows:

$$\rho[T_{2_1}^{(i)}(\mathbf{r})] = \rho[T_{2_1}^{(0)}(\mathbf{r})], \quad i \in \{0, 1\}.$$

$$\begin{aligned} T_{2_1}^{(0)}(\mathbf{r}) &= x\mathbf{a}_0 \\ &+ (\frac{1}{2} + y)(\frac{1}{2}\mathbf{a}_0 + \mathbf{b}_0) \\ &+ (\frac{1}{3} + z)\mathbf{c} \\ &= (x + \frac{1}{4} + \frac{1}{2}y)\mathbf{a}_0 \\ &+ (\frac{1}{2} + y)\mathbf{b}_0 \\ &+ (\frac{1}{3} + z)\mathbf{c}, \end{aligned}$$

$$\begin{aligned} T_{2_1}^{(1)}(\mathbf{r}) &= (\frac{1}{2} + x)\mathbf{a}_0 \\ &+ (\frac{1}{2} - y)(\frac{1}{2}\mathbf{a}_0 + \mathbf{b}_0) \\ &+ (\frac{1}{3} - z)\mathbf{c} \\ &= (x + \frac{3}{4} - \frac{1}{2}y)\mathbf{a}_0 \\ &+ (\frac{1}{2} - y)\mathbf{b}_0 \\ &+ (\frac{1}{3} - z)\mathbf{c}. \end{aligned}$$

The extinction condition (while not existing) is represented similarly to (B.2) [p.41] as follows:

$$\sum_{i=0}^1 \exp[-i2\pi \mathbf{h} \cdot T_{2_1}^{(i)}(\mathbf{r})] = 0. \quad (\text{C.3})$$

Here, for mathematical convenience to calculate \sum of (C.3), let us define $f_{2_1}(\mathbf{h}, \mathbf{r})$ as follows:

$$f_{2_1}(\mathbf{h}, \mathbf{r}) = \exp\{-i2\pi[h(\frac{1}{2} + x) + k\frac{1}{2} + l\frac{1}{3}]\}.$$

Therefore, \sum of (C.3) can be deformed as fol-

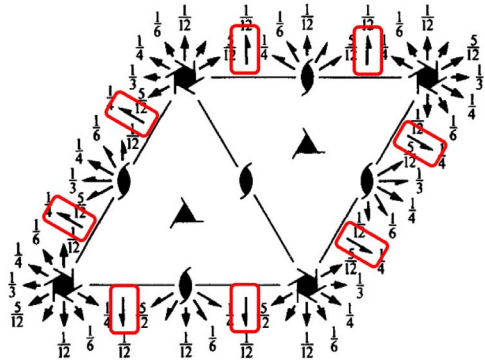


Figure C.4: *International Tables for Crystallography* (2006) Vol.A, Symmetric elements. $P6_122$ (#178).

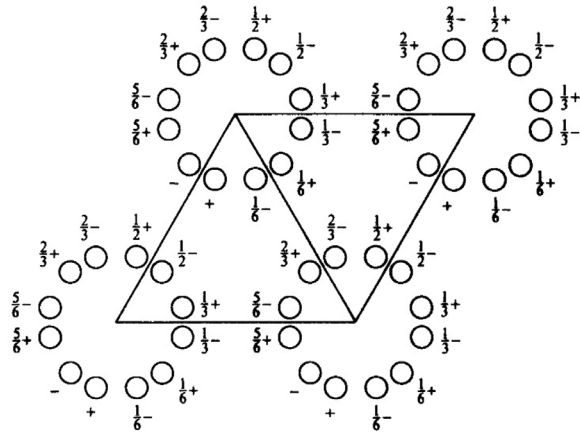


Figure C.5: *International Tables for Crystallography* (2006) Vol.A, Positions of atoms. $P6_122$ (#178).

lows:

$$\begin{aligned}
 & f_{2_1}(\mathbf{h}, \mathbf{r}) \times \\
 & \left\{ \exp\left\{-i2\pi\left[h\left(\frac{1}{4} - \frac{1}{2}y\right) - ky - lz\right]\right\} \right. \\
 & \left. + \exp\left\{-i2\pi\left[-h\left(\frac{1}{4} - \frac{1}{2}y\right) + ky + lz\right]\right\} \right\} \\
 & = f_{2_1}(\mathbf{h}, \mathbf{r}) \times \\
 & \cos\left\{2\pi\left[h\left(\frac{1}{4} - \frac{1}{2}y\right) - ky - lz\right]\right\} = 0.
 \end{aligned}$$

The above equation reveals that there is no extinction due to 2_1 screw axis perpendicular to \mathbf{c} since terms of h , k and l all depend to values of y or z . The second term $-h\frac{1}{2}y$ in $\cos\{\}$ of the above equation exists since \mathbf{a}_0 is not parallel to \mathbf{a}_0^* . If there were a reciprocal primitive vector parallel to the screw axis, we can discuss the extinction under the condition that $k, l = 0$. When there is no reciprocal primitive vector parallel to the screw axis, there is no extinction due to it.

In a similar way, it can be verified that there is no extinction due to screw axes parallel to \mathbf{b}_0 or $\mathbf{a}_0 + \mathbf{b}_0$.

C.2 Case of hexagonal system

C.2.1 Figure shown in *International Tables for Crystallography* (2006) Vol.A

Fig. C.4 is a drawing for space group $P6_122$ (#178) in *International Tables for Crystallography* (2006) Vol.A that shows symmetric elements. Fig. C.5 shows coordinates of atoms.

The unit cell is usually taken similarly to that in the case of trigonal system as shown in Fig. C.1 [p.48] and C.2 [p.48]. There are 2_1 screw axes perpendicular to \mathbf{c} . However they do not cause extinction similarly to the case of trigonal system.

C.2.2 Coordinates for describing six-fold screw axes

For describing positions of atoms that are rotated by $\frac{i}{6}2\pi$ ($i \in \{0, 1, 2, 3, 4, 5\}$) from the original position, let us prepare combinations of \mathbf{a}_i and \mathbf{b}_i as follows:

\mathbf{a}_i	\mathbf{b}_i	i
\mathbf{a}_0	\mathbf{b}_0	0
$\mathbf{a}_0 + \mathbf{b}_0$	$-\mathbf{a}_0$	1
\mathbf{b}_0	$-\mathbf{a}_0 - \mathbf{b}_0$	2
$-\mathbf{a}_0$	$-\mathbf{b}_0$	3
$-\mathbf{a}_0 - \mathbf{b}_0$	\mathbf{a}_0	4
$-\mathbf{b}_0$	$\mathbf{a}_0 + \mathbf{b}_0$	5

By using the above coordinates, positions that is rotated by $\frac{i}{6}2\pi$ ($i \in \{0, 1, 2, 3, 4, 5\}$) from the

original position can be written as follows:

$$\begin{aligned} x_0 &= x, & y_0 &= y, \\ x_1 &= x - y, & y_1 &= x, \\ x_2 &= -y, & y_2 &= x - y, \\ x_3 &= -x, & y_3 &= -y, \\ x_4 &= -x + y, & y_4 &= -x, \\ x_5 &= y, & y_5 &= -x + y. \end{aligned}$$

C.2.3 Derivation of extinction rule due to 6_1 screw axis

Symmetry due to 6_1 screw axis located at the origin in the direction of \mathbf{c} , is described as follows:

$$\begin{aligned} \rho[T_{6_1}^{(i)}(\mathbf{r})] &= \rho[T_{6_1}^{(0)}(\mathbf{r})], \quad i \in \{0, 1, 2, 3, 4, 5\}. \\ T_{6_1}^{(0)}(\mathbf{r}) &= x\mathbf{a}_0 + y\mathbf{b}_0 + z\mathbf{c}, \\ T_{6_1}^{(1)}(\mathbf{r}) &= (x - y)\mathbf{a}_0 + x\mathbf{b}_0 + \left(\frac{1}{6} + z\right)\mathbf{c}, \\ T_{6_1}^{(2)}(\mathbf{r}) &= -y\mathbf{a}_0 + (x - y)\mathbf{b}_0 + \left(\frac{2}{6} + z\right)\mathbf{c}, \\ T_{6_1}^{(3)}(\mathbf{r}) &= -x\mathbf{a}_0 - y\mathbf{b}_0 + \left(\frac{3}{6} + z\right)\mathbf{c}, \\ T_{6_1}^{(4)}(\mathbf{r}) &= (-x + y)\mathbf{a}_0 - x\mathbf{b}_0 + \left(\frac{4}{6} + z\right)\mathbf{c}, \\ T_{6_1}^{(5)}(\mathbf{r}) &= y\mathbf{a}_0 + (-x + y)\mathbf{b}_0 + \left(\frac{5}{6} + z\right)\mathbf{c}. \end{aligned}$$

Similarly to (B.2) [p.41], the extinction condition is described as follows:

$$\sum_{i=0}^5 \exp[-i2\pi\mathbf{h} \cdot T_{6_1}^{(i)}(\mathbf{r})] = 0. \quad (\text{C.4})$$

For mathematical convenience, let us define $f_{6_1}(\mathbf{h}, \mathbf{r})$ as follows:

$$f_{6_1}(\mathbf{h}, \mathbf{r}) = \exp[-i2\pi(lz)].$$

From (C.4), the extinction condition is obtained as follows:

$$\begin{aligned} f_{6_1}(\mathbf{h}, \mathbf{r}) \times \\ \left\{ \exp\{-i2\pi[hx + ky]\} \right. \\ + \exp\{-i2\pi[h(x - y) + kx + l\frac{1}{6}]\} \\ + \exp\{-i2\pi[-hy + k(x - y) + l\frac{2}{6}]\} \\ + \exp\{-i2\pi[-hx - ky + l\frac{3}{6}]\} \\ + \exp\{-i2\pi[h(-x + y) - kx + l\frac{4}{6}]\} \\ \left. + \exp\{-i2\pi[hy + k(-x + y) + l\frac{5}{6}]\} \right\} = 0. \end{aligned}$$

The extinction can be discussed only when $h = k = i = 0$. Under this condition, the above extinction condition can be described as follows:

$$\begin{aligned} 1 \\ + \exp(-i2\pi l\frac{1}{6}) \\ + \exp(-i2\pi l\frac{2}{6}) \\ + \exp(-i2\pi l\frac{3}{6}) \\ + \exp(-i2\pi l\frac{4}{6}) \\ + \exp(-i2\pi l\frac{5}{6}) = 0. \quad (\text{C.5}) \end{aligned}$$

When $l = 6n$, reflections do not distinguish. When $l = 6n + i$ ($i \in \{1, 2, 3, 4, 5\}$), reflections distinguish since phase interval of the six term is an identical value $-2\pi\frac{i}{6}$. The reflection condition (not extinct) can be described as follows,

$$hkil : l = 6n.$$

Similarly, the same reflection condition can be derived also for 6_1 screw axis.

In Fig. C.4, 2_1 and 3_1 screw axes in the direction of \mathbf{c} are found. However, the logical product of reflection conditions due to 6_1 , 2_1 and 3_1 screw axes gives the same reflection condition as described in the above equation.

C.2.4 Derivation of the extinction due to 6_2 screw axis

The extinction condition due to 6_2 screw axis is given similarly to (C.5) [p.52] as follows:

$$\begin{aligned}
 &1 \\
 &+ \exp(-i2\pi l \frac{1}{3}) \\
 &+ \exp(-i2\pi l \frac{2}{3}) \\
 &+ 1 \\
 &+ \exp(-i2\pi l \frac{1}{3}) \\
 &+ \exp(-i2\pi l \frac{2}{3}) = 0.
 \end{aligned}$$

When $l = 3n$, reflections do not distinguish since the six term have an identical value unity. When $l = 3n + i$ ($i \in \{1, 2\}$), reflections distinguish since phase interval of the six term is an identical value $-2\pi \frac{i}{3}$. Then, the reflection condition (not extinct) is given by

$$hkl : l = 3n.$$

In a similar way, the same reflection condition

can be derived for 6_4 screw axis.

C.2.5 Derivation of extinction rule due to 6_3 screw axis

An equation for 6_3 screw axis that corresponds to (C.5) [p.52] is given by

$$\begin{aligned}
 &1 \\
 &+ \exp(-i2\pi l \frac{1}{2}) \\
 &+ 1 \\
 &+ \exp(-i2\pi l \frac{1}{2}) \\
 &+ 1 \\
 &+ \exp(-i2\pi l \frac{1}{2}) = 0.
 \end{aligned}$$

When l is even, all terms are unity giving no extinction. When l is odd, reflections distinguish since phase interval of the six terms is an identical value $-2\pi \frac{1}{2}$ giving extinction. Therefore, the reflection condition (not extinct) is given by

$$hkl : l = 2n.$$

End of the document.

Index

Symbols

2_1 screw axis	38, 41
<i>A</i> base-centered lattice	41
<i>B</i> base-centered lattice	41
<i>C</i> base-centered lattice	41
<i>c</i> glide plane	38, 41
<i>n</i> glide plane	41
[Ctrl]+[R]	23
[Ctrl]+[T]	20
'Face-centered monoclinic'	35

A

<i>Aba2</i> (#41)	38
<i>Abm2</i> (#39)	38
Absolute structure	13
Absorption Correction	17
α -cyclodextrin	20, 21, 23
<i>Ama2</i> (#40)	38
<i>Amm2</i> (#38)	38
Anisotropic temperature factor	10, 22
Auto button	i
AutoChem	20

B

Base-centered lattice	41, 42
Benzene ring	25
Body-centered lattice	42
Body-centered monoclinic lattice	37
Bragg reflection plane	32
Bragg's reflection condition	30, 32, 37
Bravais lattice	35, 37

C

<i>C12/c1</i>	40
<i>C2/c</i> (#15)	39, 40
Cell choice	38
Complex lattice	37, 38, 41, 42
Contact Letter	15
Crystal information	15
Crystal system	37
Crystl system	38
Cubic	35
Cyclodextrin	21, 23

D

D amino acid	39, 43
Dell computer	i
Determination of space group	34, 35
Diffraction	16
Direct method	7
Disorder	23
Draw	i
Drawing of Miller	33

E

Electron density peak	23
Ethylene group	25
Ewald, P. P.	30–32
Ewald construction	30–32
Ewald sphere	30, 32
Ewald's reflection condition	32
Extinction effect	28
Extinction rule	i, 30, 34, 35, 37, 38, 43

F

Face-centered lattice	43
Flack parameter	10, 13

G

Glide plane	41, 43
Graphic symbol of 2_1 screw axis	38
Graphic symbol of <i>c</i> glide plane	38
Graphic symbol of symmetric center	38

H

H-M full notation	38, 41
H-M notation	38, 39
Hauptman	8
Hermann-Mouguin full notation	38
Hermann-Mouguin notation	38, 39
Hexagonal	i, 35
Horizontal translation	i
Hydroxy group	12, 25
Hydroxy ion	25

I

Image due to 2_1 screw axis	38
Image due to <i>c</i> glide plane	38

In-plane rotation	i	$P2_1/c$ (#14)	34–37, 39, 40
Initial phase	7, 20	$P2_1/c$ (#14)	35
Intensities of Q peaks	23	$P2_1/c11$	38
Isotropic temperature factor	22	$P2_1/n11$	38
isotropic temperature factors	9	$P2_111$	41
		$P2_12_12_1$ (#19)	39–41
K		$P3_121$ (#152)	48
Karle	8	$P6_122$ (#178)	50–52
		$P\bar{1}$ (#2)	39, 40
L		Password	i
L amino acid	39, 43	PATH	5
Laue, M. T. F. von	30, 31	Phase problem	37, 40
Laue group	35, 37, 38	phase problem	8
Laue's reflection condition	30–32	PLATON	4
Login name	i	Position of atom	38
		Primitive lattice	37
		Primitive translation vector	31
		process.out	35
		Publication	17
M		Q	
Maximum peak intensity	22, 23	Q peak	9–11, 23–25
Methine group	25		
Methyl group	25	R	
Methylene group	25	R-factor	i, 9, 10, 12, 25–29
Miller indices	33	Racemic compound	40
Monoclinic	37, 40	Reasonableness of using four indices	48
Monoclinic	35, 37, 38, 40, 41	Reciprocal lattice	30–32
mSprit	24	Reciprocal lattice vector	32
		Reciprocal space	31, 32
N		Refine	i
Nishikawa, S.	36	registration of user information	1
		Report	i
O		S	
Occupancy	24, 27	Schönflies notation	38
OLEX ²	20	Screw axis	38, 41, 45, 46, 48
OLEX ²	7	Sheldrick	8
Olex2	1	SHELX	1, 17
OlexSys	1	ShelXL	22
Open project	7, 20	ShelXT	8
Operator	15	sign-in URL	1
Optical isomer	43	Six-fold screw axis	48
Ordinal number of space group	38	Solve	i
Orthorhombic	35, 41	solvent molecule	20
		Space group	i, 34, 35, 37
P		Submitter	15
$P112_1$	41	Sucrose	i, 12
$P112_1/a$	38	Symmetric center	21, 22, 38, 40
$P112_1/b$	38	Symmetric element	36
$P112_1/n$	38	symmetrical operation	20
$P12_1/a1$	38, 39	Symmetry	30
$P12_1/c1$	38, 39		
$P12_1/n1$	38, 39		
$P12_11$	40, 41		
$P2_1$ (#4)	39–41		
$P2_1/b11$	38		

T			
Taurine	34–36	user information	1
Tetragonal	35	V	
Thermal ellipsoid	11	Vertical translation	i
Three-fold screw axis	48	W	
Triclinic	35, 40	Wyckoff, R. W. G.	36
Trigonal	i, 35	Z	
U		Zoom	i
Unique axis	38		